

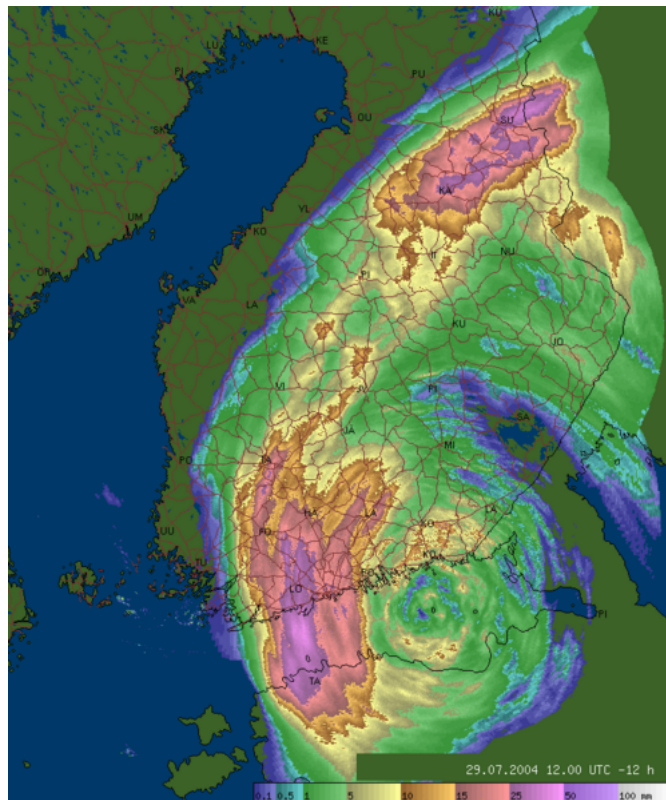


---

---

## Workshop Report

### HIRLAM/NetFAM Workshop on Convection and Clouds Tartu, 24 - 26 January, 2005



Accumulated 12 hour precipitation retrieved from FMI radar network, 7th July, 2004, 12UTC



## Introduction

The HIRLAM/NetFAM workshop on clouds and convection was arranged at the Physics building of Tartu University in January, 24-26, 2005. The aim of the workshop was to join HIRLAM and ALADIN-Meteo France researchers working in the area of convection and cloud processes to review the state of art, discuss the strategy, tasks and plans in the way towards explicit convection and microphysics in fine scale HIRLAM/ALADIN, interactions with the nonhydrostatic dynamics. The topics suggested for discussion included:

1. Interactions between shallow convection and moist turbulence
2. Parametrized and explicit deep convection
3. Development of explicit microphysics for fine scale models
4. Validation methods for convection, clouds and precipitation
5. Case studies with hydrostatic and nonhydrostatic models.

In addition, principles of coupling the model dynamics and physics were discussed, and a short coordinating meeting of the Nordic Network on Fine-scale Atmospheric Modelling (NetFAM) arranged.

The workshop programme consisted of general sessions and working groups, see the attached programme for the details. 30 participants from 15 countries and 18 institutes attended the workshop. In the present report, the extended abstracts follow the order of the workshop programme. Reports of the four working groups then follow. The present report is printed as black and white. However, many contributions contain colours. The original files (pdf) are available at the NetFAM web site <http://netfam.fmi.fi>.

## Acknowledgements

The Department of Environmental Physics of Tartu University hosted the meeting and arranged an excellent venue and environment for the fruitful work during the workshop. Arrangement of the workshop was made possible by the funding of NetFAM by Nordic Research Board (NordForsk), which covered the travel expenses of many of the workshop participants. The international HIRLAM project included the present report into the series of HIRLAM workshop publications.

On behalf of the organisers

Helsinki 25.4.2005  
Laura Rontu

## **Programme of the workshop**

### **Monday 24.1.2005**

8.45 - 9.00

Opening of the workshop: Rein Rõõm, University of Tartu

General topics 9.00 - 10.50

Chairman: Jean Quiby

9.00 - 9.20

Per Unden

Physical parametrizations on the way from HIRLAM to AROME

9.25 - 9.45

Rein Rõõm and Aarne Männik

Nonhydrostatic semi-implicit semi-lagrangian dynamics (NH SISL) for HIRLAM: overview and perspective for application to VHR modeling

9.50 - 10.10

Bart Catry

Towards a consistent formulation of interfaces between dynamical and physical processes

10.15 - 10.35

Bent Hansen Sass

A brief review of some key issues related to modelling of clouds and precipitation forecasting

10.40 - 11.00

coffee break

Parametrizations 11.00 - 17.20

Chairman: Rein Rõõm

11.00 - 11.40

Paul Schultz, NOAA

Explicit Microphysics and Diabatic Initialization

11.45 - 12.15

Jean-Pierre Pinty, J.-P. Chaboureau, Y. Seity and Eric Bazile

Experiments with the MesoNH-AROME microphysical scheme and evaluation by remote sensing tools

12.20 - 13.20

lunch break

13.20 - 13.40

Javier Calvo

Kain-Fritsch and Rasch-Kristjansson in HIRLAM

13.45 - 14.05

Colin Jones

Coupling a statistical cloud scheme with moist turbulence and parameterised convection. Initial results and future prospects.

14.10 - 14.30

Wim de Rooy

Experiences with a statistical cloud scheme in combination with Kain-Fritsch convection in Hirlam

14.35 - 14.55

Jean-Francois Geleyn

Why do moisture convergence deep convection schemes work for more scales than those which they were in principle designed for?

15.00 - 15.20

Luc Gerard

An integrated prognostic approach for clouds, precipitation and convection

15.25 - 15.45

coffee break

15.50 - 16.10

Francois Bouyssel - Yves Bouteloup - Pascal Marquet

Implementation and validation of a prognostic large-scale cloud and precipitation scheme in ARPEGE

16.15 - 16.35

Karl-Ivar Ivarsson

Separate prognostic treatment of cloud water and ice in Hirlam - some preliminary results.

16.40 - 17.00

Dmitri Mironov

Useful analogies between the mass-flux and the Reynolds-averaged second-moment modelling frameworks

17.05-17.25

Tomislav Kovacic

Testing of bulk parameterisation of microphysics in ALARO 10

Starting the working groups 17.30 - 18.15

- defining the topics and accepting the agenda
- starting discussions

Convection and turbulence parametrizations

Chairman: Colin Jones

Development of microphysics for the fine scale

Chairman: Laura Rontu

## **Tuesday 25.1.2004**

Working groups (continuation) 8.30 - 10.15

Convection and turbulence parametrizations  
Development of microphysics for the fine scale models

10.15 - 10.30  
coffee break

Validation and diagnostics 10.30 - 12.40

Chairman: Marko Kaasik

10.30 - 10.50  
Irene Sanz  
Use of radar reflectivities to validate HIRLAM

10.55 - 11.15  
Christoph Zingerle  
Cloud verification using satellite data

11.20 - 11.40  
Kalle Eerola  
Precipitation and cloud forecasts in two HIRLAM versions (RCR and H635) in  
September 2004

11.45 - 12.05  
Carl Fortelius  
What can a LAM-NWP tell us about the atmospheric water cycle

12.10 - 12.20  
Anna Kanukhina  
A study on convection indexes

12.25 - 13.25  
lunch break

Case studies 13.25 - 14.40  
Chairman: Aarne Männik

13.25 - 13.45  
Andres Luhamaa  
Testing different HIRLAM convection and microphysics schemes at high resolutions

13.50 - 14.10  
Sami Niemelä  
The flood case 27-29 July 2004

14.15 - 14.35

Paulius Jalinskas

Case studies based on one dimensional model with Kain-Fritsch convection parameterization scheme

14.40 - 15.05

coffee break

Working session on analysis, diagnostics and validation 15.05 - 17.30

Chairman: Carl Fortelius

- A review on cloud-related observations and their assimilation into fine-grid models - Paul Schultz
- Short description of the Helsinki testbed observations - Laura Rontu (based on Jani Poutiainen's presentation at FMI)
- Short presentation of the one-dimensional HIRLAM as a tool for validation - Javier Calvo

discussion + recommendations

19 – Workshop dinner

**Wednesday 26.1.2004**

Parallel sessions 8.30 - 10.00

NetFAM project meeting

Chairman: Laura Rontu

Working session on dynamics-physics coupling in the mesoscale  
HIRLAM-AROME-ALADIN

Chairman: Per Unden

General session 10.00 - 12.00

Chairman: Laura Rontu

- results of the working groups and working sessions
- general discussion
- closure of the workshop

Lunch 12.00 -

## List of participants

Ulf Andrae	ulf.andrae@smhi.se
Francois Bouyssel	Francois.Bouyssel@meteo.fr
Javier Calvo	j.calvo@inm.es
Bart Catry	Bart.Catry@UGent.be
Kalle Eerola	kalle.eerola@fmi.fi
Carl Fortelius	carl.fortelius@fmi.fi
Jean-Francois Geleyn	jean-francois.geleyn@chmi.cz
Luc Gerard	luc.gerard@oma.be
Karl-Ivar Ivarsson	karl-ivar.ivarsson@smhi.se
Paulius Jalinskas	paulius@meteo.lt
Colin Jones	jones.colin@uqam.ca
Marko Kaasik	mkaasik@physic.ut.ee
Anna Kanukhina	kanukhina@rshu.ru
Katherina Kourzeneva	kourzeneva@rshu.ru
Tomislav Kovacic	kovacic@cirus.dhz.hr
Andres Luhamaa	andres.luhamaa@ut.ee
Dmitri Mironov	dmitrii.mironov@dwd.de
Aarne Männik	aarne.mannik@ut.ee
Sami Niemelä	sami.niemela@fmi.fi
Thor Erik Nordeng	thor.erik.nordeng@met.no
Jean-Pierre Pinty	pinjp@aero.obs-mip.fr
Jean Quiby	jean.quiby@meteoswiss.ch
Laura Rontu	laura.rontu@fmi.fi
Wim de Rooy	wim.de.rooy@knmi.nl
Rein Rõõm	rein.room@ut.ee
Irene Sanz	isanz@inm.es
Bent Hansen Sass	bhs@dmi.dk
Paul Schultz	paul.j.schultz@noaa.gov
Per Unden	per.unden@smhi.se
Christoph Zingerle	christoph.zingerle@fmi.fi

# The HIRLAM physics towards meso-scale

Per Undén

HIRLAM-6 , c/o SMHI, S-60176 Norrköping, Sweden

## 1 Vision for Hirlam

The vision of the Hirlam Programme is to provide the best available meso-scale (1-3 km) modelling system to be operational in the member countries 2010. The reasons for this are

- Necessary to resolve weather in mountainous areas
- Needed for very short-range prediction of severe weather of precipitation and particularly connected with convection
- More detailed and higher resolution forecast for many applications such as air pollution dispersion modelling, wind energy, disastrous releases of dangerous agents, etc.

To provide such a model requires:

- Non-hydrostatic and efficient dynamics
- Meso-scale advanced physical parameterisation
- Advanced meso-scale data assimilation with many new data sources
- Probabilistic forecasting
- Transparent Boundary conditions

Most of these items are additional to the previous Hirlam Projects of synoptic scale modelling at resolutions that used to be around 50-20 km, although some of the physical parameterisation and data assimilation have common components or framework with the synoptic modelling.

At the same time, Hirlam will also continue to provide a synoptic scale system for regional (Atlantic) scales and of resolutions of around 10 km. The reasons for this are

- To provide the meso-scale forecasting system with the most recent boundary conditions, with high resolution in space and **time** and with certain consistencies in the physics
- To provide members with a high quality regional forecasting system that is at least of equal quality as available alternatives but is run more frequently (as demanded) with short cut-off after observations have been made
- To provide members with a high resolution (in space **and** in time) comprehensive set of forecast variables to be used for a wide range of forecasting applications and also to drive other models

## 2 How to achieve the goals

Hirlam is not going to develop a new meso-scale model of its own. It is a large effort and takes several years. The Project does not have enough dynamics staff currently, even though a pressure coordinate anelastic non-hydrostatic dynamical core was developed by Tartu University, outside of the Project. The time and resources are crucial and besides to embark on a new model would mean a lot of duplication in Europe.

In order to re-gain lost time and to get critical mass in all areas, the Project has concluded that it is necessary to collaborate with other partners. Hirlam has a long established collaboration with Météo-France (it is member of Hirlam since 1992) and there is good experience of this collaboration and it should be increased whenever possible. There have been large advances in the non-hydrostatic dynamics of the ALADIN model, developed in partnership with ALADIN members. By using parts of the physics from Mésó-NH in France, Météo-France has an advanced project aiming for operational meso-scale forecasting, called AROME. This coincides very much with the ambitions and needs in Hirlam and the Project sees several opportunities for mutual benefits and contributions. Furthermore, ALADIN is using the main part of the ECMWF IFS code and is synchronised with this, and this brings benefits from ECMWF as well. ALADIN and Hirlam models and data assimilation have several common components and ALADIN was developed with ideas from Hirlam.

To achieve all the benefits of collaboration, the Project has decided for a **code** collaboration with ALADIN. This will ensure that also future developments on both/all sides will go into the common system and is a vehicle to actually share the work. The price to pay is that one needs to be committed to synchronise-phase the code at regular intervals and this requires quite a lot of work. The benefits are however expected to be much larger than the extra efforts. The research plans in the areas of collaboration (first the meso-scale activities) are to be coordinated. For the next Hirlam and ALADIN projects the MoUs of the organisations need to include the collaboration and details will be regulated. Cross steering mechanisms need to be established.

It is evident that, even though the synoptic Hirlam model is thriving and used operationally and is undergoing development, in the long run it will be too much to maintain two modelling systems. The synoptic Hirlam model should be merged into the collaboration as well, and particularly the physics need to be interfaced. The dynamics are rather equivalent for the hydrostatic part, particularly if one compares with the spectral Hirlam model.

## 3 Hirlam model components and strategy

The Hirlam physics is quite state of the art for the synoptic scale ( currently around 20 km grid resolution). The radiation is relatively simple but efficient and relatively good, the turbulence is a TKE scheme and has been the focus of much attention and development, the surface scheme is ISBA and is being enhanced with an explicit snow scheme. The condensation is of Sundqvist type and the convection scheme is a regularised Kuo scheme although a mass-flux Kain-Fritsch scheme is available and used by some. Meso-scale and sub-grid scale orography parametrisation has been developed. A number of these schemes have been developed in collaboration with Météo-France and also indirectly with Mésó-NH.

The Hirlam strategy is not to try to model in the no-man's land between 8-4 km or thereabouts. Even though there are at least partially successful Hirlam applications in this range too, there are compelling reasons when dealing with resolved or parameterised convection that makes this range very difficult to model. Furthermore, the user requirements make it necessary to achieve

as high resolution as possible.

There are several Hirlam components that should be suitable also in the meso-scale. The surface ISBA scheme is also designed for high resolution and the tiling is probably relevant even below 1 km resolution, due to nature. The TKE turbulence scheme is 1D and probably this is OK down to about 1 km but not lower. The Hirlam radiation scheme has been enhanced to include sloping surfaces and may be used still for some time. The cloud physics is not so advanced and in this area much more is needed. The sub-grid scale orography still needs parametrisation at 1 km. At the same time, there are the already mentioned similarities in the Méso-NH and AROME physics. The turbulence schemes have the same origins. The ISBA scheme is not tiled at Météo-France and is being externalised. There is significantly more advanced microphysical treatment in Méso-NH and this needs to be used in Hirlam too.

While Hirlam will continue to support and improve its synoptic physics, work is going on to integrate and interface it with ALADIN. The aim is to compare with AROME physics and integrate some AROME options or some Hirlam options with AROME. Options will be switchable and a Hirlam configuration will be defined.

There are several more challenges for the meso-scale forecasting system. The meso-scale data assimilation needs to be developed, even though there are many building blocks available. It is necessary to carry out probabilistic forecasting and modelling of uncertainties. Verification aspects will also require new methods in the meso-scale.

## 4 Recent work in Hirlam

The Hirlam group has acquired the ALADIN model set it up at ECMWF for compilation and execution, to run some cases in a test period. This has been an extensive learning exercise but also some initial results could be seen, that seemed very reasonable. Work is ongoing to interface Hirlam boundaries and parts of the Hirlam physics has been interfaced.

During the recent years there has been a lot of activity to improve the Hirlam synoptic physics, in the areas of turbulence, surface parameterisation and surface fluxes mainly. It has been very important for the model to increase the surface drag and fill cyclones correctly, but without deteriorating the vertical wind profiles. Recently some good compromises, with a certain mixing also in stable stratification (but not excessive), increased orographic and vegetational roughness and a turning of the surface stress, have in combination with different roughness lengths for heat/moisture and momentum, resulted in large and important forecast improvements. The systematic errors of too moist and cold summer 2m forecasts have been much reduced and also the cold and moist spring problem are reduced. For further documentation, see Järvenoja (2005) and Eerola (2005) (from which some material was shown at the meeting and in the ppt presentation).

## References

- Eerola, Kalle, 2005: Verification of Hirlam version 6.3.5 against RCR in autumn conditions *HIRLAM Newsletter*, **47**.
- Järvenoja, Simo, 2005: Experimentation with a modified surface stress. some earlier versions and RCR. *HIRLAM Newsletter*, **47**.

# Non-hydrostatic, semi-implicit, semi-Lagrangian adiabatic core for HIRLAM

Rein Rõõm, Aarne Männik  
Tartu University, Estonia  
Rein.Room@ut.ee, Aarne.Mannik@ut.ee

## 1 Introduction

The development of the nonhydrostatic (NH), semi-implicit semi-Lagrangian (SISL) core for HIRLAM is completed in general lines. Currently (January 2005), the model is implemented with Reference HIRLAM v6.1.0 and proceeds the stage of preoperational testing at the Estonian Meteorological and Hydrological Institute (EMHI).

The NH SISL creation continued efforts of earlier NH model development in the HIRLAM framework at the Tartu University (Rõõm 2001, Männik & Rõõm 2001, Rõõm & Männik 2002).

The main goals at the NH SISL development have been:

- To bring the semi-anelastic, pressure-coordinate, NH approach to a logical and definite finish in the HIRLAM framework;
- To upgrade HIRLAM for mesoscale use, substantially enhancing the computational efficiency of the NH core, and thus making the model competitive with other mesoscale forecast models.

In the first part we will give a short description of the dynamics and numerics, employed in the model. In the second part, preliminary test results with the new core are presented and discussed.

## 2 Model description

### 2.1 Dynamics

The basic for dynamics are the semi-anelastic pressure-coordinate equations of motion and thermodynamics in Lagrangian form. In detail these equation are described in (Rõõm 2001). The only and main difference between that model and current approach is the surface pressure treatment. In the current model the surface pressure is treated as non-adjusted, satisfying the 'full' evolutionary equation, which coincides with surface pressure treatment by the primitive equations. Altogether, the set of dynamical equations is factually the HS primitive equation set, updated with an additional equation for vertical acceleration (the vertical momentum equation), which includes an additional, non-hydrostatic geopotential. This additional potential is diagnosed from the condition of the

non-divergence of motion in pressure-coordinates (the continuity equation, which also is the same as in the HS primitive-equation model).

## 2.2 Discrete model

For discretization, the hybrid coordinates of ECMWF origin are employed along with C-grid staggering. The Semi-Lagrangian (SL) trajectory calculations are applied, which factually coincide with the trajectory calculations in HS case. Thus, the existing (McDonald & Haugen 1992, McDonald 1995) routines from HS HIRLAM are possible to employ for trajectory calculations and interpolating procedures.

The two-level time stepping scheme is also appropriated from HS model.

## 2.3 NH-specific features

Separation of forces to the main (linear) forces and perturbation (nonlinear) part makes use of pressure(height)-dependent reference temperature  $\hat{T}(p)$ , Brunt-Väisälä frequency  $N(p)$ , and reference surface pressure  $\hat{p}_s(x, y)$ . To avoid fictive geopotential force generation by reference surface pressure,  $\hat{p}_s(x, y)$  must be chosen from the barometric relationship in concordance with reference temperature  $\hat{T}(p)$ . Consequently, the real dynamic variables are represented by fluctuative parts of temperature  $T$ , and surface pressure  $p_s$ .

The use of height dependent reference fields  $\hat{T}(p)$ ,  $N(p)$  insures to the benefit of increasing the weight of linear forces, which are treated implicitly, in comparison with explicit non-linear perturbations. The aim of such increase of the linear implicit forces is to maximize the stability of the model. For instance, in the ideal case of coincidence of the actual temperature  $T(x, y, p, t)$  with the reference field  $\hat{T}(p)$ , the perturbative, nonlinear hydrostatic pressure forcing disappears, and scheme becomes (at that instant) unconditionally stable for optionally large time steps.

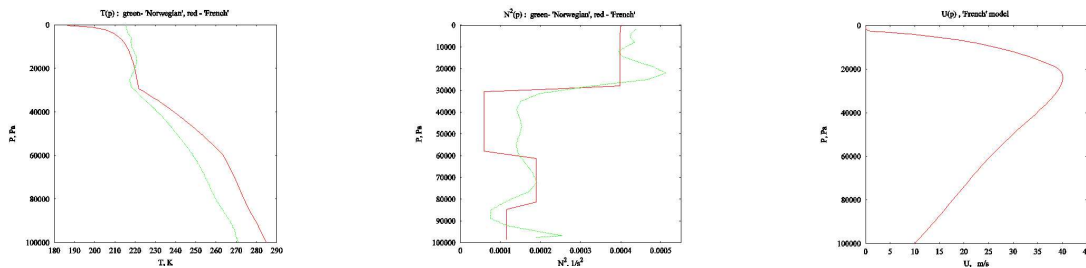


**Fig. 1.**

*Examples of reference temperature profiles (a) and corresponding Brunt-Väisälä frequencies (b). The reference wind profile (c) is used for model tests with artificial orography.*

The potential problem with sophistication of the main elliptic equation for NH geopotential due to the (more) complicated reference temperature distribution (common SISL approaches, including the HS SISL HIRLAM, make use of the constant reference temperature) is solved by using a special algorithm to solve this main elliptic equation.

In general, the developed NH SISL numerical algorithm is computationally (by time consumption rate per time-step) even more economic than the HS parent.

## 3 Testing

### 3.1 Model experiments

Aim of the model experiments is (1) debugging, and (2) model quality control. In the model experiments adiabatic stationary flow regimes over given orography are studied and compared to the known analytical solutions of the linearised dynamics.

As an example, in Fig. 2 the stationary flow over Agnesi ridge with half-width  $a_x = 3$  km and maximum height  $h = 600$  m is presented. The wind and temperature profiles are the 'French' case in Fig. 1. The grid is 276x100x100 points, horizontal resolution is 0.55 km. At such a reference state, the waves present a stationary wave-train downstream of the mountain, each wave vertically directed and penetrating the whole depth of the atmosphere. It is rather difficult to model this wave pattern correctly, the simulation quality is a good indicator of the quality of the numerical scheme. In this special case we were checking the stability of the model with respect to the time step size. In the top panel, the time step is  $\Delta t = 30$  s, in the bottom panel –  $\Delta t = 60$  s. The critical time step in this particular experiment is  $\Delta_{cr}t = \Delta x/U_{max} = 13$  s.

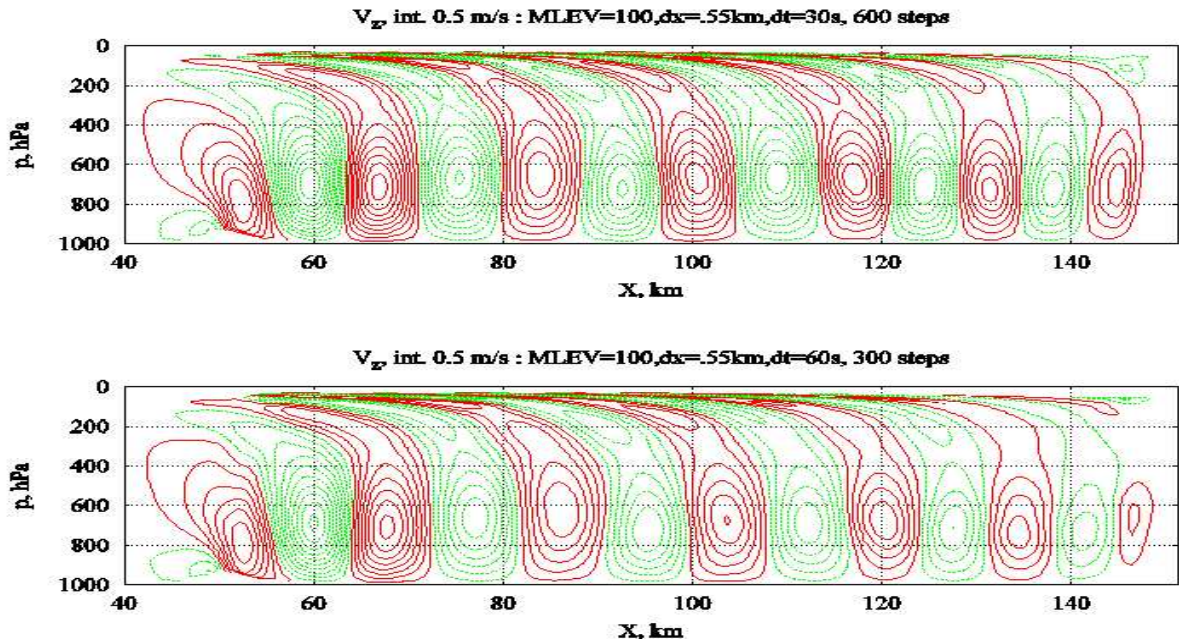


**Fig. 2.**

*Vertical velocity waves (isoline interval 0.5 m/s) at stationary flow over Agnesi ridge. Top:  $\Delta t = 30$  s, bottom:  $\Delta t = 60$  s.*

### 3.2 Time-step estimates

There is no strict upper limit for the accessible time-step  $\Delta t$  in NH SISL model. In the table, estimations of maximum reliable time-step are presented.

$Max U,$ [m/s]	$T(p)$	$\Delta x,$ [km]	$\Delta t_{cr} = \frac{\Delta x}{U}$ [min]	$\Delta t$ [min]	$\Delta t/\Delta t_{cr}$	parcel path (max), [km]
40	const	5.5	2.3	4.6	2.0	11
55	real	5.5	1.67	4.0	2.4	13.2
40	real	2.2	0.92	2.8	3.0	6.6
42	real	0.55	0.22	1.0	4.6	2.5

As one can conclude, (1) the efficiency of the model is comparable with the HS case at low resolutions; (2) the efficiency of the model increases in terms of the ratio  $\Delta t/\Delta t_{cr}$  with the resolution increase.

### 3.3 Real-condition experiments

The NH SISL adiabatic core was investigated in two cases: In mountainous region with resolution 5.5 km and in lowland conditions with resolution 3.3 km.

#### 3.3.1 Norwegian experiment (mountains)

The resolution is 5.5 km, grid size is 156x156 points, 31 levels. The reference HIRLAM is v5.0.0, physics is switched on. Forecast period is 24 h, and the time step is 4 minutes.

The model check is carried out through comparison with forecast results by HS SISL model in identical conditions. As Fig. 3 demonstrates, the surface pressure of NHY model is  $\sim 1$  mb higher on the lowlands and over the sea, and  $\sim 1$  mb lower on the mountain-tops.

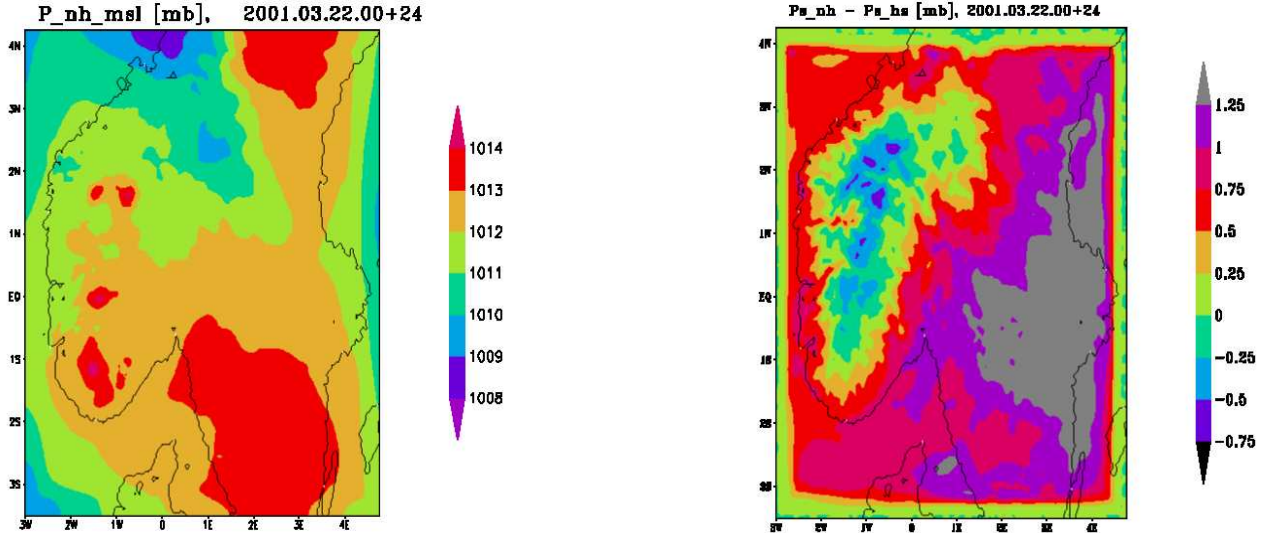


Fig. 3.

Mean sea-level surface pressure in 24 h Norwegian forecast with 5.5 km resolution and 4-minute time-step. Left: Mean sea level pressure; right: Surface pressure difference from the HS SISL results

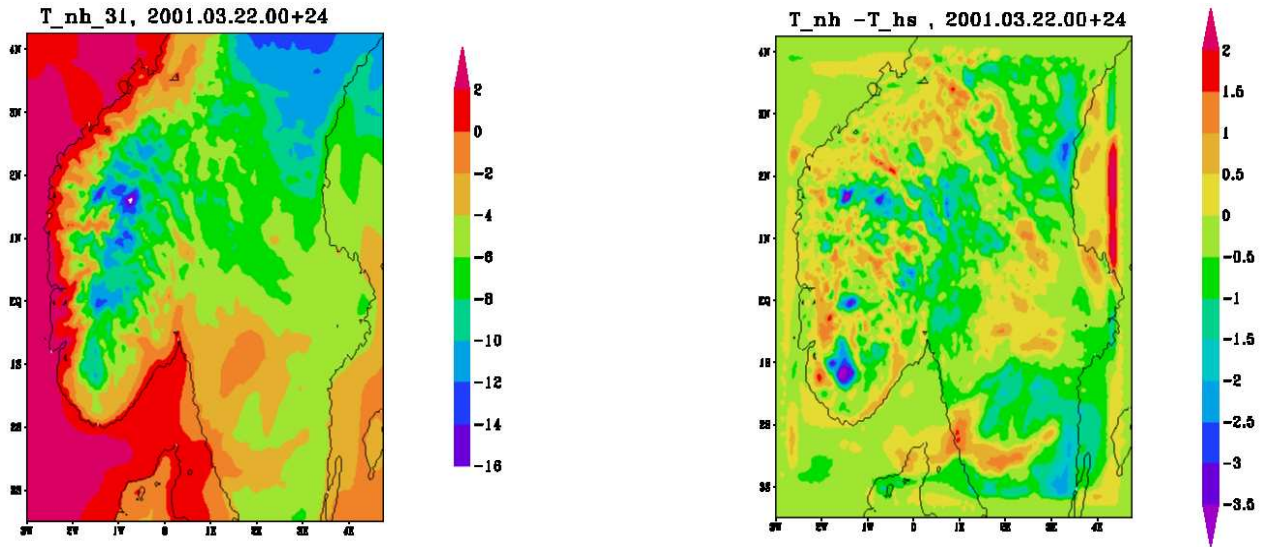


Fig. 4.

10 m temperature in 24 h Norwegian forecast with 5.5 km resolution and 4-minute time-step. Left: Temperature; right: Temperature difference from the HS SISL results

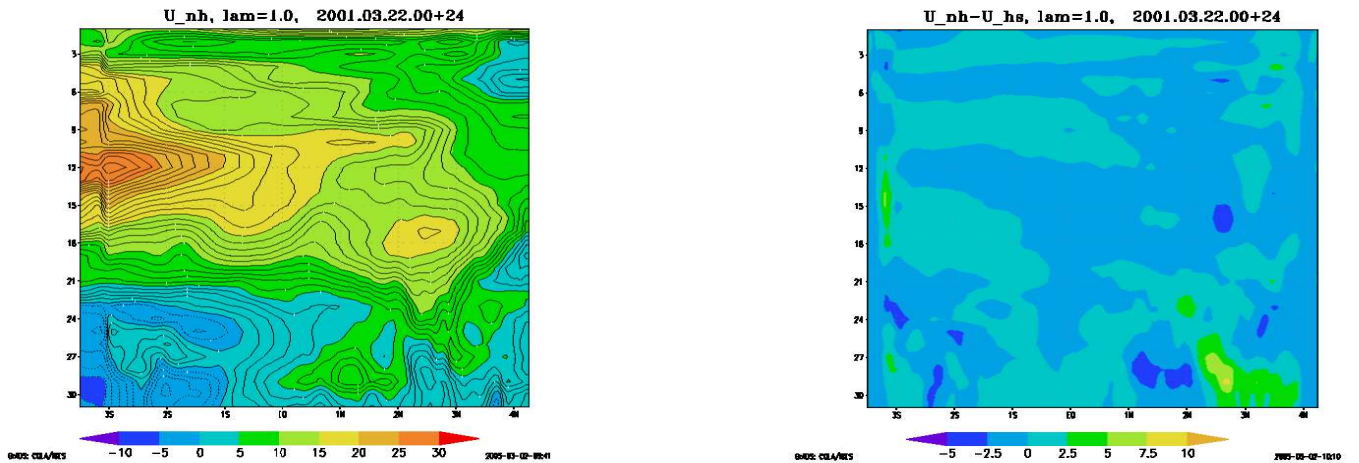


Fig. 5.

Vertical cross-section of the wind component  $U_x$  in 24 h Norwegian forecast with 5.5 km resolution and 4-minute time-step. Left: Vertical cross-section of  $U_x$ ; right: Departure of  $U_x$  from the corresponding HS SISL wind

The forecasted 10-m temperature (Fig. 4) does not differ from HS SISL results more than  $\sim \pm 0.5$  C.

However, the local differences in forecasted wind fields are substantial and may reach 10 m/s by amplitude. This is explained by slightly different placement of steep local fronts of wind fields in HS and NH models.

### 3.3.2 Estonian B-area experiments (lowlands)

Experiments similar to the previous case, were carried out with NH SISL core, implemented with the Reference HIRLAM 6.1.0, physics included, for of 3.3 km resolution Estonian B-

area. The grid in this case was 186170 points, 40 levels in vertical. The former Eulerian SI model grid was 104x100 points here. Thus, the increase in the forecast area due to implementation of SI SISL scheme is about 3.3 times. In Fig. 6, the 36 h MSL surface pressure and lowest level temperature are presented. The time-step in this experiment was 1.5 min (90 s). However, model remains stable and produces the same forecast with time step 2.5 min (150 s) also.

The differences with the HS SISL model do not exceed in the current lowland case  $\pm 0.3$  mb in surface pressure,  $\pm 0.5$  C in the lowest level temperature fields.

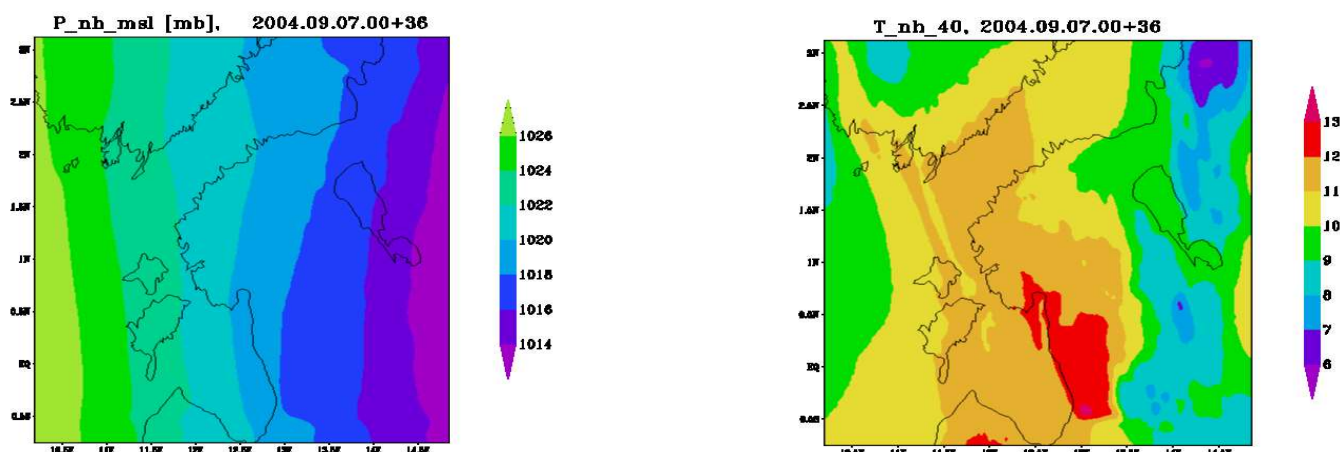


Fig. 6.

*Mean sea-level surface pressure (left) and lowest level temperature (right) 36 h forecasts in Estonian B-area domain.*

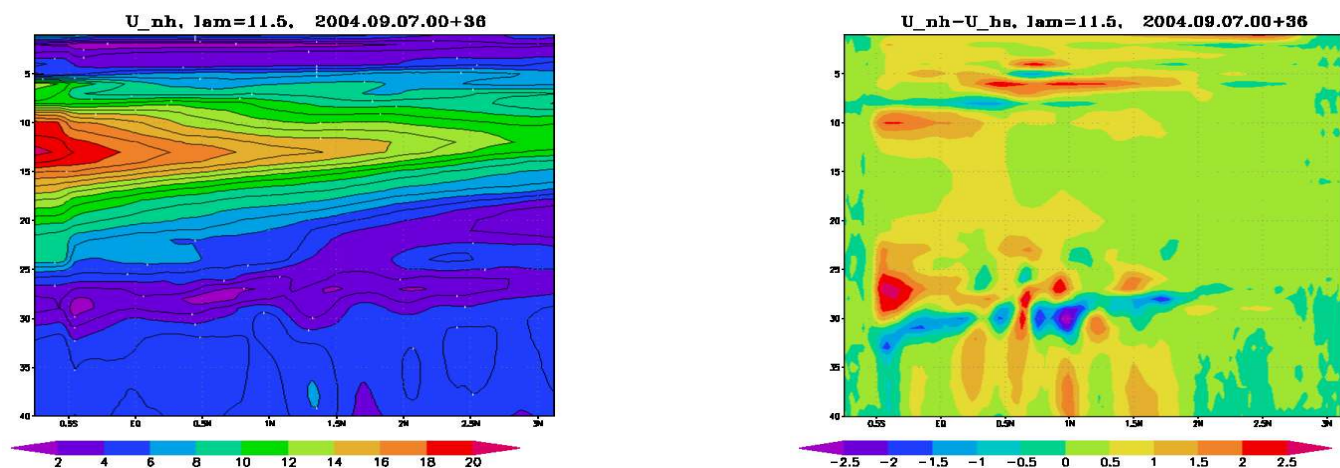


Fig. 7.

*Vertical cross-section of the wind component  $U_x$  in 36 h Estonian B-area forecast with 3.3 km resolution and 1.5-minute time-step. Left: Vertical cross-section of  $U_x$ ; Right: Departure of  $U_x$  from the corresponding HS SISL wind*

## 4 Conclusions

We consider the NH SISL development as the completed task:

- The stability and the time step characteristics of the new model are reasonable.
- Comparison with theoretical results (mountain flows), as well as with other models (NH Euler, HS SISL) shows that NH SISL is reliable and ready for applications.
- The computational efficiency increase is substantial.

Currently, the NH SISL is implemented as the adiabatic core in Estonian B-area (3.3 km resolution, grid 186x170, 40 levels, physics of HIRLAM 6.1.0) and the statistical testing is activated. As the experimentation experience reveals, the NH-specific effect is moderate at these resolutions for the given physical parameterization and lowlands condition. More NH behavior will be expected at higher resolutions (0.5 - 1km, 100 levels) with explicit moist convection physics and complex orography. NH SISL will be a suitable tool for physics development (complex terrain, boundary layer, moist convection) at these very high spatial resolutions.

## 5 References

Männik, A. and R. Rõõm, 2001: Non-hydrostatic adiabatic kernel for HIRLAM. Part II: Anelastic, hybrid-coordinate, explicit-Eulerian model. *HIRLAM Technical Report*, **49**, 54p.

Rõõm, R., 2001: Nonhydrostatic adiabatic kernel for HIRLAM. Part I: Fundamentals of nonhydrostatic dynamics in pressure-related coordinates. *HIRLAM Technical Report*, **48**, 26p.

Rõõm, R. A. Männik, 2002: Nonhydrostatic adiabatic kernel for HIRLAM. Part III: Semi-implicit Eulerian scheme. *HIRLAM Technical Report*, **55**, 29p.

McDonald, A., 1995: The HIRLAM two time level, three dimensional semi-Lagrangian, semi-implicit, limited area, gridpoint model of the primitive equations. HIRLAM Technical Report No. 17. Norrköping, 1995, 25 pp.

McDonald A., J.-E. Haugen, 1992: A two-time-level, three-dimensional, semi-lagrangian, semi-implicit, limited-area gridpoint model of the primitive equations. *MWR* **120**, 2603 - 2621.

# A brief review of some key issues related to the modelling of cloud and precipitation

Bent H. Sass

Danish Meteorological Institute

## 1. Introduction

When modeling clouds and precipitation in atmospheric forecast models it is important to ask the following questions:

1) Can it be quantified from observations that the mesoscale structure of precipitation is significant ? The answer is : Yes

2) Can we summarise typical weaknesses and/or limitations of the methods for cloud and precipitation prediction used in the operational weather prediction models ?

3) Which modelling strategies for high resolution are expected to lead to increasingly realistic operational schemes in the coming years ?

The answers to 3) will appear as concluding remarks after answering 1) and 2).

## 2. Examples of mesoscale precipitation features

The influence of orographic features is well established, not only for high mountains, but also for small hills with a height of less than 50 m. For example, Tor Bergeron writes in Uppsala report No. 6 (1968): "Unexpectedly, small orographic features are reflected in the fine structure of rainfall distribution" (averaged over months). Only a 20m -30m plateau in the Uppsala field is needed to produce approximately a 20 % precipitation increase.

Other studies have pointed to significant mesoscale structures of precipitation. For example, Austin and Houze ( J. Appl. Meteor.,925-935 , 1972) in a study of 9 storms in New England concluded that different scales can be identified, from a 'synoptic scale' (100 km \* 100km) down to small mesoscales of 3km \* 3km. The associated time scales range from typically 24h to 0.5h , respectively. The associated peak precipitation rates increase as the scale is reduced, and heavy rain is observed in both stratiform and showery conditions.

Recently very fine scale structures of precipitation (typically 20-30 % variation) has

been measured in Denmark with 9 rain gauges of the same design evenly spaced over a 500m by 500m flat field. The measurement campaign took place over a period of 65 days during Autumn 2003 (for details see <http://www.exigo.dk/project/summary>).

### **3. Model uncertainties/weaknesses**

Uncertainties exist in the current HIRLAM physics (and in other models) concerning the following processes:

#### **3.1. Microphysics**

The formation of ice clouds in the atmosphere has little relation to ice saturation and the onset of cloud formation is complicated (concentration and the type of ice nuclei vary across the globe). A lot of research activities exist, e.g. a COST 723 action ([www.cost723.org](http://www.cost723.org)). In HIRLAM a modified cirrus cloud formation has been implemented recently. Is there a need for further updates ?

Some presently used parameterizations might be too inaccurate, and more detailed microphysics will then be needed. Is it relevant to explicitly forecast droplet/particle size distributions in the near future ?

#### **3.2. Turbulence and convection**

The CBR turbulence scheme with conserved moist variables has recently been tested. It provides a better description of the vertical moisture transports in stratus/stratocumulus conditions (e.g. ASTEX), but has difficulties to describe cloud fields for shallow cumulus situations such as BOMEX where the convection scheme takes well care of the vertical transports (has been verified in 1D-HIRLAM simulations with 'moist' CBR and STRACO cloud scheme).

The ideal assumptions connected to convection schemes break down at (very) high horizontal resolution of meso-scale models, but the use of convection schemes might still be desirable (as indicated above), provided that they are used with care (conditionally). Research is probably still needed to optimise the use of convection schemes at very high resolution.

There are still uncertainties about the triggering of convection, that is, how to parameterize the fluctuations of momentum, heat and moisture responsible for initiation of convection.

Assumptions of 'instantaneous' precipitation fallout in the vertical air column becomes increasingly unrealistic at high horizontal resolution due to the actual drift of precipitation with the wind. This effect can easily account for horizontal displacements of more than 10 km, especially for drifting snow.

### 3.3. Dynamics

Hydrostatic model dynamics is expected to be less realistic than non-hydrostatic dynamics at grid sizes below about 5 km. - Furthermore, if it is a general problem to describe convective cloud cover (and vertical humidity transports) for shallow cumulus conditions from turbulence physics alone (no convection scheme used), does this mean that a reasonable description of shallow cumulus requires explicit dynamics of a LES model ? (e.g. about 100 m or less ). The answer depends to some extent of the turbulence scheme used and of the cloud parameterization in use.

### 4. Tentative recommendations

The following tentative recommendations are made, based on the discussion above:

- 1) Continue to make high quality ‘physiographic databses’, partly because stationary forcing (e.g. from orography) shows up in observed precipitation statistics (also very small scale orography has impact).
- 2) Introduce ‘prognostic’ 3D precipitation fields with several hydrometeors (rain, snow, etc.) to avoid unrealistic fallout of precipitation.
- 3) For a given model resolution investigate whether the vertical and horizontal humidity transports can be adequately described by the turbulence parameterization and the dynamics. -If not, continue to develop and use a convection scheme for high resolution, perhaps even at finer scales than 2 km. More restricted use of the convective parameterization is likely at such high resolution.

The observations showing precipitation variability at scales down to about 100 m indicate that very fine scale dynamics on the ‘turbulent scale’ is playing a role to explain this. A formulation of 3-dimensional turbulence is a natural framework to incorporate these variations. In a real forecasting system a probabilistic component will probably be needed as an additional tool to describe the high variability of the precipitation intensity in space and time.

# Explicit Microphysics and Diabatic Initialization

Paul Schultz  
January 24, 2005

The presentations I gave at the NetFAM Workshop on Clouds and Precipitation are based on my work, and that of my colleagues, on the Local Analysis and Prediction System (Albers et al. 1996). Equations and graphics from the powerpoint presentation that accompanies this article will not be replicated here; the reader may find additional clarity by referring occasionally to the presentation material.

LAPS is a software package that ingests meteorological observations, creates hourly three-dimensional grids of state variables and clouds, and produces initialization grids for mesoscale models. LAPS is designed for efficiency, specifically to enable real-time numerical weather prediction on affordable computers. For example, it runs on AWIPS, which is the weather forecasting workstation used by the US National Weather Service in all of its forecast offices.

One very attractive reason for using high-resolution mesoscale models is to avoid using parameterizations of deep convection. Algorithms of this type detect conditions suitable for deep convection and then adjust the model's vertical profiles of moisture and temperature to resemble post-convective environments. Surface precipitation is diagnosed as a result of these adjustments. These methods can generate reasonable surface precipitation rates, but the convection is fixed in place (unless the forcing is moving as in the case of a front) because there is nothing the model can advect. Furthermore, there is no way to represent the nonhydrostatic effects that are crucial in steering and configuring deep convection. That is why explicit representation of deep convection is attractive. With explicit microphysics, cloud liquid is created in supersaturated grid boxes, which causes local warming by latent heat release, which causes vertical motions that initiate moist convective updrafts, quite like the sequence of physical processes in nature. As the updrafts continue to rise, they cool, more cloud liquid is generated, which eventually coalesces into rain. If the environment is cold enough, such processes as freezing of rain, generation of cloud ice, and aggregation of cloud ice into snow can occur. Precipitation species like rain and snow begin to respond to gravity, evaporate on the way downward, and may reach the surface. Convective downdrafts, cold pools, anvils, and nonhydrostatic storm steering all occur as a result of modeled processes, and require no additional parameterization. All these similarities to nature appeal to physical scientists who are motivated by the congruence of nature and algorithm.

Historically, explicit microphysics algorithms (e.g., Rutledge and Hobbs 1983; Lin et al. 1983; Reisner et al. 1998) have been associated with large computational burden. They were conceived as fortran manifestations of laboratory results and were coded primarily for faithfulness to theoretical treatments of how particles interact, collision efficiencies, measured rates of diffusion toward liquid and various ice surfaces, etc. This algorithmic complexity, and the associated compute load, was a daunting obstacle to those interested in using them for real-time applications. This motivated the development of the algorithm I call "NWP Explicit Microphysics", or NEM, although unfortunately it seems have been informally renamed to "Schultz microphysics" since the original paper (Schultz 1995). The NEM code is about 700 lines including comments, and is designed to be easy to read,

understand, and modify. Gains in efficiency were attained by using simple mathematical functions to replace more complicated formulas.

Although several mostly minor changes have been made since Schultz (1995), there was a major change made recently.

Weisman et al. (1997) document several problems associated with using all-explicit cloud physics (i.e., without a parameterization for deep convection) on grids not fine enough to resolve all moist convection. These problems include late initiation, excessive CAPE buildup, and excessive precipitation rates, often by a factor of two or more. This is because most explicit microphysics algorithms require 100% RH before cloud liquid begins to form. This prevents the model from generating boundary layer cumulus clouds in the preconvective environment. Although these clouds, like all liquid-water clouds, have in-cloud relative humidity of 100%, the saturated volume is quite small relative to grid boxes of 5 km or so; the grid-volume-average relative humidity may be as low as 80%. As a result, the model's earth surface gets direct sunshine while it should be shaded, at least partially. Another important effect of boundary layer cumuli is to release some of the CAPE that normally builds up in the morning boundary layer. The effect, then, is that the vertical mixing and latent heat release that is accomplished in nature by shallow cumuli is erroneously retarded. CAPE builds up artificially and the suppressed latent heat release is eventually aliased into the resolvable scale, which causes explosive and sudden vertical accelerations when condensation finally occurs. This can cause numerical "point-CISK", in which enormous updrafts cause surface pressure drops and straight-line surface winds of 50 m/s or more blowing directly into the updraft.

Thus, the recent change to the NEM algorithm is to allow condensation to occur in grid cells that are moist, but not saturated, and with low static stability. Saturation is still required in stable environments; i.e., conditions associated with stratiform clouds. Early tests show that the modeled convection is still late, but much less so, and still produces excessive precipitation, but much less so. The grid increment is also considered in determining the relative humidity threshold above which condensation can occur, so that a relatively fine grid (with  $\Delta x$  of 1-2 kilometers) uses a higher threshold than a coarser grid (with  $\Delta x$  of 10 or more kilometers).

The original HIRLAM microphysics package (Sundqvist 1978), which facilitates partial cloudiness, has recently been modified along the lines of Rasch and Kristjánsson (1998), and now incorporates consideration of grid-scale static stability.

By design, the water species represented in the NEM algorithm are similar to those analyzed by the LAPS cloud analysis, which enables straightforward model initialization with LAPS grids. However, there are additional steps required to ensure a successful model initialization with active clouds and precipitation processes, or diabatic initialization. For example, simply inserting nonzero mixing ratios of cloud liquid into the model will yield very bad results. Even if the grid box is saturated (or above NEM's threshold), any mixing with dry air will cause evaporation of the cloud liquid, then cooling, then subsidence warming, then more evaporative cooling, and eventually a synthetic downdraft precisely where a cloud was diagnosed. Thus, the paired additional steps of ensuring saturation in grid boxes with nonzero cloud liquid, and inserting upward vertical velocities in cloudy grid boxes, are required. Vertical velocities are estimated empirically in the LAPS cloud analysis, and the full 3D wind field is then variationally adjusted so that the initialized divergence field is

consistent with the diagnosed vertical motions. We refer informally to this procedure as “hot start” initialization.

Diabatic initialization of global models, which have grid resolutions that are coarse enough to require deep convective parameterization, is performed by adjusting the model fields of moisture, CAPE, and/or divergence so that the convective parameterization is triggered to produce observed surface rain rates (e.g., Kasahara et al. 1996). Surface rain rates are of little use in the diabatic initialization of fine-grid models using explicit microphysics, because surface precipitation is the result of 15-45 minutes of complex antecedent cloud dynamics. Instead, three-dimensional estimates of cloud properties are required, which is accomplished by using volumetric radar data, satellite data, and METAR reports of cloud bases and layers.

## References

- Albers, S.A., J.A. McGinley, D.L. Birkenheuer, and J.R. Smart, 1996: The Local Analysis and Prediction System (LAPS): Analyses of clouds, precipitation, and temperature. *Wea. Forecasting*, **11**, 273-287.
- Kasahara, A., J.-I. Tsutsui, and H. Hirauchi, 1996: Inversion methods of three cumulus parameterizations for diabatic initialization of a tropical cyclone model. *Mon. Wea. Rev.*, **124**, 2304–2321.
- Lin, Y.-L., R.D. Farley, and H.D. Orville, 1983: Bulk parameterization of the snow field in a cloud model. *J. Clim. Appl. Meteorol.*, **22**, 1065-1092.
- Rasch, P. J., and J. E. Kristjánsson, 1998: A comparison of the CCM3 model climate using diagnosed and predicted condensate parameterizations, *J. Climate*, **11**, 1587-1614.
- Reisner, J., R.M. Rasmussen, and R. Bruintjes, 1998: Explicit forecasting of supercooled liquid water in winter storms using the MM5 model. *Quart. J. Roy. Meteor. Soc.*, **124**, 1071-1107.
- Rutledge, S.A. and P.V. Hobbs, 1983: The mesoscale and microscale structure and organization of clouds and precipitation in midlatitude cyclones. VIII. A model for the "seeder-feeder" process in warm-frontal rainbands. *J. Atmos. Sci.*, **40**, 1185–1206.
- Schultz, P., 1995: An explicit cloud physics parameterization for operational numerical weather prediction. *Mon. Wea. Rev.*, **123**, 3331-3343.
- Sundqvist, H., 1978: A parameterization scheme for non-convective condensation including prediction of cloud water content. *Quart. J. Roy. Meteor. Soc.*, **104**, 677-690.
- Weisman, M.L., W.C. Skamarock, and J.B. Klemp, 1997: The resolution dependence on explicitly modeled convection. *Mon. Wea. Rev.*, **125**, 527-548.

# EXPERIMENTS WITH THE MESONH-AROME MICROPHYSICAL SCHEME AND EVALUATION BY REMOTE SENSING TOOLS

Jean-Pierre Pinty(\*), Jean-Pierre Chaboureau(\*),  
Evelyne Richard(\*), Frank Lascaux(\*) and Yann Seity(\*\*)

(\*) Laboratoire d'Aérodynamique, Observatoire Midi-Pyrénées, Toulouse, France

(\*\*) Météo-France, Toulouse, France

## 1. INTRODUCTION

The trend is now to develop new operational forecast systems for scales much lower than 10 km in order to better resolve mesoscale flows such as breezes, isolated storms, orographic flows and organized convective systems. Some of these projects, the Unified Model (UK MetOffice), the Local Model (DWD, Germany), WRF (NCAR-NOAA, USA), AROME (Météo-France), ALARO (ALADIN community), have already incorporated advanced features in NWP models. Among these are non-hydrostatic dynamics cores, turbulence schemes with 3D capabilities and multi phase microphysical schemes. Here we focus on the explicit resolution of clouds and precipitation at a few km scale for which standard and sometimes sophisticated microphysical schemes currently used in research mesoscale models could be adapted for NWP purpose.

Many operational NWP systems employ several techniques, semi-Lagrangian and semi-implicit numerical schemes or variational data assimilation schemes, which are far less popular in mesoscale models. This leads to new aspects in explicit cloud modeling. For the numerics, the traditional explicit, conservative, positive definite schemes tend to be substituted by two time level robust schemes to perform the temporal integration with large time steps. This question is crucial for the treatment of the sedimentation fluxes of precipitation which may fall from several levels in a single time step. Another debate is the desirable initialization of the water cycle in order to reduce the model spin up in the formation of cloud fields. Assimilation of cloudy satellite radiances and radar data is known to be a strong issue to obtain high resolution analyses of the cloud and humidity fields. Last, the development of verifying tools and the definition of new scores to appreciate the quality of nebulosity and ground precipitation forecasts are also foreseen.

---

*Corresponding author's address:* Jean-Pierre Pinty, Lab. Aérodynamique, OMP, 14 av. E. Belin, 31400, Toulouse, France; e-mail <pinjp@aero.obs-mip.fr>.

## 2. EXPLICIT CLOUD MODELING

### 2.1 Generalities

The clouds are at the origin of many interactions with the dynamics, the radiation, the surface properties, the aerosols, the chemistry and the atmospheric electricity. There are many cloud types to simulate. The fogs, the extended warm cloud sheets, the cirrus, the cumulus and the heavily precipitating clouds contain a wide range of particle size and particle habit. A numerical difficulty arises because the microphysical fields are sparse and discontinuous with sharp cloud boundaries. So it is important to realize that simulating the localization and persistence of the clouds and the generation of precipitation is still a difficult task.

A key-question in cloud modeling turns around the optimal number of different ice species to carry out and the way, number concentrations should be described. It is now commonly accepted that mixing ratios (mass of water scaled by the mass of dry air) lead to the simplest equations of conservation of the water substance. As the prediction of number concentrations critically depends on yet poorly known aerosol properties (activation and nucleation) this issue seems out of reach to NWP models for the moment. Most of mixed-phase microphysical schemes consider two variables for the water (cloud droplets and rain drops) and three variables for the ice phase (small ice crystals, unrimed or aggregated large crystals and a graupel, frozen rain, hail mixed category). Other combinations, including a separate prediction of snow and hail, have been also advocated as well as simplified schemes with a single non-precipitating and precipitating category of water but with additional assumptions.

Besides a limited number of water species, the microphysical schemes share many common features. The size distribution of the particles are described by a continuous parametric distribution law in the  $0 < D < \infty$  range, where  $D$  is a characteristic dimension (diameter of water drops). The mass-size and fall speed-size relationships are simple enough to enable analytical integrations. However all the

schemes suffer from uncertainties about bulk coefficients and about the representation of some processes. For example, the collision-sticking efficiencies of the collection kernels of ice-ice interactions are poorly known. Many questions concern the treatment of the autoconversion processes that govern the onset of precipitating particles. The common practice of adjustment to saturation in mixed-phase clouds is also questionable.

## 2.2 The MESONH microphysical scheme

In its essence, the MESONH scheme follows the approach of Lin et al. (1983) that is a three-class ice parameterization coupled to a Kessler's scheme for the warm processes. The scheme predicts the evolution of the mixing ratios of six water species:  $r_v$  (vapor),  $r_c$  and  $r_r$  (cloud droplets and rain drops) and  $r_i$ ,  $r_s$  and  $r_g$  (pristine ice, snow/aggregates and frozen drops/graupels defined by an increasing degree of riming). The concentration of the precipitating particles is parameterized as in Pinty and Jabouille (1998) with a total number  $N = C\lambda^x$ .  $\lambda$  is the slope parameter of the size distribution,  $C$  and  $x$  are empirical adjustments drawn from observations. The size distribution of the hydrometeors follows a generalized Gamma distribution:

$$\begin{aligned} n(D)dD &= Ng(D)dD \\ &= N \frac{\alpha}{\Gamma(\nu)} \lambda^{\alpha\nu} D^{\alpha\nu-1} \exp(-(\lambda D)^\alpha) dD \end{aligned} \quad (1)$$

where  $g(D)$  is the normalized distribution while  $\nu$  and  $\alpha$ , adjustable parameters ( $\nu = \alpha = 1$  gives the Marshall-Palmer distribution law). Finally, suitable power laws are taken for the mass-size ( $m = aD^b$ ) and for the velocity-size ( $v = cD^d$ ) to perform useful analytical integrations using the moment formula:

$$M(p) = \int_0^\infty D^p g(D) dD = \frac{\Gamma(\nu + p/\alpha)}{\Gamma(\nu)} \frac{1}{\lambda^p}, \quad (2)$$

where  $M(p)$  is the  $p^{\text{th}}$  moment of  $g(D)$ . A first application of (2) is to compute the mixing ratio  $\rho r_x = aNM_x(b)$ , where  $\rho$  is the air density. Table 1 provides the complete characterization of each ice categories and of the cloud droplets/raindrops.

The microphysical scheme is sketched in Diagram 1 where the colored boxes represent the different category of water substance. The pristine ice category is initiated by homogeneous nucleation (**HON**) when  $T \leq -35^\circ\text{C}$ , or more frequently by heterogeneous nucleation (**HEN**, the small ice crystal concentration is a simple function of the local supersaturation over ice). These crystals grow by water vapor deposition (**DEP**, see below) and by the Bergeron-Findeisen effect (**BER**). The snow phase is initiated by autoconversion (**AUT**) of the pristine ice crystals; it grows by deposition (**DEP**) of

water vapor, by aggregation (**AGG**) through small crystal collection and by the light riming produced by impaction of cloud droplets (**RIM**) and of raindrops (**ACC**). The graupels are produced by the heavy riming of snow (**RIM** and **ACC**) or by rain freezing (**CFR**) when supercooled raindrops come in contact with pristine ice crystals. According to the heat balance equation and to the efficiency of their collecting capacity, graupels can grow either in the (**DRY**) mode or in the (**WET**) mode when riming is very intense (as for hailstone embryos). In the latter case, the excess of non-freezable liquid water at the surface of the graupels is shed (**SHD**) and evacuated to form raindrops. When  $T \geq 0^\circ\text{C}$ , pristine crystals immediately melt into cloud droplets (**MLT**) while snowflakes are progressively converted (**CVM**) into graupels that melt (**MLT**) as they fall. The other processes are those described by the Kessler scheme: autoconversion of cloud droplets (**AUT**), accretion (**ACC**) and rain evaporation (**EVA**). Cloud droplets excepted, each condensed water species has a substantial fall speed so giving an integrated sedimentation rate (**SED**).

	$r_i$	$r_s$	$r_g$	$r_c$	$r_r$
$\alpha$	3	1	1	3	1
$\nu$	3	1	1	3	1
$a$	0.82	0.02	19.6	524	524
$b$	2.5	1.9	2.8	3	3
$c$	800	5.1	124	$3.2 \cdot 10^7$	842
$d$	1.00	0.27	0.66	2	0.8
$C$		5	$5 \cdot 10^5$		$10^7$
$x$		1	-0.5		-1

Table 1: Characteristics of water-ice categories.

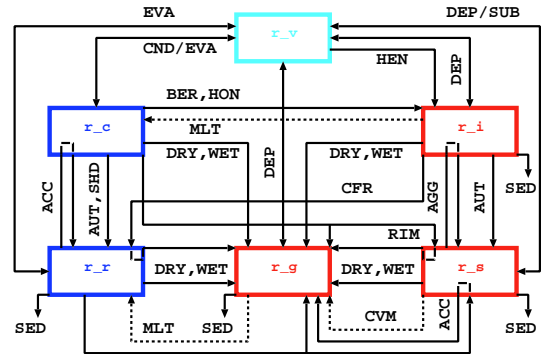


Diagram 1: Processes in the mixed-phase scheme.

The possible coexistence of cloud droplets and small ice crystals in mixed-phase clouds necessitates a careful treatment of the fast water vapor exchanges (**DEP** and **CND**). As is usually done, the "floating" water vapor saturation pressure  $r_{v,c,i}^{\text{sat}}$ , is defined

by a barycentric formula using the vapor saturation curves over water and ice and the mass amounts  $r_c$  and  $r_i$ , respectively. In the parameterization, the **DEP** and **CND** terms result from an implicit adjustment relative to  $r_{v,c,i}^{sat}$ , but with an original closure where any deficit/excess of  $r_v$  due to the adjustment, is compensated/absorbed by each condensed phase in proportion to its actual amount. The algorithm is non-iterative and 2<sup>nd</sup> order accurate.

The other processes that need a special attention are the collection processes. When non ( $r_c$ ) or very slowly ( $r_i$ ) precipitating categories are involved, the collection rates are computed analytically using the geometric sweep-out concept of the collection kernels defined for the large collecting particles (raindrops, snowflakes or graupels). When both interacting particles are precipitating, an analytical integration over the spectra is no longer possible and pre-tabulated kernels are used. For each ice-ice interaction, a major point of concern is the tuning of the sticking efficiencies which are still poorly understood functions of the temperature in most cases. After a series of experiments, the last set of coefficients retained by Ferrier et al. (1995) has been adopted. Finally, the microphysical processes are integrated one by one after carefully checking the availability of the sinking categories.

The detailed documentation of the scheme can be obtained at <http://aero.obs-mip.fr/mesonh/>.

### 3. EXAMPLES WITH MESONH/AROME

#### 3.1 Generalities

MESONH is a multi-purpose non-hydrostatic anelastic mesoscale model, jointly developed by Météo-France and Laboratoire d'Aérodologie (Lafore et al., 1998). It contains multiscale physical parameterizations to simulate academic and real flows with the grid-nesting technique. In addition and in order to facilitate the comparison between observations and model results, many diagnostics such as radar reflectivities or satellite images are available. This section illustrates the behaviour of the microphysical scheme of MESONH for real flow studies.

#### 3.2 The Gard flash flood experiment

The Gard flash flood event that occurred in the South of France on Sept. 8<sup>th</sup> 2002 was very devastating. A peak of 300 mm of accumulated precipitation was recorded by the Nîmes radar between 12-22 UTC (see Fig. 1a). The heavy rainfall found there are the result of a southerly flow over the Gulf of Lions (Mediterranean sea) which is forced to lift because of the Cevennes ridge in the south edge of the Massif Central. Obviously, there is a strong interest to simulate this extreme event at high resolution.

Several numerical experiments are performed for

this case study. Best results are obtained using ARPEGE analyses and additional mesoscale observations, such as mesonet surface observations, radar reflectivities, and Meteosat data (Ducrocq et al., 2002). Fig. 1b shows the cumulated rainfall as simulated by MESONH with a double grid nesting at 10 km and 2.5 km horizontal resolution. The boundary conditions are provided by 3 hour ALADIN forecasts. The comparison with the radar derived cumulated rainfall (Fig. 1a) shows a good agreement for the location of the precipitating area and a slight underestimation of the peak value. Previous experiments indicate that the relatively high quality of the present simulation is mostly due to the enhanced analyses at high resolution.

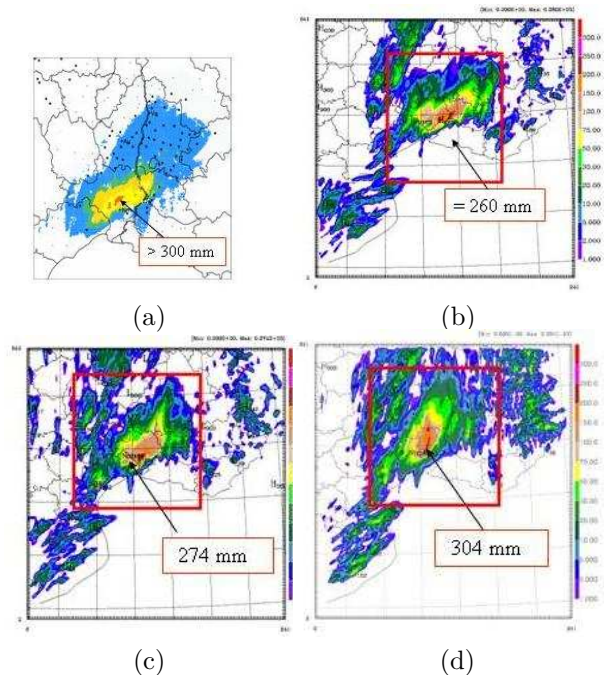


Figure 1: Gard experiment: a) 12-22 UTC Nîmes radar cumulated rainfall, b) MESONH with grid-nesting, c) MESONH as single model, d) AROME, 2.5 km simulations.

For comparison purpose, the simulation is redone by MESONH with a timestep of 4 s. but without grid-nesting and by an AROME prototype allowing for a larger timestep (60 s.). Both models are initialized the same way and run at 2.5 km resolution. For short the AROME version is based on the ALADIN dynamics but incorporates the physical package of MESONH without modification. Results are shown in Fig. 1c and 1d. The differences between the two MESONH simulations (Figs 1b and 1c) are attributed to the grid nesting. The first simulation performs slightly better for the location of the precipitating area while the peak value is improved in the second one. The AROME results shown in Fig. 1d compare reasonably well with those of MESONH but the orientation of the

rainy area pattern seems less accurate. A conclusion drawn from this test is that the microphysical scheme of MESONH is rather flexible and can be integrated with large timesteps as compared to the usual practice.

### 3.3 The "MAP" orographic precipitation

The MAP experiment was set up to study the flow across, above, around the Alpine bow and to relate the precipitation patterns to the fine scale orography (Bougeault et al. 2001). A field experiment with Intensive Observing Periods (IOP) took place during fall 1999 for which many numerical simulations were performed to evaluate quantitative precipitation forecasts at high resolution. The 2 km simulation domain shown in Fig. 2, encompasses the north of Italy and the south of Switzerland.

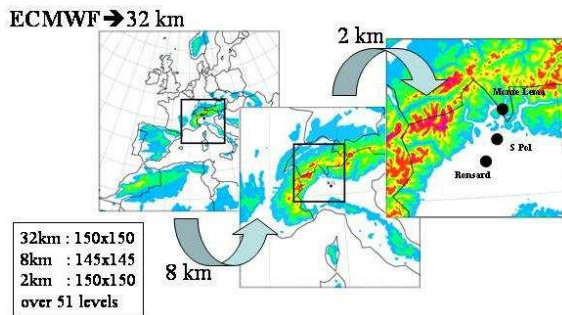


Figure 2: Configuration of MESONH for 3 level grid-nested simulations of MAP. Dots indicate radar locations.

Fig. 3 shows results obtained for the simulation of IOP2a at 2 km resolution. MESONH is initialized and takes boundary conditions from ECMWF analyses at 32 km. The simulation starts on sept. 17<sup>th</sup> 1999 at 12 UTC. At the end of the afternoon, a major squall line formed on the foothills of the southeastward facing slopes of the Lago Maggiore region in Italy and intensified during its propagation to the east as a three-dimensional convective cluster (Richard et al., 2003). This intense orogenic system with lots of lightning impacts and precipitation amounts of more than 70 mm in 6 hours, was well observed by the three radars. Two twin experiments are performed with MESONH for this case. In the first one, the standard microphysical scheme of MESONH is used while in the second one, an explicit hail category of ice is added. In the latter case, the formation of hail particles is derived from the **WET** and **DRY** growth modes of the graupels. Once formed hail grows exclusively in the **WET** growth mode. No reverse conversion to the graupel category is possible. Hailstones fall and melt into rain at a rate which is explicitly computed.

Examination of the radar reflectivity fields in Fig. 3 suggests that MESONH is able to timely capture the formation and displacement of the convective

system (similar "horseshoe" pattern at  $z = 2000$  m). Indeed it seems that considering hail as a fourth category of ice is beneficial in this case, at least to reproduce the high reflectivity cores at  $z = 6000$  m.

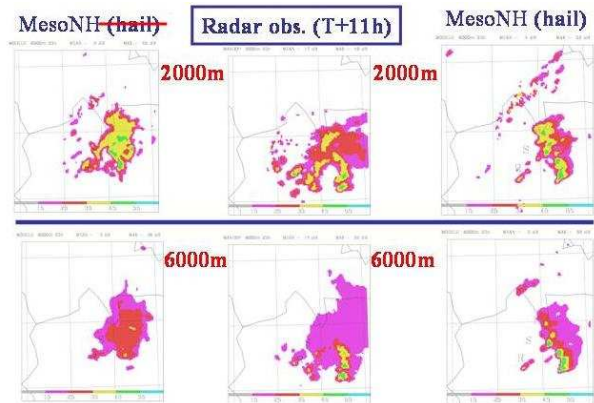


Figure 3: Radar reflectivity maps at  $z = 2000$  m (top) and at  $z = 6000$  m (bottom). Data are in the central column.

In order to illustrate the variable distribution of microphysical species on the vertical, the mixing ratios are averaged on the horizontal over the rainy areas. The left plot in Fig. 4 (IOP2a case) shows that the 1D profiles are those of deep convective clouds topping at 12 km with a remarkable stratification. The lightest particles (cloud ice) are aloft while the densest ones (hail) are peaking at 4 km high and even can reach the ground. The IOP2a vigorous convection case of MAP is in contrast with the IOP8 case showing a shallower precipitating system. In the IOP8 case on the right side of Fig. 4, snow is the dominant type of ice particle as in stratiform systems. These MAP numerical simulations let us to conclude that the microphysical scheme of MESONH is able to simulate very different types of precipitating clouds forming on the same area.

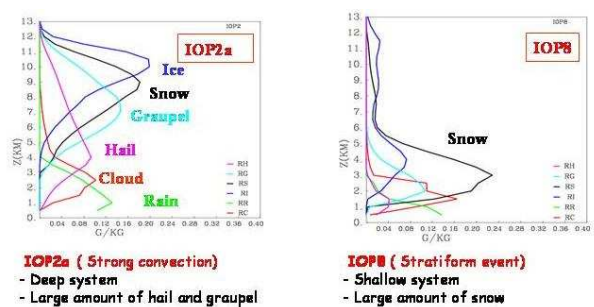


Figure 4: 1D vertical profiles of the horizontally averaged mixing ratios of IOP2a (left) and IOP8 (right) MAP cases.

### 3.4 Storms over Germany on Aug 12<sup>th</sup> 2004

MESONH is used to study a moving deep convective system which intensifies over the south of Germany. The simulation is performed with three

grid-nested models running at 40, 10 and 2.5 km resolution, respectively. Model results at 10 km scale are shown in Fig. 5. The purpose of this case study is to illustrate how multichannel satellite observations can be very powerful to pertain the quality of a simulation. The top row of Fig. 5 corresponds to satellite images with in order, the brightness temperature (BT) of the SEVIRI (MSG) 10.8  $\mu\text{m}$  IR channel, a BT difference between 10.8  $\mu\text{m}$  and 12  $\mu\text{m}$  (the split window technique to show up cirrus clouds) and the coincident microwave temperature at  $183 \pm 1$  GHz from AMSUB (NOAA15). As far as clouds are concerned, the plots picture the cloud top temperature, then the extent and opacity of high level clouds and finally the amount of large scattering particles of ice. The second row of Fig. 5 provides the corresponding simulation results obtained with the fast radiative transfer code RTTOV-7 (Saunders et al., 2002) using MESONH outputs valid for the same time 17 UTC (the simulation started at 00 UTC from the ECMWF analysis).

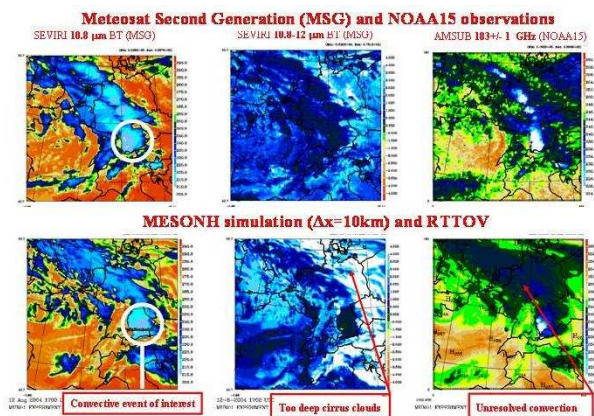


Figure 5: Satellite pictures from MSG and NOAA 15 (top row) and MESONH outputs with RTTOV (bottom row).

The first column of Fig.5 shows that the convective event of interest (circled in white) is well captured by MESONH. The high resolution model at 2.5 km is centered over this area. It is the feedback from this model to the 10 km one (two-way grid-nesting) which brings a significant contribution to the cloud field since at 10 km scale, most of the convection comes from the deep convection scheme. The central column reveals a bias of bright  $\Delta\text{TB}$  in MESONH suggesting that the model tends to produce too much ice in the upper levels. This feature can be easily circumvented by readjusting the ice autoconversion parameterization as shown by Chaboureaud et al. (2002). The last column of Fig. 5 provides an indication of the presence of large ice particles, snow or graupel. The detection of these particles is efficient for the part of storm over the south of Germany. However the bright spots tracing the convective bow in the AMSUB data are not

present in the picture deduced from MESONH. The reason is again that convection is not explicitly resolved so without feedback from a high resolution model at these locations, the amount of snow and graupel is poorly estimated. The unresolved clouds of the deep convection scheme are transparent in our RTTOV-7 implementation for the moment.

#### 4. CONCLUSION

The study reports results obtained with the microphysical scheme developed in the French mesoscale model MESONH. Several meteorological cases are simulated at high resolution, down to the 2 km scale. The results show that the microphysical scheme coupled to MESONH or to AROME is able to capture an extreme precipitating event. Other experiments made for a variety of precipitating systems over orography and for a deep convective event confirm the benefit of explicit cloud modeling. The last point to mention is that many data are now available from ground radars and spaceborne sensors. In this context, the extensive use of these data is the coming step in explicit cloud modeling.

#### 5. REFERENCES

- Bougeault, P., P. Binder, A. Buzzi, R. Dirks, R. Houze, J. Kuettner, R. B. Smith, R. Steinacker, H. Volkert and all the MAP scientists, 2001: The MAP special observing period. *Bull. Am. Meteor. Soc.*, **82**, 433-462.
- Chaboureaud, J.-P., J.-P. Cammas, P. J. Mascart, J.-P. Pinty, and J.-P. Lafore, 2002: Mesoscale model cloud scheme assessment using satellite observations. *J. Geophys. Res.*, 107(D16), 4301, doi:10.1029/2001JD000714.
- Ducrocq, V., D. Ricard, J.-P. Lafore, and F. Orain, 2002: Storm-scale numerical rainfall prediction for five precipitating events over France: On the importance of the initial humidity field. *Wea. Forecasting*, **17**, 1236-1256.
- Ferrier, B. S., W.-K. Tao, and J. Simpson, 1995: A double-moment multiple-phase four-class bulk ice scheme. Part II: Simulations of convective storms in different large-scale environments and comparisons with other bulk parameterizations. *J. Atmos. Sci.*, **52**, 1001-1033.
- Lafore, J.-P. et al., 1998: The Meso-NH Atmospheric Simulation System. Part I: adiabatic formulation and control simulations. Scientific objectives and experimental design. *Ann. Geophys.*, **16**, 90-109.
- Lin, Y.-L., R. D. Farley, and H. D. Orville, 1983: Bulk parameterization of the snow field in a cloud model. *J. Climate Appl. Meteor.*, **22**, 1065-1092.
- Pinty, J.-P. and P. Jabouille, 1998: A mixed-phase cloud parameterization for use in a mesoscale non-hydrostatic model: simulations of a squall line and of orographic precipitation. In *Conf. on Cloud Physics*, Everett, WA. Amer. Meteor. Soc., 217-220.
- Richard, E., S. Cosma, P. Tabary, J.-P. Pinty, and M. Hagen, 2003: High-resolution numerical simulations of the convective system observed in the Lago Maggiore area on 17 September 1999 (MAP IOP 2a). *Quart. J. Roy. Meteor. Soc.*, **129**, 543-563.
- Saunders, R., Brunel P., Chevallier F., Deblonde G., English S., Matricardi M., and Rayer P., 2002: RTTOV-7 science and validation report. Met Office Tech. Rep. FR-387, 51 pp.

# Performance of Kain-Fritsch/Rasch-Kristjansson in Hirlam. A review

Javier Calvo, INM, Spain

## 1 Introduction

Different studies about the performance of a new moist physics package in Hirlam have been carried out over the last years. The package includes three new components for Hirlam: Kain-Fritsch (KF) convection, Rasch-Kristjansson (RK) large scale condensation and microphysics and a diagnostic cloud fraction scheme. The new scheme is included in the Hirlam reference system as an option since September 2004. The aim of this paper is summarizing the main findings of these studies. The results of the new scheme (hereafter, KFRK) are compared with observations and with the results obtained using the reference moist physics scheme.

## 2 The reference scheme

The reference scheme in Hirlam, known as STRACO, is described in Sass (2002). Convection is of Kuo type and microphysics follows Sundqvist ideas. The scheme tries to accomplish smooth transitions between convective and large scale regimes, includes some treatment of shallow convection and sets some resolution depending tuning. Most current Hirlam components have been developed using this scheme and it is the scheme used in most Hirlam operational implementations.

## 3 Components of the new moist package

### *(a) Kain-Fritsch convection*

The scheme is described by Kain and Fritsch (1990, 1993). It has been mostly developed and used within the MM5 community. Many studies have shown that KF is specially suitable for mesoscale middle-latitude simulations (10-30 km resolution) including severe weather phenomena. There is a long operational experience using the scheme over the USA (MM5, Eta model and WRF model).

There is a completely recoded version of KF (Bechtold et al, 2001) which has been extensively tested in the Météo-France research model MesoNH, giving realistic systems from synoptic scales to Cloud Resolving Model (CRM) scales. In Météo-France operational models, ARPEGE-ALADIN, this scheme has not been able to improve the reference convection (Bougeault, 1985).

In Hirlam we use a version close to the Eta model KF convection. The main differences concern the treatment of shallow convection with a Turbulent Kinetic Energy (TKE) closure. It was implemented by C. Jones using J. Kain's code. Some of the updates to KF described by Kain (2004) are not included in the Hirlam implementation.

### *(b) Rasch-Kristjansson large scale condensation and microphysics*

The Hirlam implementation by Ødegaard (1998) is based on the Community Atmospheric Model (CAM) code as described by Rasch and Kristjánsson (1998) with some tuning modifications. A

slightly different code is currently used in the CAM model (Zang et al, 2003).

### *(c) Diagnostic cloud fraction*

Large scale clouds basically depend on relative humidity (RH) loosely following Slingo (1987). Marine stratocumulus (Sc) also depend on static stability. Convective clouds are function of the parameterized mass-flux following Xu and Krueger (1991). A treatment for the 'passive clouds' associated with shallow convection is include as described by Jones and Sánchez (2002): they depend on resolved RH and cumulus (Cu) cloud water vapor and condensate. There is memory of shallow clouds (they may prevail the active clouds) and they may generate precipitation through large scale microphysics.

## **4 Single Column Model cases studies from the EUROCS project**

The aim of EUROCS project was to improve the representation of clouds in climate and weather prediction models. It tried to cure systematic errors in the models by designing idealized cases based on observations, by comparing Single Column Models (SCM) and Cloud Resolving Models (CRM), and by evaluation of the developments in the complete models. A special issue with the main findings of the project has been published in the *Q. J. R. Meteorol. Soc* (October 2004 Part C)

### *(a) Diurnal cycle of Stratocumulus over ocean*

Stratocumulus (Sc) clouds are not represented correctly in climate and weather prediction models. Over tropical oceans, cloud cover and liquid water path (LWP) associated with these clouds are greatly underestimated which leads to a significant understimation of the short-range radiation reaching the ground. A EUROCS case was design to address this problem (Duynderke et al, 2004). SCM tended to produce too thin clouds and with cloud tops lower than observations and Large Eddy Simulation models (LES). Cloud top entrainment was a key issue to represent correctly these clouds. Within this EUROCS exercise, the implementation of more sophisticated turbulence schemes has been able to improve the results significantly. Hirlam showed similar results with KFRK and STRACO: lack or insufficient cloud top entrainment, drizzle acting to control liquid water and significant sensitivity to microphysics. The results improve significantly using a moist conservative turbulence scheme, explicit parameterization of cloud top entrainment and higher vertical resolution (Jones, 2004).

### *(b) Diurnal cycle of shallow cumulus over land*

Over land, shallow cumulus (Cu) greatly modify the radiation reaching the ground and play an important role preconditioning deep convection. A non-stationary case was designed to improve the parameterization of shallow Cu (Lenderink et al, 2004). Most common deficiencies in SCM are: too large values of cloud cover and LWP, unrealistic thermodynamical profiles and results too noisy. In Hirlam, the discrimination between shallow Cu and Sc seemed to be a problem which also happens in 3D simulations. For this case, the mass-flux approach (KF) describes better the growth and daily evolution of the clouds. An important improvement was achieved for KFRK including the 'passive clouds' associated with shallow Cu (Jones and Sánchez, 2002): these may reach 30 % cloud cover in contrast with 5 % of active clouds.

### *(c) Diurnal cycle of deep convection over land*

An idealized case was defined to address a common failure in the representation of the diurnal cycle of precipitation by atmospheric models: a tendency to produce precipitation too early in the day. The case was able to reproduce the problem (Guichard et al, 2004). In contrast with CRM simulations, SCM onset convection too early, they were not able to simulate the progressive

growth of the clouds and tended to produce a too moist boundary layer when downdrafts start. Compared with other SCM, Hirlam-KF did a reasonably good job, delaying the precipitation to noon and not producing a too moist boundary layer when downdrafts are onset.

## 5 Representation of the Hadley Circulation

This EUROCS intercomparison tried to assess the representation of clouds in climate and weather prediction models (Siebesma et al, 2004). Monthly means of model results along a trajectory over the Pacific were compared with satellite observations. Along this path, Sc, shallow Cu and deep Cu occur in a persistent and geographically separated manner. Most models strongly underpredict cloud cover and LWP in the Sc regions but overpredict them over the shallow Cu regions. Both Hirlam configurations, KFRK and STRACO, showed this behavior. Also, both schemes tended to produce too much light precipitation in the Sc and shallow Cu regions, a problem already noted in the SCM case studies. Discrimination between Sc and shallow Cu also seems to be a problem. The Intertropical Convergence Zone (ITCZ) was correctly located but convective clouds were underestimated. Over the ITCZ, STRACO as most models, tended to overestimate significantly the precipitation whereas KFRK gave values closer to observations.

## 6 A typhoon case study (COMPARE III)

An intercomparison exercise (Nagata et al, 2001) was established to assess the ability of weather prediction models to represent the explosive intensification of a typhoon (100 hPa in 3 days). The track prediction was relatively well predicted by the models giving the proper initial conditions but the intensity prediction seemed to remain been a difficult task. The increase of horizontal resolution was crucial to improve the intensity prediction. For Hirlam significant differences were found using STRACO and KFRK. Whereas the reference produces almost no deepening of the cyclone, even increasing the resolution, KFRK was able to reproduce qualitatively the intensification although greatly underestimating it. There are many ingredients contributing to the deepening as the partition between shallow and deep convection in the surroundings of the cyclone core or the surface flux formulation. In Hirlam a very important aspect is the partition between convective and large scale (explicit) condensation. Due to the strong rotation, we have slantwise convection in the core region. As slantwise convection is not explicitly parameterized, the model tends to treat it triggering the explicit condensation. However, this is not the case for STRACO where the precipitation is mostly convective in the cyclone core.

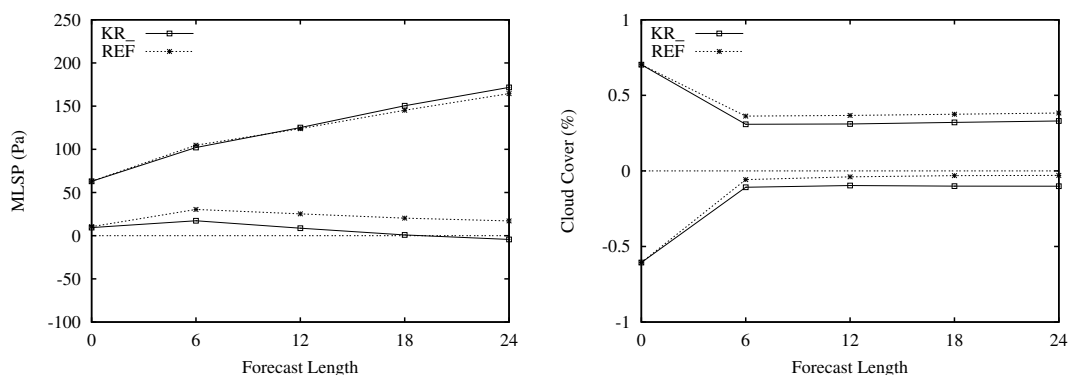


Figure 1: Objective verification against EWGLAM observations: RMSE and Bias of (a) Mean Sea Level Pressure, (b) cloud cover. REF/dash means reference STRACO and KR\_/solid means KF/RK

## 7 Case studies and parallel runs

Early studies comparing the new KFRK scheme with reference STRACO scheme, Finkele (2001), McGrath and Finkele (2001), Niemelä and Fortelius (2002), have shown little impact of the new scheme in terms of objective synoptic scores but more realistic simulation of cloud systems as seen by subjective evaluation. In a recent study by Calvo (2004) comparing an updated version of KFRK with reference STRACO for a period of three months over different seasons (see fig. 1 and 2), it was seen that the new scheme systematically improves the humidity profiles which leads to a better representation of the cloud cover. A slight deterioration of the mean sea level pressure field, probably due to tendency to deep too much the low pressure systems, is found in most studies. From the precipitation verification we have not seen big differences between the schemes except over Iberia where the new scheme improves the precipitation forecasts. This is probably related to the bigger contribution of convective regimes in this area. Besides, the new scheme tends to produce too much light precipitation (less than 1 mm/day). Concerning the computer cost, the KFRK forecast takes 10-20 % than the reference STRACO one. On vector computers the cost is higher and a vectorization is under way.

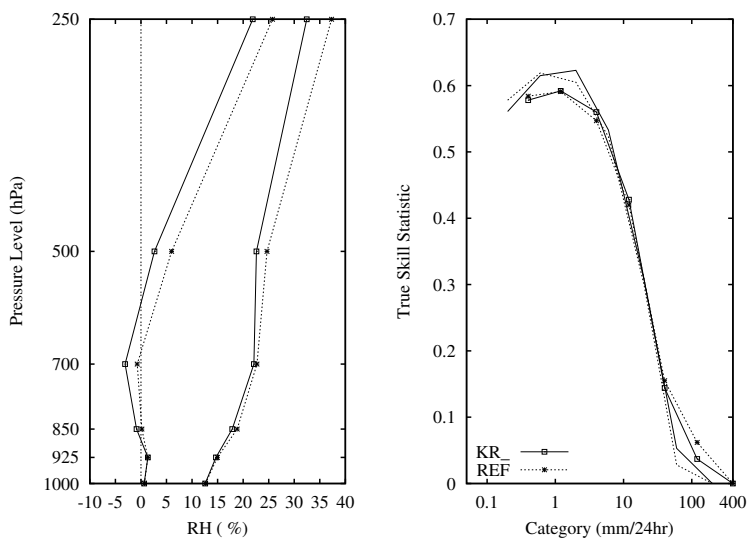


Figure 2: *Objective verification against EWGLAM observations: (a) RMSE and Bias of RH, (b) True Skill Score of precipitation for observations accumulated in 6 and 12 hr. REF/dash means reference STRACO and KR\_/solid means KF/RK*

## 8 Results from other studies

In a reanalysis exercise for one year, Fortelius et al (2002) showed that Hirlam-KFRK was capable of simulating the essential features of the energy and water cycle over the catchment area of the Baltic sea. This moist physics package is also used in a climate modelling version of Hirlam model (Rossby Center Atmospheric Climate Model). Jones et al (2004) showed that the model was able to simulate the recent climate and variability over Europe with a high degree of realism. In the Swedish Meteorological Institute (SMHI), Hirlam-KFRK at resolutions of 0.20 and 0.10 degrees is used for operational weather prediction. Duty forecasters seem to be very satisfied with the results (K.-I. Ivarsson, personal communication).

## 9 Conclusions and perspectives

A new moist physics scheme (KFRK) based on Kain-Fritsch convection and Rasch-Kristjansson large scale condensation scheme has been implemented in Hirlam. Here we have summarized the main findings of several studies from Hirlam researchers using this moist package. The system is able to produce realistic cloud systems and water cycle. The results have been compared with observations and with results using the reference STRACO scheme. It seems that the new scheme is able to improve the results in terms of humidity and cloud cover. An improvement in the precipitation forecast is found over the southern part of Europe (Iberia). The new scheme deteriorates slightly the mean sea level pressure field and the forecast takes 10-20 % more computer time than the reference system.

Now research focuses on improving the cloud fraction formulation: turbulence in moist conservative variables and statistical cloud scheme, controlling the over-prediction of light precipitation, and implementing more sophisticated microphysics: more cloud water species and more complex microphysics. Also we are optimizing the code for vector computers.

*Acknowledgments.* The KF convection was implemented in Hirlam by C. Jones for the RCA model based on J. Kain's code. RK was introduced by V. Odegard based on CAM's code. The operational experience at SMHI has been reported by K.-I. Ivarsson. The EUROCS project was partly funded by the European Commission.

## References

- P Bechtold, E Bazile, F Guichard P Mascart, and E Richard, 2001. A mass-flux convection scheme for regional and global models *Q. J. R. Meteorol. Soc.*, **127**,869–886
- P Bougeault, 1985. Simple Parameterization of the Large-scale Effects of Cumulus Convection *Mon. Wea. Rev.*, **113**,2108–2121.
- J Calvo, 2004. Progress on Kain-Fritsch/Rasch-Kristjansson *HIRLAM Newsletter*, **45**,176–183.
- P Duynkerke, S de Roode, M C van Zanten, J Calvo, J Cuxart, S Cheinet, A Chlond, H Grenier, P Jonker, M Köhler, G Lenderink, D Lewellen, C-L Lappen, A P Lock, C-H Moeng, F Miller, D Olmeda, J-M Piriou, E Sanchez, and I Sednev, 2004. Observations and numerical simulations of the diurnal cycle of the EUROCS stratocumulus case *Q. J. R. Meteorol. Soc.*, **130**,3269–3296.
- K Finkele, 2001. Simulation of a FASTEX storm at different resolutions. *HIRLAM Newsletter*, **37**,47–51.
- K Fortelius, U Andrae, and M Forsblom 2002. The BALTEX regional reanalysis project. *Boreal Env. Res.*, **7**,193–201.
- F Guichard, J C Petch, J-L Redelsperger, P Bechtold, J-P Chaboureau, S Cheinet, W Grabowski, H Grenier, C G Jones, M Köhler, J-M Piriou, R Taulleux, and M Tomasini, 2004. Modelling the diurnal cycle of deep precipitating convection over land with cloud-resolving models and single-column models. *Q. J. R. Meteorol. Soc.*, **130**,3139–3172.
- C G Jones, U Willen, A Ullerstig, and U Hansson, 2004. The Rossby Centre Atmospheric Model part 1: Model climatology and performance for the present climate over Europe. *Ambio*, **33**, 199–210.
- C Jones and E Sánchez, 2002. The representation of shallow cumulus convection and associated cloud fields in the Rossby Atmospheric Model (RCA). *HIRLAM Newsletter*, **41**,91–106.

- C Jones, 2004. Representing stratocumulus clouds in numerical models: Sensitivity to model physics and vertical resolution. *HIRLAM Newsletter*, **45**,168–175.
- J S Kain and J M Fritsch, 1990. A One-Dimensional Entraining/Detraining Plume Model and Its Application in Convective Parameterization. *J. Atm. Sci.*, **47**,2784–2802.
- J S Kain and J M Fritsch, 1993. Convective Parameterisation for Mesoscale Models: The Kain-Fritsch Scheme. In: The representation of cumulus convection in numerical models. Eds: K. A. Emanuel and D. J. Raymond. *AMS Monograph*, **46**,246p.
- J S Kain, 2004. The Kain-Fritsch Convective Parameterization: An Update *J. Appl. Meteor.*, **43**,170–181.
- G Lenderink, A P Siebesma, S Cheinet, S Irons, C G Jones, P Marquet, F Mller, D Olmeda, J Calvo, E Sánchez, and P M M Soares, 2004 The diurnal cycle of shallow cumulus clouds over land: A single-column model intercomparison study *Q. J. R. Meteorol. Soc.*, **130**,3339–3364.
- R McGraph and K Finkle, 2001 Verification of Kain-Fritsch/Rasch-Kristjánsson convection/condensation scheme. *HIRLAM Newsletter*, **38**,110–114.
- M Nagata, L Leslie, H Kamahori, R Nomura, H Mino, Y Kurihara, E Rogers, R Elsberry, B Basu, J Calvo, M Desgagné, S-Y Hong, J Katzfey, D Majewski, P Malguzzi, J McGregor, A Murata, J Nachamkin, M Roch, and C Wilson, 2001. A mesoscale model intercomparison: A Case of Explosive Development of a Tropical Cyclone (COMPARE III) *J. Met. Soc. Japan*, **79**,999–1033.
- S Niemelä and C Fortelius, 2002. Comparison of convection and condensation schemes under non-hydrostatic Hirlam model. A case study. *HIRLAM Newsletter*, **41**,125–130.
- V Ødegaard, 1998. Status of the implementation of the Rasch-Kristjánsson scheme in Hirlam *Proceedings of HIRLAM 4 Workshop on Physical Parameterization*, Madrid, Nov 1998.
- P J Rasch and J E Kristjánsson, 1998. A comparison of the CCM3 model climate using diagnosed and predicted condensate parameterizations. *J. Climatol.*, **11**,1587–1614.
- B H Sass, 2002. A research version of the STRACO cloud scheme. *DMI Technical Report*, **02-10**, Danish Meteorological Insititute. 1–25.
- A P Siebesma, C Jakob, G Lenderink, R A J Neggers, J Teixeira, E van Meijgaard, J Calvo, A Chlond, H Grenier, C Jones, M Köhler, H Kitagawa, P Marquet, A P Lock, F Mller, D C Olmeda, and C Severijns, 2004 Cloud representation in general-circulation models over the northern Pacific Ocean: A EUROCS intercomparison study *Q. J. R. Meteorol. Soc.*, **130**, 3245–3267.
- J M Slingo, 1987. The development and verification of a cloud prediction scheme for the ECMWF model. *Quart. J. Roy. Met. Soc.*, **113**,899–927.
- K Xu and S K Krueger, 1991. Evaluation of cloudiness parameterizations using a cumulus ensemble model. *Mon. Wea. Rev.*, **119**,342–362.
- M Zhang, W Lin, C Bretherton, J Hack, and P J Rasch, 2003. A modified formulation of fractional stratiform condensation rate in the NCAR Community Atmospheric Model (CAM2). *J. Geophys. Res.*, **108** ACL 10-1/11.

# Combining a Statistical Cloud Parameterisation and Moist Conservative Turbulence scheme in the HIRLAM model.

Colin Jones  
 Canadian Regional Climate Modelling Network  
 University of Quebec at Montreal  
 email : jones.colin@uqam.ca

## 1. Introduction and Motivation

The Rossby Centre Regional Climate Model (RCA) physics package is used at SMHI within the HIRLAM NWP system for short-range weather prediction. Within this physics package there can potentially be 3 active cloud fractions in a single grid box. These cloud fractions must be combined before being used for microphysical and radiation calculations. The 3 cloud fractions are:

1. Large scale (resolved) fractional clouds
2. Shallow cumulus cloud amounts, associated with parameterised shallow convection.
3. A cloud fraction associated with parameterised deep convection.

Each of these cloud types also has an independently generated cloud water amount. This makes a consistent treatment of clouds within the model physics package a difficult challenge.

Recently, a moist conservative turbulence scheme has been introduced into the physics package (Lenderink and Holtslag 2004) this builds on the original dry, prognostic turbulent kinetic energy (TKE) scheme due to Cuxart et al (2000). A key difference between the original dry TKE scheme and the new moist scheme is the need to calculate static stability and turbulent mixing lengths taking into account that a grid box may be partially cloudy. The vertical fluxes of heat, moisture and momentum are directly sensitive to the derived mixing lengths in the TKE scheme. These mixing lengths are highly dependent on the static stability in the model (see Lenderink and Holtslag 2004 and Bougeault and Lacarrare 1989 for more details). The static stability inside a cloud may be radically different to that in the surrounding clear sky regions, mainly as a result of latent heat release. This difference directly leads to the amount of turbulence and hence vertical transport being considerably larger inside clouds than in the surrounding clear air. Including this non-linear contribution to the subgrid scale vertical fluxes is a key motivation for introducing a moist version of the TKE mixing scheme. The static stability in a partially cloudy boundary layer can be expressed as a combination of the stability in the cloud free regions and in the cloudy portion of the grid box (Cuijpers and Dunkerkye 1993).

$$\frac{g}{\theta_v} \frac{\partial \bar{\theta}_v}{\partial z} \approx N^2 = c_f \left( A_m \frac{\partial \bar{\theta}_l}{\partial z} + B_m \frac{\partial \bar{r}_l}{\partial z} \right) + (1 - c_f) \left( A_d \frac{\partial \bar{\theta}_l}{\partial z} + B_d \frac{\partial \bar{r}_l}{\partial z} \right) \quad 1.$$

where  $c_f$  is the cloud fraction,  $\theta_l$  is the grid box mean liquid water potential temperature and  $r_l$  is the grid box mean total water mixing ratio. For the definition of the  $A$  and  $B$  terms refer to Cuijpers and Dunkerkye 1993.

The sudden formation of a cloud, or rapid increase in cloud fraction within a model grid box can lead to very rapid changes in the moist static stability and resulting vertical fluxes. Due to the central role cloud fraction now plays in the calculation of static stability and turbulent fluxes it is crucial that an accurate estimate of the cloud fraction be available in the TKE scheme. In the initial implementation of the moist TKE scheme, we used the resolved cloud fraction, diagnosed as a function of relative humidity, for calculating the moist static stability inside the TKE scheme. Due to the rapid nature of the turbulent fluxes and cloud fraction changes, this approach led to numerical instability in the model as the vertical resolution was increased. To alleviate this problem we implemented a calculation of cloud fraction (and cloud water) directly within the moist TKE scheme. The cloud fraction is estimated within the TKE scheme, using a statistical cloud approach following the original ideas of Sommeria and Deardorff (1977) and Mellor (1977). We implemented the parameterisation closely following the suggestions of Chaboureaud and Bechtold (2002), where the cloud fraction and diagnosed cloud water are functionally dependent on a single variable, the normalised grid box saturation deficit  $Q_1$ . The cloud fraction is expressed as:

$$C_f = \max \{0, \min [1, 0.5 + 0.36 \arctan(1.55Q_1)]\} \quad 2.$$

The need to introduce a statistical cloud fraction and cloud water estimate inside the turbulence scheme, potentially leads to a fourth cloud fraction within a model grid box. In this paper we assess whether the statistical cloud fraction approach is a suitable method for parameterising all cloud fractions (large scale, shallow and deep convective) and associated cloud water amounts and if these cloud terms can be used globally throughout the model physics (e.g as input to the cloud microphysical and radiation parameterisations). If this is the case, it would be possible to have a single, consistent treatment of cloud fraction and cloud water throughout the model physics. To assess this we have integrated a single column version of the HIRLAM model for a number of case studies that include typical subtropical oceanic stratocumulus, summer season shallow cumulus clouds and deep convective clouds and compared the cloud fractions and cloud water amounts diagnosed by the combined statistical cloud, moist turbulence approach to available estimates from Large Eddy Simulation (LES) models and Cloud Resolving Models (CRMs) and where possible direct observations.

## 2. Results

The normalised saturation deficit ( $Q_1$ ) describes the proximity to saturation of the model grid box, normalised by a measure of the subgrid scale variance of all terms (*moisture content and temperature*) contributing to local saturation conditions within a grid box.

$$Q_1 = \frac{\overline{r_i} - r_{sat}(\overline{T_l})}{\sigma_s} \quad 3.$$

$\sigma_s$  is the subgrid scale variance of terms contributing to the local variation of saturation conditions about the grid box mean value.  $r_{sat}$  is the grid box mean saturation mixing ratio, evaluated with respect to the grid box mean liquid water temperature ( $T_l$ )

$$\sigma_s = \left[ a^2 \overline{r_i^{n^2}} - 2abr_i^n \overline{T_l^n} + b^2 \overline{T_l^{n^2}} \right]^{1/2} \quad 4.$$

Figure 1 shows cloud fraction as a function of  $Q_1$ , diagnosed using equation 2, as suggested by Chaboureau and Bechtold (2002). When the grid box is just at saturation ( $Q_1=0$ ) cloud fraction is 0.5, at saturated conditions ( $Q_1>0$ ) cloud fraction rapidly increases to unity and for sub-saturated conditions ( $Q_1<0$ ), cloud fraction rapidly decreases to zero. Partial cloudiness is clearly very sensitive to the specification of the variance term appearing in the denominator of the expression for  $Q_1$ . In unsaturated conditions a large value of  $\sigma_s$  will allow fractional

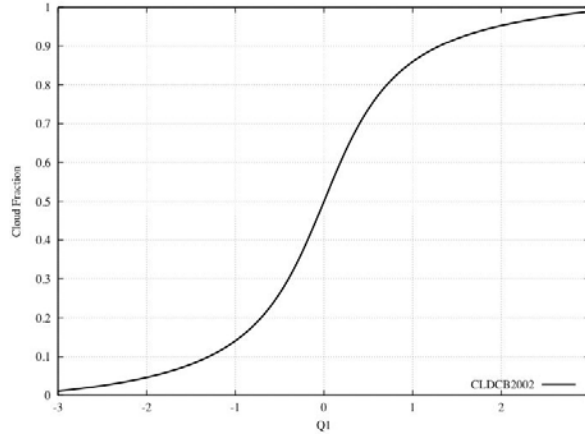


Figure 1. Cloud Fraction as a function of normalised saturation derived From equation 2, due to Chaboureau and Bechtold (2002)

cloudiness. Likewise, in saturated conditions a large value of  $\sigma_s$  will keep grid box mean cloud fractions below unity. The key term determining the quality of simulated cloud amounts and cloud water, using a statistical cloud scheme is the representation of the variance of saturation conditions about the grid box mean value ( $\sigma_s$ ). Here we parameterise this term as a combination of 3 assumed contributions.

1. A subgrid scale variation term associated with boundary layer turbulence
2. A term associated with convective scale variations
3. A value assumed to be related to subgrid scale mesoscale fluctuations in moisture and temperature within a model grid box.

## 2.1 Stratocumulus boundary layer clouds

Term 1 is parameterised in a manner analogous to the representation of down-gradient subgrid scale vertical transport in the model.

$$\sigma_{s_{turb}} = l_{tke} \left( a^2 \left( \frac{\partial \bar{r}_t}{\partial z} \right)^2 - 2abC_{pm}^{-1} \frac{\partial \bar{h}_t}{\partial z} \frac{\partial \bar{r}_t}{\partial z} + b^2 C_{pm}^{-2} \left( \frac{\partial \bar{h}_t}{\partial z} \right)^2 \right)^{1/2} \quad 5.$$

where  $h_t$  is the grid box mean moist static energy and  $l_{tke}$  is the diagnosed (moist) mixing length from the turbulence scheme. In this manner the diagnosed cloud fraction and cloud water amounts are directly linked to the amount of simulated turbulence.

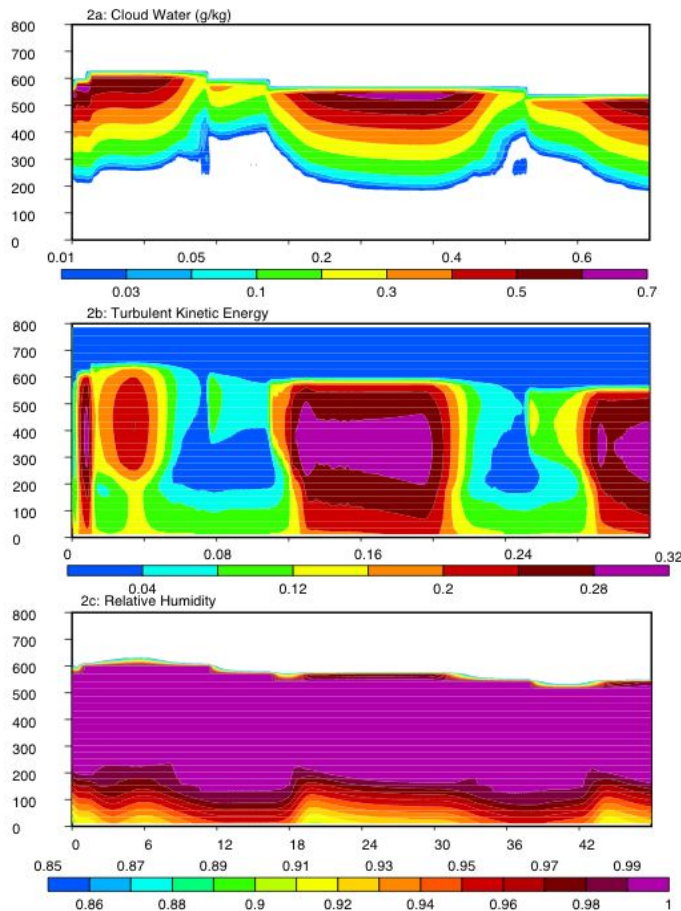


Figure 2. Time-height cross-section of the HIRLAM SCM simulated diurnal cycle of FIRE subtropical, oceanic stratocumulus clouds. X-axis shows local time with the model simulation beginning at local midnight. Y-axis is height in metres.

In a non-convective boundary layer, this estimate of the subgrid scale variation of saturation state appears sufficient to accurately simulate the evolution of this type of cloudy boundary layer. Figure 2 shows the simulated diurnal cycle of oceanic stratocumulus clouds, using the SCM version of the HIRLAM model incorporating the statistical cloud and moist TKE schemes. This case is based on a 2-day period of oceanic subtropical stratocumulus observed off the coast of California in 1987 during the FIRE campaign (Albrecht et al. 1988). It constituted a case study within the EUROCS project (EUROpean Cloud Systems Project, see Grabowski and Kershaw 2004), whereby a number of LES and SCM models simulated this diurnal cycle using a common set of large scale, external forcing terms. Results of these simulations can be found in Duynkerke et al (2004) and Chlond et al (2004). Figure 2 illustrates time-height sections of the simulated cloud water amounts, TKE and relative humidity for the case, using the moist TKE and statistical cloud scheme. The HIRLAM SCM was integrated with a vertical resolution of  $\sim 30\text{m}$  in the boundary layer.

Cloud fraction is simulated to be unity throughout the simulation, in agreement with LES models and observations (see Duynkerke et al 2004). Simulated cloud depth decreases during local afternoon, as do the cloud water amounts. This is a result of absorption of solar radiation within the cloud, leading to evaporation of cloud water. The heating, associated with the solar absorption within the cloud also leads to the development of a relatively stable layer close to the cloud base. As a result turbulent mixing is radically reduced (evidenced by the local minimum in TKE just below cloud base in the local afternoon) and the vertical flux of water from the surface required to maintain the cloud layer against depletion through solar absorption and subsidence is greatly reduced. By night, unbalanced long wave cooling generates negative buoyancy at cloud top and increased turbulence. This increases the vertical flux of water from the surface into the cloud layer and increases the cloud depth and cloud water amounts during the local night. Turbulence is simulated to be a maximum inside the cloud layer at night and the values of simulated TKE are in good agreement with LES simulated values (see Chlond et al 2004, their figure 8.). It is worth noting that during the local afternoon the relative humidity in the lowest model layer can reach 95% (see figure 2c), but no cloud is simulated by the statistical cloud scheme. This is in agreement with both observations and LES models, where a cloud base at  $\sim 300\text{m}$  is observed. The original relative humidity based cloud parameterisation would have placed a cloud in the lowest model layer given these relative humidities and thus would have (incorrectly) simulated the stratocumulus layer extending to the sea surface. Cloud-free conditions below 300m are simulated by the statistical cloud scheme during the afternoon, even with a grid box mean relative humidity of 95% ( $r_r - r_{sat}$  slightly negative (unsaturated) in equation 3), because the local static stability is very high and thus  $\sigma_s$  is small in the denominator of equation 3, leading to a large negative value of  $Q_1$  and zero cloud amounts from equation 2.

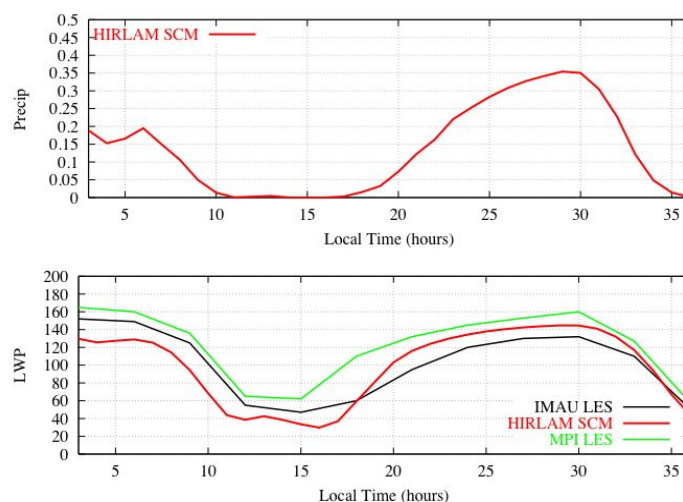


Figure 3. HIRLAM SCM (in red) simulated precipitation (mm/day) and Liquid Water Path (LWP) in mm, for FIRE stratocumulus case. Also shown are 2 simulations of the FIRE LWP (in Black and Green)

Figure 3 shows a time series of precipitation and integrated liquid water path (LWP) from the HIRLAM SCM simulation. LWP values agree quite well with typical LES values for the same case. A diurnal cycle of drizzle is

also simulated by the model with zero precipitation in the local afternoon and maximum rates of  $\sim 0.25$ mm/day at local night-time. Stevens et al (2003) observed frequent drizzle at a similar rate, from nocturnal oceanic stratocumulus clouds off the coast of California. The cloud water and cloud fraction diagnosed from the statistical cloud scheme were used as input into the cloud microphysical scheme, indicating that a smooth interaction between moist turbulence, statistical clouds and precipitation is feasible.

## 2.2 Shallow Cumulus Clouds

In the presence of convection, the variation of saturation conditions at the scale of a typical NWP grid box ( $\sim 20$ km) will increase. Localised regions of high humidity will be concentrated in the areas of convective ascent and regions of relative subsaturation in regions of convectively induced, compensating subsidence. In convective boundary layers the relative humidity is often below saturation, clouds occur as a direct result of the large variation of saturation conditions at the scale of a model grid box. To simulate partial cloudiness in a convective boundary layer it is necessary to include an estimate of the variance of saturation conditions associated with the convective scale motions. To do this we follow the suggestion of Lenderink and Siebesma (2000) and in the convective cloud layer relate the saturation variance term to the convective intensity (given by the parameterised convective mass flux) and the saturation excess/deficit of convective plumes relative to the local grid box conditions.

$$\sigma_{scu} = \left( \frac{M_{cu} (q_{1cu} - \bar{q}_1) C_{dep} \frac{\partial \bar{q}_1}{\partial z}}{\rho w_{pbl}^*} \right) \quad 6.$$

$w^*$  is a convective scale velocity and  $C_{dep}$  is the depth of convection simulated by the convective parameterisation. In convective boundary layers, the total variance of saturation conditions is assumed to be a combination of the variance due to boundary layer turbulence and that due to convective scale variations.

$$\sigma_s = \sigma_{sturb} + \sigma_{scu} \quad 7.$$

Figure 4 shows a SCM simulation of a typical diurnal cycle of shallow cumulus clouds over the ARM Southern Great Plains site during the summer IOP of 1997. This case has been extensively simulated by LES models (Brown et al 2002) and SCMs (Lenderink et al 2004). Figure 4 shows the simulated cloud fraction and cloud water amounts using the HIRLAM SCM with 30m vertical resolution in the boundary layer. Also shown is the simulated cloud water amount from one of the LES models contributing to the EUROCS case study of this event. The HIRLAM SCM uses the moist turbulence and statistical cloud scheme in combination with the Kain-Fritsch convection scheme (Kain and Fritsch 1990). The convection scheme provides tendencies of heat and moisture due to convection in regions where shallow cumulus convection is simulated to occur. At grid boxes where parameterised shallow convection is occurring heat and moisture tendencies due to moist turbulence are not communicated to the model prognostic equations. Cloud fraction and cloud water amounts associated with the shallow convection are diagnosed in the moist turbulence scheme using the combined estimate of subgrid scale saturation variation given by (7). The diagnosed cloud fraction and cloud water amounts are then used in the subsequent calculations of radiation and microphysical conversion in the same model time step. In this manner the statistical cloud fraction and cloud water are the only cloud variables being used (consistently) by all model parameterisations.

Figure 4 indicates that the statistical cloud scheme is able to simulate a reasonably good diurnal cycle of shallow cumulus cloud amounts and cloud water mixing ratios. Figure 5 shows the terms  $\sigma_{sturb}$  and  $\sigma_{scu}$  that contribute to the total subgrid scale variance of saturation conditions used in the diagnosis of  $Q_1$  and subsequently the cloud fraction and cloud water amounts. In this convective boundary layer, parameterised shallow convection is the primary contributor to the variance of saturation conditions within a model grid box. A relative maximum in  $\sigma_{sturb}$  can be seen in the shallow convective cloud layer, but the simulated cloud fraction is cleared phased with the onset of parameterised convection and the sharp increase in  $\sigma_s$  due to convection. Simulations made with parameterised convection turned off failed to simulate a shallow cumulus cloud due to the low value of  $\sigma_{sturb}$  and the subsequent large negative value of  $Q_1$ . We are presently testing using only the moist turbulence scheme for simulating shallow convection with an extra term included in the subgrid scale buoyancy flux calculation due to the non-gaussian nature of vertical transports in a partially cloudy layer (Cuijpers and Bechtold 1995). Inclusion of this contribution to the buoyancy term in the TKE equation greatly increases the simulated value of TKE in partially cloudy grid boxes. This will increase the  $\sigma_{sturb}$  term and it is hoped might allow a better estimate of shallow cumulus cloud fractions directly from the moist turbulence scheme, without requiring the  $\sigma_{scu}$  contribution from parameterised shallow convection.

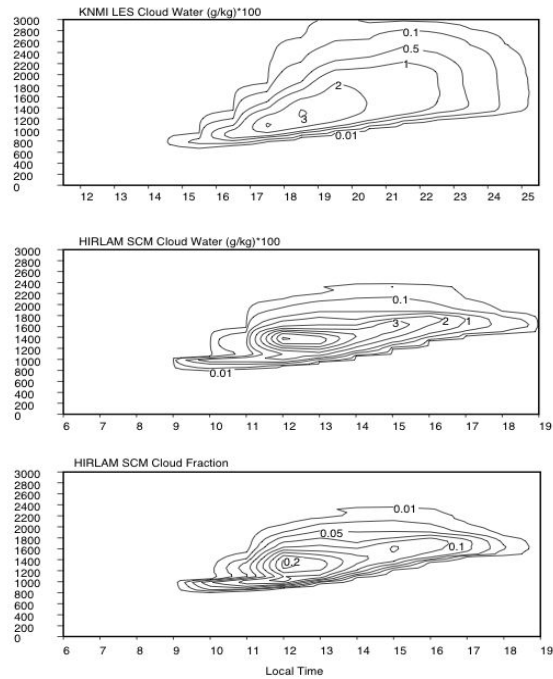


Figure 4. HIRLAM SCM simulation of the diurnal cycle of shallow cumulus clouds observed over the ARM SGP site June 21<sup>st</sup> 1997. Also shown is the KNMI Large Eddy Simulation of the cloud water evolution for this case. X-axis shows local time and y-axis is the vertical height..

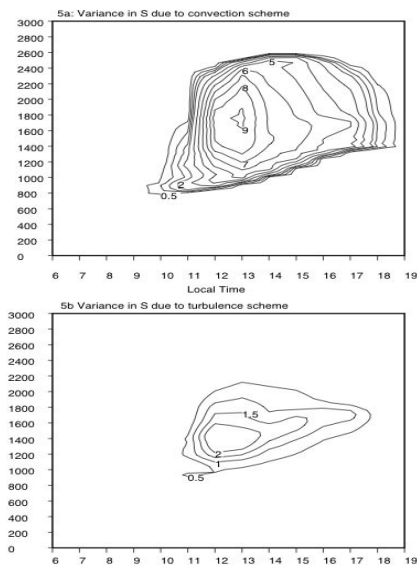


Figure 5. Time-height cross-section showing the diurnal cycle of the variance of saturation conditions ( $\sigma_s$ ) about the grid box mean saturation deficit As contributed by a) the convection parameterisation and b) turbulence scheme. X-axis local time in hours.

### 2.3 Deep Convective clouds

Finally we tested the ability of the statistical cloud scheme to simulate deep convective clouds and particularly upper level clouds forced by moistening due to detrainment of condensate from deep convective towers. The HIRLAM SCM was used to simulate a 4-day period of deep convection observed during the summer of 1997 at the ARM Southern Great Plains site (see Xu et al 2002 and Xie et al 2002). In the free troposphere, above the boundary layer, simulated values of TKE and associated  $\sigma_{sturb}$  will often become very small. Away from regions of convection the diagnosed  $\sigma_s$  term will be very small, the only contribution coming from the small  $\sigma_{sturb}$  term in the free atmosphere. In the free troposphere variations of water and saturation conditions do occur on scales smaller than  $\sim 20\text{km}$ , that are not directly associated with active convection or small-scale turbulent motions. For example variability associated with mesoscale convective circulations, enhanced turbulence following a convective event, jet streaks and frontal circulations. Neglect of these variance contributions risks making the cloud fraction and cloud water diagnosis through  $Q_1$  become an “all or nothing” scheme, with cloud fraction being either unity (in saturated conditions) or zero (in unsaturated conditions) because of the very small value of  $\sigma_s$  simulated in the free atmosphere. As an initial attempt to alleviate this problem, above the simulated boundary layer we introduce an extra variance term ( $\sigma_{sfix}$ ). This we model analogous to  $\sigma_{sturb}$  using equation 5, but we replace the prognostic  $l_{tke}$  by a fixed mixing length scale  $l_{fix}=250\text{m}$ . This is analogous to the assumption of an asymptotic mixing length used by many turbulence schemes in the free troposphere (Louis 1979). The resulting  $\sigma_s$  term is modelled as follows:

$$\begin{aligned} \sigma_s &= \sigma_{sturb} + \sigma_{scu} & z &\leq pblh \\ \sigma_s &= \max\left[\left(\sigma_{scu} + \sigma_{sturb}\right), \left(\sigma_{scu} + \sigma_{sfix}\right)\right] & z &> 2xpblh \end{aligned} \quad 8.$$

where  $\sigma_{sfix}$  uses equation 5 for diagnosing the saturation variance but with the value of  $l_{fix}$  replacing  $l_{tke}$ . The term  $pblh$  is the height of the top of the model boundary layer. The two values of  $\sigma_s$  are linearly interpolated across the vertical distance between  $pblh$  and  $2xpblh$ .

Figure 6 shows a time-height section of the simulated cloud fraction for the 4-day period of this simulation. Two periods of convection were observed to occur (Xu et al 2002), the timing and duration of which are reasonably well simulated by the HIRLAM SCM convection scheme. The sharp vertical spikes of cloud fraction in figure 6 show the cloud fraction simulated by the statistical cloud scheme associated with these periods of deep convection. Fractional cloud amounts are simulated during these periods due to the large variance term coming from the parameterised deep convection. During the period between hours 24 and 42 of the simulation an upper level cloud was observed to form (observed by the millimetre radar at the ARM site, *not shown here*) and to gradually thicken and the cloud base descend with time. During this period no convection was observed to be active and non was simulated by the HIRLAM SCM. This cloud probably occurred as a result of moistening of the upper troposphere by the period of deep convection between hours 14-24 of the simulation. Inclusion of the  $\sigma_{sfix}$  term above the boundary layer allows this cloud layer to be reasonably well captured, with cloud fractions of 20-40% gradually descending with time. Neglect of the term  $\sigma_{sfix}$  leads to the statistical cloud scheme relaxing into an all or nothing scheme in the free atmosphere and this mid to upper level cloud deck is simulated as two separate layers of 100% cloud fraction with zero cloud in between (a situation that was not observed to occur). This is due to the model atmosphere remaining sub-saturated, with high values of static stability above the boundary layer. Cloud free conditions were not observed to occur during this period and this model error is a direct result of the underestimate of the variance of saturation conditions in the free troposphere once convection has ceased and the  $\sigma_{scu}$  term is zero.

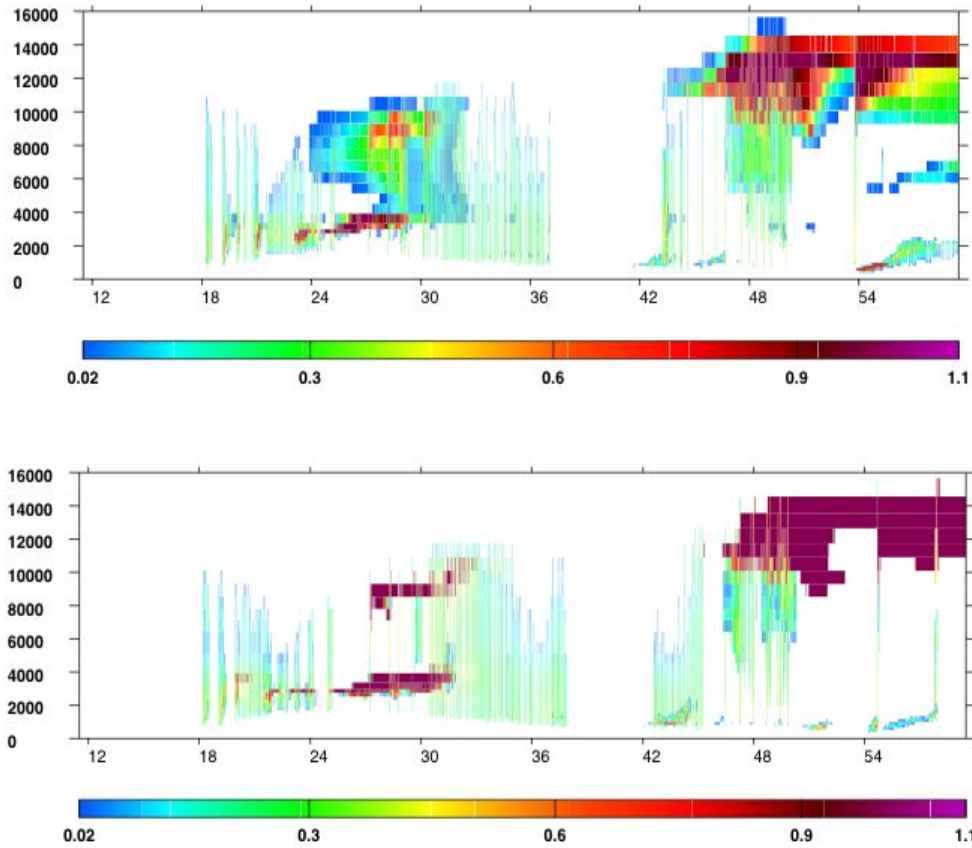


Figure 6. Time-height cross-section of clouds fraction from a run with  $\sigma_{sfix}$  included (top panel) and an identical integration but with  $\sigma_{sfix}$  equal to  $\sigma_{sturb}$  (lower panel)

For practical application of the statistical cloud scheme to represent all cloud types, an estimate of the subgrid scale variation of saturation conditions (*subgrid scale variation of total water and temperature*) resulting from processes other than convection and small-scale turbulence seems necessary. Equation 8 represents a preliminary attempt to parameterise this term.

### 3. Conclusions.

We have described the introduction of a statistical cloud scheme into the HIRLAM moist turbulence scheme. This cloud scheme is used to estimate all cloud types (*both fractional extent and water content*) in a variety of situations simulated by the HIRLAM SCM. These situations span boundary layer stratocumulus clouds, shallow cumulus and deep convective clouds. The statistical scheme links the simulated clouds to the grid box mean saturation conditions, normalised by an estimate of the subgrid scale variation of saturation conditions about the grid box mean value. The variance term has contributions from parameterised turbulence, convection and an assumed free troposphere contribution. In this manner cloud fraction and water amounts are tightly coupled to the model parameterisations of convection and turbulence. Results indicate that this approach is a promising route to simulate all cloud types by a single scheme, irrespective of their means of production. More work needs to be done to simulate subgrid scale free troposphere variations in saturation conditions. It is possible that the information on subgrid scale variation of saturation conditions might prove to be useful information for the model microphysical and radiation schemes to incorporate variability of cloud water amounts in the calculation of precipitation and cloud-radiation interaction.

## **Acknowledgements**

I would like to thank Geert Lenderink, Sander Tijm, Wim de Rooy and Pier Siebesma (all from KNMI) for valuable discussions and contributions to this work.

## **References.**

- Albrecht B.A., Randall D.A and Nicholls S. 1988. Observations of marine stratocumulus clouds during FIRE. *Bull. Am. Meteorol. Soc.* 69, 618-626
- Brown A. and co-authors 2002. Large Eddy Simulation of the diurnal cycle of shallow cumulus convection over land. *Q.J.R. Meteorol. Soc.* 128, 1075-1094.
- Bougeault and Lacarrere 1989. Parameterisation of orography induced turbulence in a mesobeta-scale model. *Mon. Wea. Rev.* 117, 1872-1890.
- Chaboureau J-P and Bechtold P. 2002. A simple cloud parameterisation derived from Cloud Resolving Model Data: Diagnostic and Prognostic applications. *Journal. Atmos. Sci* 59, 2362-2372
- Chlond A., Muller F and Sednev I. 2004. Numerical simulation of the diurnal cycle of marine stratocumulus during FIRE-An LES and SCM modelling study. *Q.J.R. Meteorol. Soc* 130, 3297-3322
- Cuijpers J.W.M and Duynkerke P.G. 1993. Large Eddy Simulation of trade wind cumulus clouds. . *Journal. Atmos. Sci.* 50, 3894-3908
- Cuijpers J.W.M. and Bechtold P. 1995. A Simple Parameterisation of Cloud Water Related Variables for use in Boundary Layer Models. *Journal. Atmos. Sci* 52, 2486-2490.
- Cuxart J, Bougeault P and Redelsperger J-L 2000. A turbulence scheme allowing for mesoscale and large-eddy simulations. *Q.J.R. Meteorol. Soc* 126, 1-30.
- Duynkerke P.G and co-authors 2004. Observations and numerical simulations of the diurnal cycle of the EUROCS stratocumulus case. *Q.J.R. Meteorol. Soc* 130, 3269-3296.
- Kain J.S and Fritsch J.M. 1990. A one-dimensional entraining/detraining plume model and its application in convective parameterisation. *Journal. Atmos. Sci* 47, 2784-2802.
- Lenderink G. and Holtslag A.A.M 2004. An updated length-scale formulation for turbulent mixing in clear and cloudy boundary layers. *Q.J.R. Meteorol. Soc* 130, 3405-3428.
- Lenderink G. and co-authors 2004. The diurnal cycle of shallow cumulus clouds over land: A single column model intercomparison study. *Q.J.R. Meteorol. Soc* 130, 3339-3364.
- Lenderink G. and Siebesma A.P. 2000. Combining the mass-flux approach with a statistical cloud scheme. pp66-69 in Proceedings of the 14<sup>th</sup> symposium on boundary layers and turbulence, Aspen USA. American Met. Soc. Boston USA.
- Louis J-F 1979. A parametric model of vertical fluxes in the atmosphere. *Boundary Layer Meteorol.* 17, 187-202.
- Mellor G. 1977. The Gaussian cloud model relations. *Journal. Atmos. Sci* 34, 356-358
- Sommeria G. and Deardorff J.W 1977. Subgrid scale condensation in models of non-precipitating clouds. *Journal Atmos. Sci.* 34, 344-355.
- Stevens B. and co-authors 2003. Dynamics and chemistry of marine stratocumulus- DYCOMSII. *Bull. Amer. Meteorol. Soc* 84, 579-593.
- Xie S.C. and co-authors 2002. Intercomparison and evaluation of GCM cumulus parameterisations under summertime mid-latitude continental conditions. *Q.J.R. Meteorol. Soc* 128, 1095-1135.
- Xu K-M and co-authors 2002. An intercomparison of cloud-resolving models with the ARM 1997 summer IOP data. *Q.J.R. Meteorol. Soc* 128, 593-624.

# Experiences with a statistical cloud scheme in combination with Kain-Fritsch convection in Hirlam

Wim de Rooy

KNMI, De Bilt, The Netherlands

## Introduction

The goal of this project is to develop a new statistical cloud scheme for Hirlam, keeping in mind the use of it in a very high-resolution, possibly non-hydrostatic, model. Using the ideas of Lenderink and Siebesma (2000), we want to couple the cloud scheme not only to a turbulence scheme but also to a mass flux convection scheme.

## Fundamentals of a statistical cloud scheme

Temperature ( $\bar{T}$ ) and total specific humidity ( $\bar{q}_t$ ) from a NWP model represents the grid box average values (denoted with an overbar). In reality T and  $q_t$  can vary within the grid-box, with possibly saturated areas although the mean state might be unsaturated. Instead of using T and  $q_t$  it is convenient to go over to one variable, the distance to the saturation curve:

$$s \equiv q_t - q_{sat}(p, T) \quad (1)$$

The temperature information is now included in the temperature dependence of the saturation specific humidity,  $q_{sat}$ . Variable s is subsequently normalized by the standard deviation (SD) in s,  $\sigma_s$ :

$$t \equiv \frac{s}{\sigma_s} \quad (2)$$

If we assume a certain probability density function (PDF) of t in the grid-box we can calculate the fractional cloud cover and liquid water content. For example, for cloud cover, the integral of the PDF over all positive values of t results in the cloud cover as a function of just one variable,  $\bar{t}$ , which is simply given by the grid-box model output. Similarly, the liquid water content can be determined. The main challenge for the development of a statistical cloud scheme is to get reasonable estimates of  $\sigma_s$  (or the variance in s,  $\sigma_s^2 \cong \overline{q_t'^2}$  (for simplicity we neglect the temperature terms in the variance)).

How can this variance be parameterized?

After a few approximations (e.g. steady state) the budget equation for humidity variance, can be written as a balance between variance production (left hand side) and variance dissipation (right hand side):

$$\overline{w'q'} \frac{\partial q_t}{\partial z} = \tau^{-1} \overline{q_t'^2} \quad (3)$$

In a mass flux convection scheme the turbulent flux,  $\overline{w'q'}$ , on the left hand side can be written as:  $\overline{w'q'} = M(q_t^u - q_t)$ , where M is the mass flux and  $q_t^u$  is the total specific humidity in the updraft. The dissipation time scale,  $\tau$ , can be written as:  $\tau = \frac{l_{cloud}}{w_*^{cu}}$ , where  $l_{cloud}$  is the depth of the

cloud and  $w_*^{\text{cu}}$  is a convective velocity scale. In this way, we come to a parameterization, first mentioned by Lenderink and Siebesma (2000), which link the convective activity with the humidity variance  $\overline{q'^2}$ .

In most statistical cloud schemes, the turbulent flux and dissipation time scale in (3) are taken solely from the turbulence scheme. This leads to a parameterization like:

$$\overline{q_t'^2} \cong l_{\text{turb}}^2 \left( \frac{\partial q_t}{\partial z} \right),$$

where  $l_{\text{turb}}$  is a turbulence length scale. For example in Chaboureau and

Bechtold (2002)  $l_{\text{turb}}$  is taken as  $0.2 \cdot z$  up to 900m, and 180 above 900m (so even in the free troposphere where there is almost no turbulent or convective activity!). They fitted the length scale to two cases with convective activity so their length scale also includes the effect of convective activity. For the case that we used (BOMEX), this length scale is much too large, leading to too high variance values, even when we skip the parameterization of the variance due to the convection. The opposite is true if we take the stability dependent length scale from the turbulence scheme itself, as implemented by Colin Jones. Now the variance contribution due to turbulence is insignificantly small. So it is not yet clear how to deal with  $l_{\text{turb}}$ . Note that also in layers without turbulent or convective activity, we need some variance to get reasonable cloud cover with a statistical cloud scheme.

## Experiments

The set-up of this project is to start simple, with 1D experiments (starting with BOMEX, a shallow cumulus case), just looking at the cloud cover diagnosed from the statistical cloud scheme without any feedbacks to e.g. radiation. The idea is to couple the variance for the statistical cloud scheme to the turbulence scheme (in the results presented here we used  $l_{\text{turb}}=40$  (as implemented in the NOGAPS model by Pier Siebesma), and the Hirlam mass flux convection scheme, Kain-Fritsch (KF)).

Apart from the complex, difficult to understand Hirlam KF code, we experienced many problems when using this convection scheme for the BOMEX case. Some of these problems are:

- Intermittent character (on/off, and sometimes deep convection)
- The updraft (virtual) temperature results in a negative buoyant cloud (and consequently a negative variance)
- An artificially looking closure for shallow convection
- The mass flux does not decrease enough with height leading to much too high variances in the upper part of the cloud.

Besides this, the results of the standard KF scheme were unsatisfactory for the BOMEX case with non-steady  $q$  and  $q$  profiles (note that observations show app. constant profiles), reflecting the too active convection (see Fig.1 for the  $q$  profile at different forecast times).

To avoid the above-mentioned problems, we made several changes to the KF scheme. Some of the most important changes are:

- Fractional entrainment and detrainment rates for shallow convection according to Siebesma et al. (2003).
- A vertical velocity equation according to Gregory (2001) resulting in an increase in the depth of convection.
- A closure for shallow convection according to Grant (2001), which makes the timescale plus some other (tunable) parameters redundant.

After these adaptations the mass flux,  $\theta$ , and  $q$  profiles improved considerably (now almost steady, see Fig. 2 for the  $q$  profile).

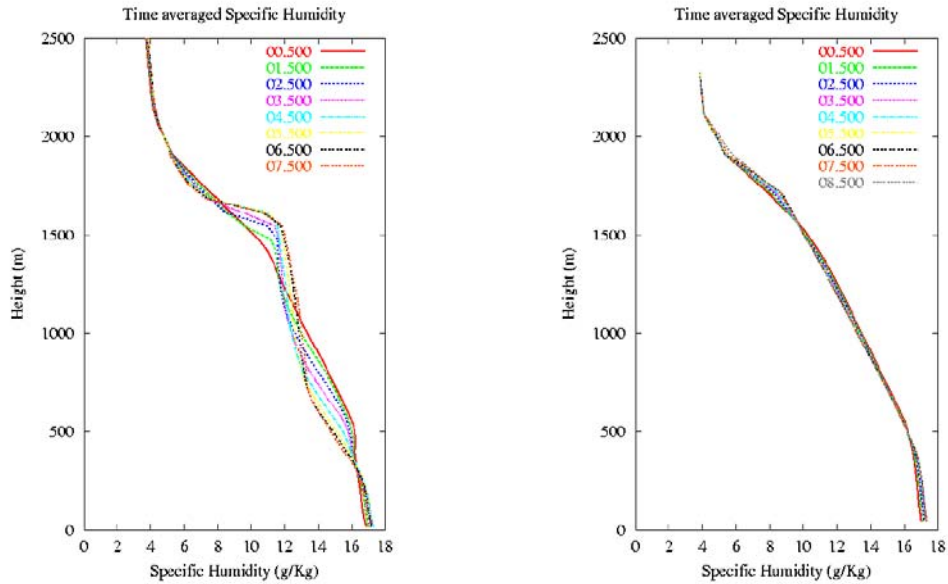


Fig. 1 (left panel) The specific humidity vertical profiles for the BOMEX case running the standard Hirlam 1D model. The different colors represent different forecast periods, e.g. green (1.5) is the output averaged over the +1 to +2h forecasts. Note that for this case the profiles should be steady.

Fig.2 (right panel) As Fig. 1 but with the modified convection scheme (as mentioned in the text)

With the modified KF scheme, also variance profiles are now in reasonable agreement with LES results, especially considering the relatively coarse vertical resolution of the 1D model (40 layers), showing a double peak at cloud base and top (see Fig. 3)

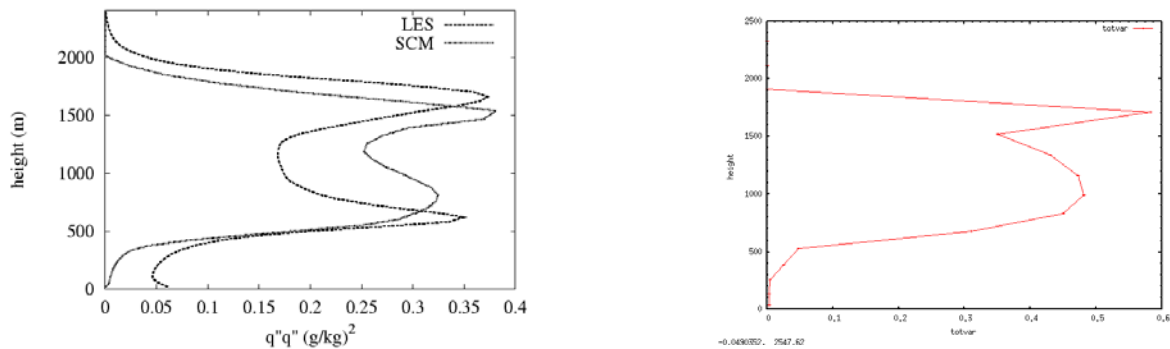


Fig. 3 (left panel) Vertical profiles of the humidity variance for the BOMEX case running an LES model and a very high-resolution (40m) 1D model (from Lenderink and Siebesma 2000). Fig.4 (right panel) As Fig.3 but with Hirlam 1D, 40 layers in the vertical, with the modified convection scheme (as mentioned in the text). Note that the x-axis maximum is now 0.6 instead of 0.4.

Finally, the cloud cover, calculated as a function of the normalized saturation deficit following Cuijpers and Bechtold (1995), nicely resembles observations with maximum values at cloud base height of about 5% (not shown)

So with the above mentioned adaptations, good results with the convection and the statistical cloud scheme are obtained for BOMEX. However, all possible situations should be covered (also deep convection, precipitation etc.). Building a new scheme from scratch would take too much time, just like rebuilding the KF code. Therefore, we considered two alternative convection schemes, namely the ECMWF and the Meso-NH scheme. Peter Bechtold is the developer of the Meso-Nh scheme and is now working on the further development of the ECMWF scheme, so he is a pre-eminently suitable advisor. Peter suggests using the ECMWF convection scheme because this code is faster, gives better results and there will be continuous research for improvements. The use of the ECMWF scheme will also facilitate the synergy within KNMI (between Hirlam and the climate research department) at the area of convection and cloud schemes.

There is however a big minus, someone has to implement this convection scheme in the Hirlam code. Although giving more work than expected, the ECMWF (28r1 version) is now implemented in Hirlam 1D. For Bomex, good results are obtained except from the deep convection, which sometimes occurs after a few hours of simulation. This aspect still has to be investigated but we are probably quite close to a proper implementation. Hereafter, more tests (1D and 3D) with the ECMWF convection scheme in combination with a statistical cloud scheme will be done.

### **Acknowledgements**

Sander Tijm is thanked for his help with the Hirlam Kain-Fritsch code. Pier Siebesma and Geert Lenderink are thanked for useful discussions and advice.

### **References:**

- Chaboureau, J.-P., P. Bechtold, 2002: A Simple Cloud Parameterization Derived from Cloud Resolving Model Data: Diagnostic and Prognostic Applications. *J. Atmos. Sci.*, **59**, 2362-2372
- Cuijpers, J.W.M., and P. Bechtold, 1995: A simple parameterization of cloud water related variables for use in boundary layer models. *J. Atmos. Sci.*, **52**, 2486-2490
- Kain, J.S., and J.M. Fritsch, 1990: A one-dimensional entraining/detraining plume model and its application in convective parameterization. *J. Atmos. Sci.*, **47**, 2784-2802
- Lenderink, G., and A.P. Siebesma, 2000: Combining the massflux approach with a statistical cloud scheme. Preprints, *14th Symp. On Boundary Layers and Turbulence*, Aspen, CO, Amer. Meteor. Soc., 66-69
- Grant, A.L.M., 2001: Cloud-base fluxes in the cumulus capped boundary layer. *Quart. J. Roy. Meteor. Soc.*, **127**, 407-422
- Siebesma, A.P. et al., 2003: A Large Eddy Simulation Intercomparison Study of Shallow Cumulus Convection. *J. Atmos. Sci.*, **10**, 1201-1219
- Sommeria, G., and J.W. Deardorff, 1977: Subgrid-scale condensation in models of nonprecipitating clouds. *J. Atmos. Sci.*, **34**, 344-355

# Why do moisture convergence deep convection schemes work for more scales than those they were in principle designed for?

J.-F. Geleyn<sup>1</sup> and J.-M. Piriou<sup>2</sup>

<sup>1</sup> Czech HydroMeteorological Institute, Prague, Czech Republic, on leave of absence from Météo-France

<sup>2</sup> Centre National de Recherches Météorologiques, Météo-France, Toulouse, France

## I) Introduction

The title of this note is intentionally provocative, but it reflects two underlying realities. First of all it stems out of the content of a mail written (on 12/01/2004, personal communication) by Philippe Bougeault (who proposed twenty years ago the first operational deep convective parameterisation that combined a mass-flux approach with a single-cloud profile and a Kuo-type closure, Bougeault (1985)) and that will be reproduced (after translation) here.

*“I was well conscious about this limitation (authors’ note: of the moisture convergence closure) in 1985, but the problem is that I mostly wanted to fit GATE data, where there is no correlation between CAPE and rainfall, while there is a strong correlation between moisture convergence and rainfall. But, as Mapes rightly says, the latter does not guarantee a causal link because one might mix cause and consequence. **But, since it works on this basis at Meteo-France as well as at ECMWF for 20 years, this cannot be that wrong either!**”*

Second, and prolonging the ideas expressed by Mapes (1997), it is our opinion that the heavy debate about which measure of Quasi-Equilibrium (QE thereafter) is the most appropriate one for any parameterisation scheme’s closure (cloud work function, CAPE-CIN, moisture convergence, ...) is ill-placed and reflects a wrong choice of priority. We believe that future parameterisation schemes will put this question to the second rank and first address a far more fundamental one.

The aim of this note is thus to introduce this change of emphasis and to explore some tracks about how to concretise it without throwing away much of the progress that deep convective parameterisation made in the past twenty to thirty years on others aspects. For this reason, our reference tool, when needed, will be the current operational version of the Bougeault scheme. For differences with the 1985 published version, the reader is referred to Gerard and Geleyn (2005).

In Section 2 the basic concepts leading to the mass flux approach and to its above-mentioned combination with a single ascent and a moisture convergence closure will be recalled. Section 3 will be a short introduction on controversies around closure and QE issues. In Section 4 we shall introduce our own search of tracks meant to go around the underlying problems (those of the basic analysis by Mapes), before a short concluding Section 5.

## II) Bougeault’s mass-flux approach and its particularities

We start from the following principles:

- any deep-convective parameterisation requires some knowledge of the host model’s ‘resolved’ tendencies for its closure;
- given the scales we are targeting at, we must parameterise in an hydrostatic-type framework an essentially non-hydrostatic phenomenon (the integral link between pressure and geopotential cannot be the same for the ‘environment’ and the ‘cloud’ if they have the same basis and top);
- parameterised convection is basically intermittent at a given grid-point and we must account for that fact (conditional activity);

- most importantly, while ‘visible’ convection appears like a local auto-organised process, its ‘invisible’ conditions of existence and back-influences on the basic flow are very much of a large-scale type.

Hence, even if parameterisation schemes look at first glance like being built to maintain the correct local vertical gradients of temperature and humidity, we must consider that their main role in the host model is to ultimately interact with the intensity and with the horizontal scale of larger-scale dynamical adjustment motions, up to those of the Hadley cell in case of the ITCZ. The need to establish this distinction is emphasised by tropical observations (Fig. 1): while the convectively active areas are characterised by unstable profiles (the local ‘return to neutrality’ is all but instantaneous), the averaged tropical situation is hardly favourable to a global convective activity (the time-rate of ‘return to neutrality’ cannot therefore be dictated only by the intensity of local imbalances).

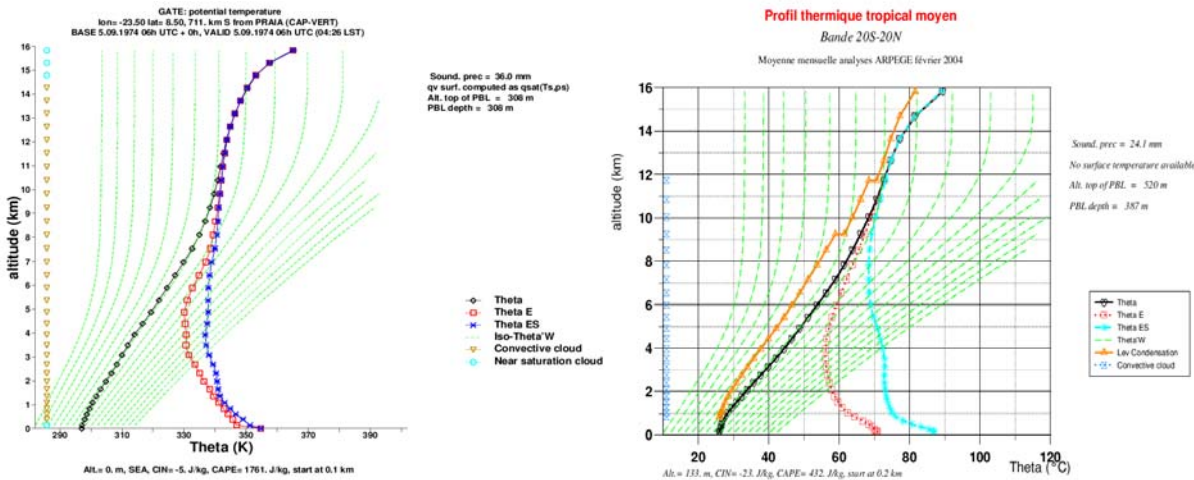


**Figure 1:** Tephigrams of a GATE sounding (left) and of the averaged tropical state (right). CAPE being proportional to the area on the right of the most right curve but colder than the warmest point below on the curve next to the left, one sees a lot of conditional instability (of the ‘first kind’) in the ‘perturbed’ case (left) and relatively little in the ‘mean’ one (right).

We now look at the most basic version of the single-ascent mass-flux framework, obtained under the hypothesis (i) of steady cloud-ascent behaviour and (ii) of negligible updraft area:

$$\left[ \frac{\partial \bar{\psi}}{\partial t} \right]_{CV} = - \frac{\partial}{\partial p} [M_c (\bar{\psi} - \psi_c)]$$

$$\frac{\partial M_c}{\partial p} = D - E$$

$$M_c \frac{\partial \psi_c}{\partial p} = E (\psi_c - \bar{\psi})$$

where the first equation expresses the sole convective tendency with  $\psi$  a generic notation for any conservative property,  $M_c$  represents the mass-flux expressed in units of a ‘negative omega’ vertical velocity,  $D$  and  $E$  are respectively the detrainment and entrainment rates expressed in inverse time units. The subscript  $c$  marks the cloud-ascent specific properties and the averaging sign the host model resolved (‘large-scale’ (LS)) values.

We don’t address here the question of deriving an expression for  $\psi_c$ . So, assuming that  $\psi_c$  has been computed by some existing method, the closure problem becomes that of expressing two out of the

three quantities  $M_c$ ,  $D$  and  $E$ . In Bougeault (1985) the approach is somewhat different and can be symbolised (on the basis of the same notations) as follows:

$$\begin{aligned} \frac{d\bar{\psi}}{dt} &= -\omega_{LS} \frac{\partial \bar{\psi}}{\partial p} - \left[ M_c \frac{\partial \bar{\psi}}{\partial p} + \bar{D} \cdot (\bar{\psi} - \psi_c) - g \frac{dJ_\psi}{dp} \right] - g \frac{dJ_\psi}{dp} \\ \frac{\partial M_c}{\partial p} &\neq D - E \text{ but } \left\{ \int \left( \frac{\partial h}{\partial t} \right)_{cv} = 0 \Rightarrow \bar{D} \right\}; \left( M_c \frac{\partial \psi_c}{\partial p} = E(\psi_c - \bar{\psi}) \right) \\ \int M_c \frac{\partial \bar{q}}{\partial p} &= \int -\omega_{LS} \frac{\partial \bar{q}}{\partial p} - g \frac{dJ_q}{dp} \text{ (Closure)} \end{aligned}$$

where the bracketed terms of the first equation correspond to the full RHS of the first equation of the previous set, the second equation of the previous set has been replaced by an integral constraint on a now uniform detrainment rate and the closure indeed expresses the local consumption (LHS) of the total moisture convergence (RHS).  $J_\psi$  represents the non-convective sub-grid scale fluxes (turbulent ones in general) and, for the sake of simplicity, horizontal advection has been omitted.

Basically, for the convective parameterisation alone, the straight link between  $M_c$ ,  $D$  and  $E$  has been replaced by a rule of compensation between convective motions and the turbulent part of their feeding. This has the important consequence that the  $\omega_{LS} + M_c$  residual value (what the large scale ‘feels’ as effective vertical motion) creates terms that are in balance with all local motions while, at steady state, the controlling moisture budget becomes independent of this effective vertical motion:

$$\int \bar{D} \cdot (\bar{q} - q_c) \cong \int g \cdot \frac{dJ_q}{dp}$$

This is in essence the way in which the basic Bougeault scheme tries to make the above-mentioned crucial distinction (illustrated by Figure 1) and probably one of the main reasons of its long-lasting value. Indeed all improvements made later to the scheme never touched this crucial point. But we must also point out that the associated advantage bears in itself its own limitations, because it is obtained only under the too restrictive conditions of (a) cloud stationary behaviour, (b) no possible storage or destorage of moisture from one time step to the next and (c) independence of the moisture source from local convective activity.

### III) Some controversies and their link with this note

As any phenomenon being in quasi-equilibrium with its environment -at least at some scales-, deep convection needs both a dissipative mechanism (friction) and a self-enhancing-type activation. Concerning the latter, two theories (CISK for Conditional Instability of the Second Kind & WISHE for Wind Induced Surface Heat Exchange) have been fighting for recognition in the past twenty years. We shall here limit ourselves to the static view of the problem (already complicated enough), therefore without reference to wave propagation arguments.

The CISK approach is to say “condensation  $\Rightarrow$  buoyancy  $\Rightarrow$  updraft motion  $\Rightarrow$  surface pressure drop  $\Rightarrow$  low level convergence  $\Rightarrow$  more moisture  $\Rightarrow$  condensation ...”, but the WISHE advocates then ask ‘*Where does the moisture comes from?*’.

The WISH approach is to say “condensation + ascent  $\Rightarrow$  balanced profile maintenance  $\Rightarrow$  sinking in dry regions balanced by radiation  $\Rightarrow$  need of a return flow  $\Rightarrow$  stronger wind leading to more evaporation  $\Rightarrow$  more available moisture  $\Rightarrow$  condensation + ascent ...”, but the CISK advocates then ask ‘*What determines the balanced profile?*’.

In fact the truth seems to be situation- and scale-dependent, but there is an important induced difference in the link between what we named earlier the ‘visible’ and ‘invisible’ parts of the convective circulations. In the CISK case, ‘convection’ drives the ‘large-scale circulation’ while, in the WISHE case, ‘convection’ controls the ‘large-scale circulation’.

This brings us back to the question of the separation between local and larger-scale properties of a given parameterisation scheme. Experimentally it can be shown (Geleyn and Rochas, 1987) that the Bougeault scheme, although having a closure assumption clearly of the CISK type, can have both CISK and WISHE behaviours, something surely related to our previous remark about the virtue of replacing the link between  $M_c$ ,  $D$  and  $E$  by a rule of compensation.

Given this reassuring practical result and since, when coming to parameterisation issues, the CISK/WISHE controversy boils down to something we already announced as of second importance, it is time to come to the second and more recent controversy, about the nature and role of QE in understanding and parameterising deep convection.

Historically speaking, the evolution of the QE concept is roughly the following (cf. Mapes, 1997):

- whatever feedback and causality might be at work, it was realised quite early that QE is verified at large scales but not necessarily at scales below;
- studying the phenomenology of convection did lead to the mass-flux concept that helped to codify the issues around QE (Arakawa and Schubert, 1974);
- this shifted the old problem of convective closure from budgets to complex questions about the dynamics of convective circulations;
- but the (likely misleading) answer was to replace a tractable question “which convective clouds are likely to develop in a given environment and which feedback do they have on this environment?” by a more difficult one “which are the quantities that QE convection leaves unchanged?”.

Beside that last issue, there is also the problem that QE is not considered under the same angle of view depending whether one prefers the CISK or WISHE theory. In the CISK case, convective circulations are determining the ‘larger-scale’ vertical motions that in turn force convection. In the WISHE case, only the residual aspects matter (weight and counter-weight motions need a small additional push corresponding to the targeted additional transport, if we take a mechanical analogy).

All this giving the impression that the QE concept has been over-used and/or over-interpreted, it is not surprising that some ‘anti-QE’ thinking started to appear. Mapes (2003) synthesises it as follows:

- scales are not separable since the ‘invisible part’ of convection is at the scale of the Rossby radius of deformation;
- forcing and answer are not really separable either (even if we may add that the return flow must be accounted for at the grid-box scale in any parameterisation scheme);
- there is no ‘under-law’ of convective regions’ dynamics that aggregates local behaviours to a simple balance.

We shall see later how to try and convert these negative statements into some positive proposals, but let us mention here that this way to bring back QE to its simplest expression indirectly confirms some impossibility to arbitrate between CISK and WISHE ideas. Indeed, following Le Châtelier’s chemical rule, if convective heating follows cooling by adiabatic ascent (somehow equivalent to the control role of convection) the resulting effect would be cooling but if convective heating precedes cooling by adiabatic ascent (somehow equivalent to the driving role of convection) the resulting effect would be heating. Testing this on the basis of statistical observed differences between active and non-active periods at some tropical locations however shows conflicting results (see Figure 2, adapted from Mapes (1997)).

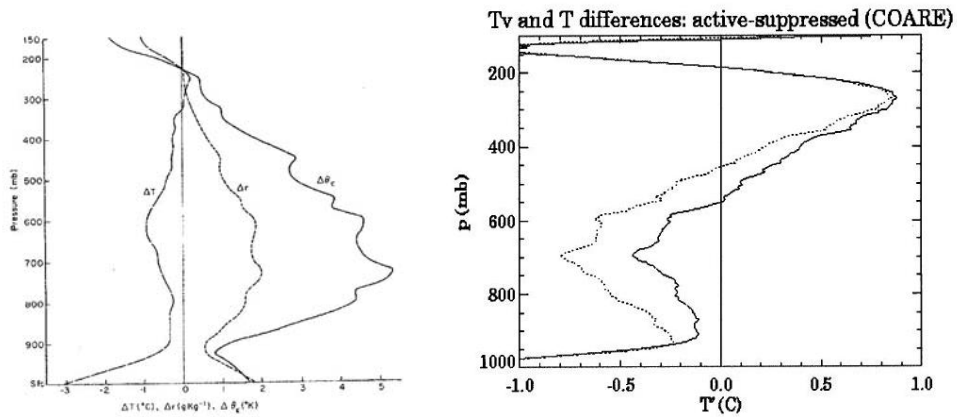


Figure 2: Left, ~300 Venezuelan sounding (Betts, 1974); right, TOGA-COARE experiment. The left curves of both diagrams represent the difference between convective and non-convective periods in terms of averaged temperatures. One sees that, away from the PBL where turbulence might bias the results, the trend is ambiguous.

IV) A possible path to revise the basic parameterisation concepts

If believing in the need for a new perspective, Figure 3, also adapted from Mapes (1997), shows how to link the changes in our nature's understanding to changes in modelling paradigms.

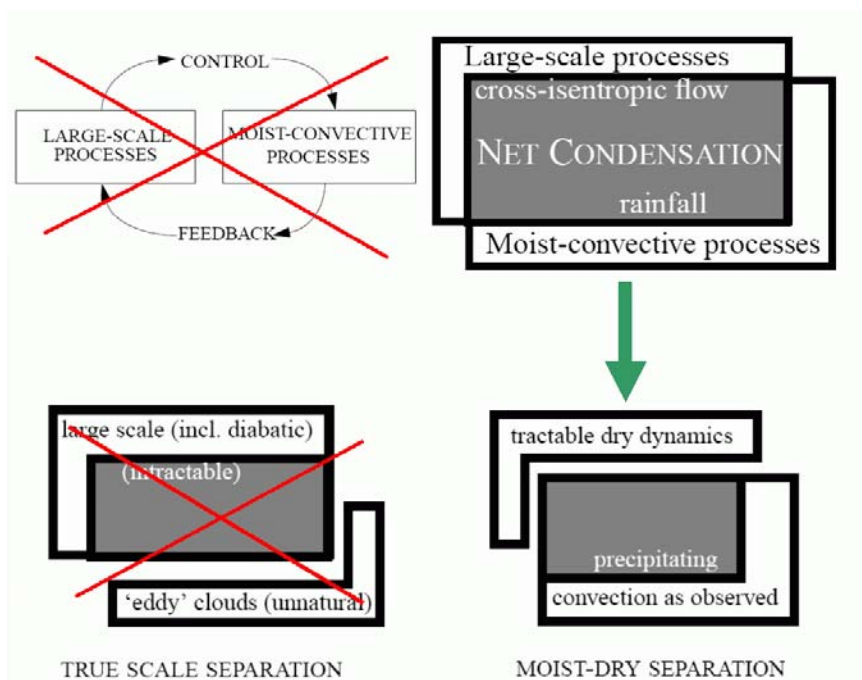


Figure 3: Top row, nature's understanding; bottom row, parameterisation schemes' boundary choices. Left column, impossible (?) problematic; right column, path not yet enough explored.

A first immediate consequence is that there is an important intermediate result that is missing (in the 'physical' sense since there is always a mathematical equivalent) in current deep convective parameterisation schemes: the vertical distribution of the condensation rate inside the 'cloud-ascent'. Let us call it BCC (Bulk Convective Condensation) and remark that, if we make it an obliged path for parameterisation calculations, (A) the moist-dry separation of Fig. 3 becomes far easier to track and (B) the distinction between 'resolved' and 'convective' types of precipitation may be ironed out via an appropriate addition of both forms of condensation before other computations relying on this quantity.

This mention of the ‘large-scale-type’ precipitations (linked to negative large scale  $\omega_{LS}$ ) brings us to the question of the representativity of the large-scale vertical velocity for the parameterisation of sub-grid scale condensation. Let us go back to the first equation of Bougeault’s interpretation of the mass-flux concept. In deep convective conditions the absolute value of  $M_c$  will be slightly greater than that of  $\omega_{LS}$  and both will be much bigger than the absolute value of the environmental vertical velocity  $\omega_e = \omega_{LS} + M_c$ . In other words, the computed large-scale vertical velocity is just the average of the (rare but intense) cloud ascents and of a slightly sinking environment everywhere. Hence the large scale vertical advection term is dynamically meaningless (*but model-wise unavoidable*) and has to be compensated by a good estimate of the mass flux, slightly bigger thanks to surface evaporation. Thus, if QE is doubtful, the mass-flux parameterisation schemes **should not use the diagnosed large-scale vertical velocity as input**, to avoid the risk of a double counting or of an uncontrolled feedback loop.

But what is then left as possible input for the closure assumption? Basically we have CAPE (Convective Available Potential Energy), CIN (Convective INhibition energy) and moisture convergence (the ‘good old concept’ introduced by Kuo (1965) in order to get rid of the convective adjustment framework and that still shows some usefulness when skilfully used, cf. Section 2). If we come back to our new ‘BCC’ goal, there is an obvious link with moisture convergence but one that certainly should not lead to identity. Hence the idea to find a ‘moisture availability’ that goes back to moisture convergence in the ideal case of fulfilled QE but that also encompasses the CAPE and CIN information in the more general case of an evolving behaviour of convective activity. But we may even go further in the way to eradicate hidden QE thinking from the design of parameterisation schemes if we decide to relax the first hypothesis of the basic mass-flux equations, i.e. the one about steady cloud-ascent behaviour. For reasons that would be too long to develop here, this becomes possible if the parameterisation scheme is organised around the provision of BCC to further calculations, this closing a hopefully virtuous circle.

## V) Conclusion

The ideas expressed in Section 4 are for the time being not yet fully concretised or tested. There are however encouraging signs that they may lead to a positive evolution of deep convection parameterisation. Furthermore they are not contradicting what was the answer to our ‘title question’, namely that the link between moisture convergence and convective rainfall is strong enough to allow schemes carefully based on such a closure to be robust and applicable even when the balance is less accurate. Hence we may conclude that Bougeault’s special application of the mass-flux concept somehow anticipated the steps we are now advocating, the present proposal being an evolution of the former in order to cover meso-scale-organised and/or rapidly evolving environmental conditions.

### References:

- Arakawa, A. and W.H. Schubert, 1974: Interaction of a cumulus cloud ensemble with the large-scale environment; Part I. *J. Atmos. Sci.*, **31**, pp. 674-701.
- Betts, A.K., 1974: Thermodynamic classification of tropical convective soundings. *Mon. Wea. Rev.*, **102**, pp. 760-764.
- Bougeault, P., 1985: A simple parameterisation of the large-scale effects of cumulus convection. *Mon. Wea. Rev.*, **113**, pp. 2108-2121.
- Geleyn J.-F. and G. Rochas, 1987: A study of the ‘feed-back’ aspects of diabatic forcing in the French large-scale hemispheric model ‘Emeraude’. *‘Diabatic forcing’ ECMWF Workshop*, pp. 177-208.
- Gerard, L. and J.-F. Geleyn, 2005: Evolution of a subgrid deep convection parameterisation in a Limited Area Model with increasing resolution. To appear in *Q. J. R. Meteorol. Soc.*
- Kuo, H.L., 1965: On formation and intensification of tropical cyclones through latent heat release by cumulus convection. *J. Atmos. Sci.*, **22**, pp. 40-63.
- Mapes, B.E., 1997: Equilibrium vs. activation control of large-scale variations of deep convection. In *‘The physics and parameterisation of moist convection’*, **Kluwer Academic Publishers**, pp. 321-358.
- Mapes, B.E., 2003: An information-based approach to convective closure. In *‘Current issues in the parameterisation of convection’*, **BMRC Research Report N°93**, pp. 89-96.

# An integrated prognostic approach for clouds, precipitation and convection

Luc Gerard, RMIB, luc.gerard@oma.be

As long as convection is not completely resolved by the model grid, a subgrid deep convection scheme has to provide its contribution to the clouds and precipitation. How to combine this with the contribution from resolved condensation, in a way to get results independent of numerical issues, is a tough problem.

From the Clausius-Clapeyron and the energy equations, it can be shown that the saturation moisture decreases when the vertical velocity increases. This is also true at the scale of the grid box averages. In presence of convective updraughts on a fraction of the grid box  $\sigma_u \ll 1$ , the resolved vertical velocity  $\bar{\omega}$  results from averaging large updraught velocities  $\omega_u$  with a near zero upwards velocity  $\omega_e$  in the updraughts environment. Considering a single equivalent updraught (mass flux scheme):

$$\bar{\omega} = \sigma_u \omega_u + (1 - \sigma_u) \omega_e \approx \sigma_u \omega_u$$

In this case, the reduction of the grid box area induces a proportional increase of the updraught area and of the resolved upwards velocity. The saturation moisture is then lower. Also in weak convective situations, the vertical velocity is likely to take higher extreme values when reducing the grid box width.

But the lowering of the saturation moisture will imply more condensation only where the local moisture is correlated with the upwards motion. Therefore it is difficult to foresee the trend of the resolved precipitation when varying the mesh size.

The model normally forecasts mean grid box values, which correspond to the maximum precipitation only for stratiform rain bands which are wider than the individual grid boxes. For convective precipitation covering only a fraction of the grid box, the presented mean values are lower than the peak precipitation.

So even in a perfect model, the precipitation amounts do not have to be conserved when varying the mesh size; but this does not free us from the need to be coherent in the water budgets. In the case of a closure of the convective scheme by moisture convergence, the double counting may be avoided by considering that the total moisture convergence towards the grid box is parted between the detrainment of moisture by the updraught and the *total* condensation, i.e. convective and resolved. This was applied for a while with some success in the Aladin model. But it did not solve everything: we are still attempting to superimpose two separate non linear schemes.

The quasi-equilibrium (QE) hypothesis has been widely used in the convection parametrization. It assumes that the adjustment time of the convection ( $\tau_D \sim 10^3 - 10^4 s$ ) is much smaller than the so-called ‘large scale’ forcing ( $10^5 s$ ). But the actual processes affecting the forcing of the convective scheme may include anvil clouds, or local turbulent processes, which have much shorter characteristic times, at least comparable to  $\tau_D$ . The QE hypothesis is then no longer bearable and it becomes necessary to include some memory of the convective activity from one time step to the next. Representing the updraught mass flux as the product of a mesh fraction  $\sigma_u$  by an updraught velocity  $\omega_u$  allows to use a vertical motion equation for the latter. Using  $\omega^* = \omega_u - \omega_e$  the relative updraught velocity, it takes the form

$$\frac{\partial \omega_u^*}{\partial t} = -F_{\text{buoy}} + \frac{\omega_u^{*2}}{p} (1 + \mathcal{K}_f) - \frac{1}{2} \frac{\partial \omega_u^{*2}}{\partial p}$$

where the RHS is composed of a buoyancy term, a dissipation term and a vertical advection term. This equation is actually valid for a single bubble or plume. In a mass flux scheme, we represent the grid box variability composed of various updraughts of different lifetimes, by a single equivalent updraught. Applying the same prognostic equation to this mean updraught may be questionable. Using a closure by moisture convergence, a prognostic equation for the mesh fraction  $\sigma_u$ , may be derived, expressing that the latent heat brought by the moisture convergence is either absorbed in

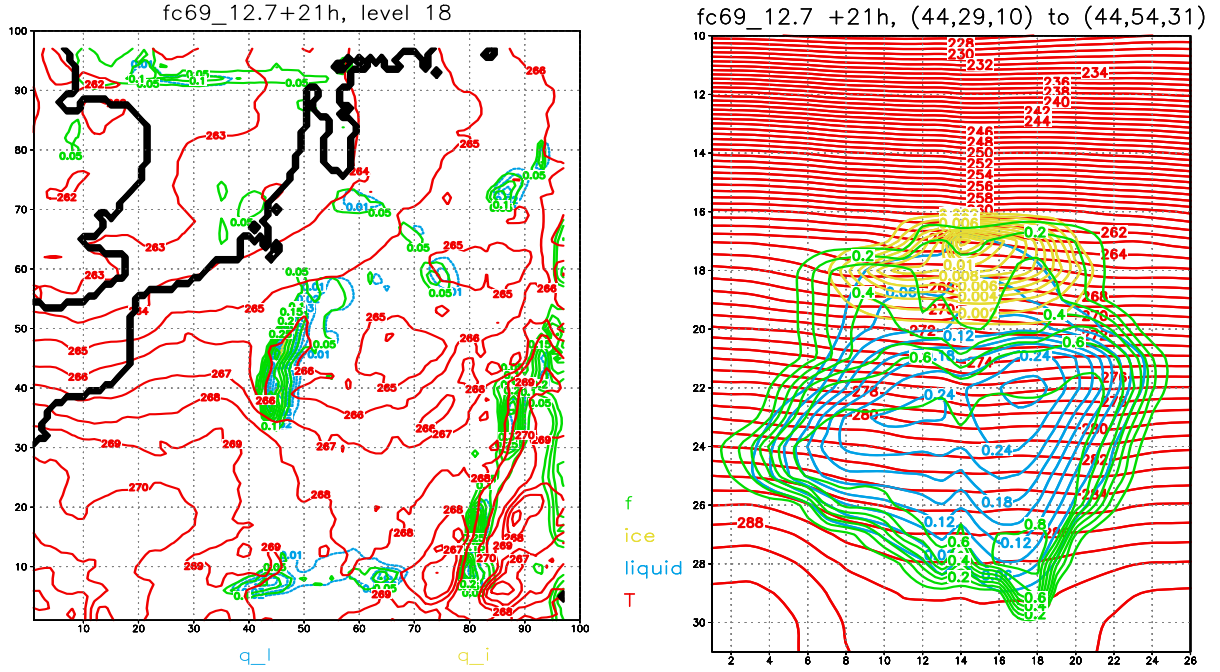


Figure 1: Left: temperature (red), cloud ice (yellow) and liquid (blue), cloud fraction (green) at model level 18 (around 575 hPa). Right: vertical cross section along a cloudy area (Y axis: model levels).

the updraught activity or stored in an increase of  $\sigma_u$ :

$$\underbrace{\frac{\partial \sigma_u}{\partial t} \cdot \int_{p_b}^{p_t} (h_u - \bar{h}) \frac{dp}{g}}_{\text{storage}} = \underbrace{L \int_{p_b}^{p_t} \sigma_u \omega_u^* \frac{\partial \bar{q}}{\partial p} \frac{dp}{g}}_{\text{-consumption}} + \underbrace{L \cdot TMC}_{\text{input}}$$

The profile of the updraught properties (temperature, moisture contents of the different phases, horizontal momentum) should normally also be memorized from one time step to the next, unless we keep considering it as a sequence of quasi-equilibria. The question is whether the time needed by a parcel to raise along the whole profile may be considered smaller than the characteristic time of the external forcing. In our current scheme we make this hypothesis.

The prognostic variables  $\sigma_u$ ,  $\omega_u$  are advected by the mean wind, and a geographical separation of the trigger and effect is possible, as well as a time separation. In this context, we can separate the downdraught from the updraught, allowing the former to survive the latter.

Using an explicit evaluation of the mesh fraction  $\sigma_u$  allows to take into account the updraught properties over it in the grid box averaging, which is important when the grid dimensions are no longer much wider than the scale of the convective events.

The integrated scheme we propose uses a microphysical package (derived from Lopez, 2002) with two cloud water variables (ice and liquid). The updraught is called first and outputs, beside the convective fluxes, detrained cloud water contents on a detrainment area. The resolved condensation is estimated outside the updraught and its detrainment area, and both are combined to enter the rest of the microphysics (auto-conversion to precipitation, Bergeron effect, collection and evaporation of precipitation). The grid box is parted geometrically between the updraught and its detrainment area, the stratiform cloud outside it, the total cloudy area, the precipitation area, the downdraught. There is also a mass flux scheme for a moist downdraught, based on the total precipitation evaporation.

The general structure of our deep convection scheme is still based on Bougeult (1985)'s approach, and this induces some weaknesses which are difficult to overcome. The triggering of the convection is not well modeled. The use of prescribed entrainment profiles makes it impossible to write a local mass budget from which we could either compute the mesh fractions or the detrainment. So, we merely consider (like many schemes) a constant updraught mesh fraction along the vertical, which implies a bad mass flux representation.

An example of model fields is shown in Figure 1. At the present stage, the structure of the forecasted fields appears correct in the 3D cases we tried, but the amounts of precipitation are too low. This seems to be associated to a lack of realism of the detrainment profile of the updraught, and its link to the updraught mass flux. The problem is directly related to the a priori imposition of the entrainment profile mentioned above. New tracks are now investigated, to get out of this trap.

## References

- [BOUGEAULT(1985)] Ph. BOUGEAULT. A simple parameterization of the large-scale effects of cumulus convection. *Mon. Wea. Rev.*, 113:2108–2121, 1985.
- [GERARD and GELEYN(2005)] L. GERARD and J.-F. GELEYN. Evolution of a subgrid deep convection parametrization in a limited area model with increasing resolution. *submitted to Q.J.R. Meteorol. Society*, 2005.
- [LOPEZ(2002)] Ph. LOPEZ. Implementation and validation of a new prognostic large-scale cloud and precipitation scheme for climate and data assimilation purposes. *Q. J. R. Meteorol. Soc.*, 128 (579):229–258, 2002.

## **Towards an operational implementation of Lopez's prognostic large scale cloud and precipitation scheme in ARPEGE/ALADIN NWP models**

*F. Bouyssel, Y. Bouteloup, P. Marquet*

*Météo-France, CNRM/GMAP, 42 av. G. Coriolis, 31057 Toulouse Cedex, France.*

### I) Motivations

The large scale precipitation and the cloudiness schemes used operationally at Météo-France in the global ARPEGE and limited area ALADIN numerical weather prediction (NWP) models for short range forecasting are described in details in the on-line documentation of physical parameterisations prepared and maintained by Luc Gérard (\*). The brief description below is from Geleyn (2003).

The operational large scale precipitation scheme includes neither storage of the liquid and solid phases in the clouds, nor consideration of partial cloudiness. The large scale precipitation occurs when water vapor is above wet bulb water vapor and falls in one time step. A revised Kessler (1969) method is used for computing precipitation evaporation, melting and freezing. A ratio of the falling speed for the two types of precipitation allows distinguishing some aspects in the liquid/ice partition. The diagnostic scheme for the "radiative" clouds link the cloudiness to the production of stratiform and convective precipitations, and to the existence of inversions. The cloudiness functionally depends on the diagnosed total cloud condensate (Xu and Randall, 1996). The convective cloud condensate is obtained from the rate of generation of convective precipitation at the previous time step. The stratiform cloud condensate is estimated from the instantaneous super-saturation of the air properties averaged along a certain delta-theta thickness below, with respect to the local saturation state multiplied by a "critical relative humidity" vertical profile. The partition between ice and liquid state depends only on temperature with a progressive transition below 0°C.

Used operationally since many years, these schemes have proved their robustness and utility for short range forecasting. However the use of more sophisticated microphysics is promising for improving the simulation of clouds, precipitations and surface conditions. Therefore the large scale cloud and precipitation scheme developed by Lopez (2002) has been implemented for evaluation in the last research version of ARPEGE and ALADIN NWP models and also in the ARPEGE climate model which includes the statistical scheme for large scale precipitation and cloudiness developed by Ricard and Royer (1993).

### II) Original Lopez's scheme

A brief overview of the scheme is given below, taken from the whole description available in Lopez (2002).

In short, the scheme of Lopez is based on the approach of Fowler and Randall (1996), where the prognostic cloud contents and the precipitations are not split into separate liquid and solid components, and where any time-stepping is overcome by the use of a semi-lagrangian scheme for the falling of rain and snow, valid for the long NWP and GCM time-steps.

The large scale cloud and precipitation scheme is based on the addition of two prognostic quantities: the amount of cloud condensate (liquid and ice water) and the precipitation content (rain and snow). A prognostic treatment of precipitation has been chosen to provide a finer description of the temporal evolution of the vertical distribution of precipitation (especially snow) and, thus, of the effects of latent-heat release associated with sublimation and evaporation. Furthermore, the scheme has been also designed for future variational assimilation of cloud and precipitation observations for which a prognostic treatment for precipitation should lead to a more direct link between model variables and observations.

The calculations of large scale condensation/evaporation and cloud fraction are based on a triangular probability-density functions (Smith, 1990). The width of this function is adjusted via a critical relative humidity threshold, above which clouds start to appear. The parameterized microphysical processes that involve precipitation are autoconversion, collection and evaporation/sublimation. The autoconversion rate of cloud droplets (ice crystals) into precipitating drops (snowflakes), is given by the simple formulation of Kessler (1969). Three types of collection processes are considered: accretion, aggregation and riming for which the classical continuous collection equation has been integrated over the Marshall-Palmer (1948) exponential particle spectra for specified distributions of particle fall speed and mass. Precipitation evaporation is calculated by integrating the equation that describes the evaporation of a single particle over the assumed spectra of particle number, mass, and fall speed. The fall of rain and snow is considered as a specific process, and is computed using a semi-Lagrangian approach that is separate from the standard semi-Lagrangian advection scheme used in ARPEGE/ALADIN model. Constant values of 5m/s and 0.9m/s are assumed for rain and snow fall speeds, respectively.

At each time step, the partitioning of stratiform cloud condensate into cloud liquid water and cloud ice is diagnosed from the local temperature. Rain is supposed to be present whenever the local temperature is above freezing point, and snow is present otherwise. Falling snow is, therefore, assumed to melt instantaneously as soon as it enters a model layer with temperature above 0°C, provided the associated cooling does not lead to freezing.

The original scheme has been widely validated with satellite observations (METEOSAT, SSMI) on FASTEX (Fronts and Atlantic Storm-Track Experiment) case studies, with remote sensing observations over the Southern Great Plains (ARM) and by comparison with meso-scale models (Met Office’s Unified Model and Méso-NH). The validation has then continued in GCM mode, prior to the present validation in NWP mode.

### III) Some modifications and tunings

The separation of total cloud condensates in two prognostic variables, liquid and solid cloud condensates, has been done to take into account the latent heat exchange resulting from a possible phase change due to the time evolution of the local temperature. This modification makes easier future scientific sophistications and code maintenance since IFS and AROME models use also two prognostic variables for liquid and ice water contents.

The influence of evaporation and collection processes on precipitating water evolution has been improved. The autoconversion process is continuous during the time step and not anymore supposed at the beginning of it. These modifications improve the realism of the 3D field of precipitating water and reduces beneficially the amount of surface precipitations.

An analytical formulation has been designed to describe the dependency of “critical relative humidity” with height and horizontal resolution (figure 1a) in order to fit the experimental values obtained from a large number of aircraft in situ measurements collected during FASTEX (Lopez, 2002).

The partition of stratiform cloud condensate into cloud liquid water and cloud ice has been tuned to allow the coexistence of liquid and ice water at temperatures between -25°C and 0°C (figure 1b).

The cloudiness reduction applied for thick vertical layers is suppressed to increase the consistency between the moist adjustment and the precipitation scheme. Consequently the threshold values for solid water specific humidity, from which start autoconversion, have been strongly reduced (factor 10).

An improved version of the original Lopez scheme has also been developed by Gérard (2005) to be part of an integrated scheme for clouds, precipitation and convection. This version uses two separate prognostic variables for liquid and solid water content and some refinements in the autoconversion process. The precipitating water is not advected anymore ; it is either a pseudo-historic or a diagnostic variable.

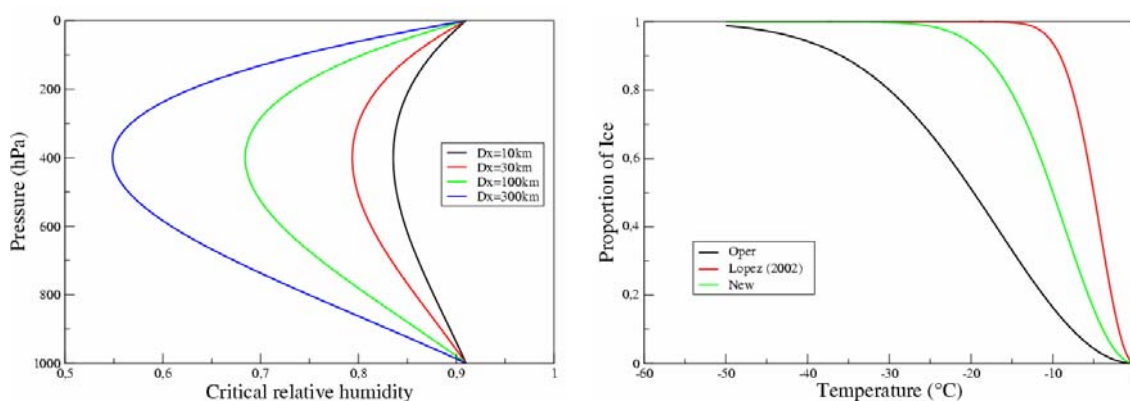


Figure 1a (left): “Critical relative humidity” as a function of pressure and horizontal resolution.  
 Figure 1b (right): Function of temperature which determines the fraction of ice for stratiform cloud condensate.

### IV) Diffusion of conservative variables

The operational scheme for the surface and upper-air exchanges is designed according to Louis (1979) and Louis et al. (1981), with the shallow convection incorporated according to Geleyn (1987) and recently modified to cure a tendency to an on/off behavior in time and along the vertical. The turbulent exchange coefficients’ dependency on the Richardson number in case of stable situations has been improved. The dynamical and thermal mixing lengths

are computed according to a diagnosed PBL height (Troen and Mahrt, 1986 ; Bazile et al., 2005). The dry static energy and the water vapor are diffused.

This scheme has been recently modified in the GCM version of ARPEGE to diffuse the cloud-conserved thermodynamic and water content variables: the moist static energy and the total water content, with the use of cloud cover as a weighting factor to include the subgrid variability of cloud water content. However, for the time being, only the vertical diffusion scheme is changed but not the computation of the turbulent exchange coefficients. This modification stabilizes the scheme as shown on the simulation of a stratocumulus case with the single column model (figure 2a).

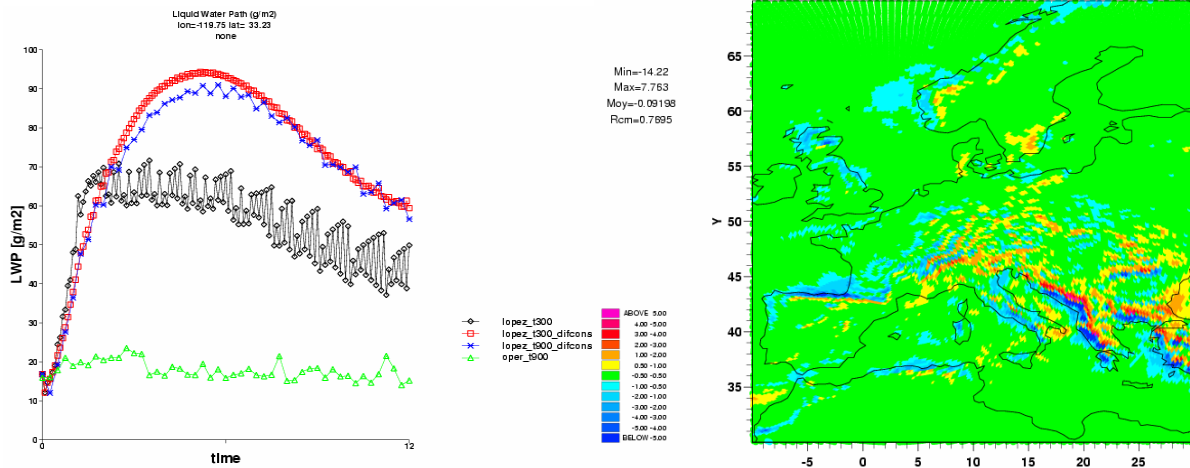


Figure 2a (left): Temporal evolution on 12 hours of Liquid Water Path (g/m<sup>2</sup>) on Eurocs stratocumulus case with the operational scheme ( $\Delta t=900s$ ) and the Lopez's scheme for 2 different time steps ( $\Delta t=300s$  and  $\Delta t=900s$ ) and with and without diffusion of conservative variables ("difcons").

Figure 2b (right): Cumulated precipitation difference (mm/day) between Lopez and operational schemes computed with fifteen 96h ARPEGE forecasts over the period 11-25/02/2005.

## V) Validation

Validation forecasts have been performed with the modified Lopez's scheme and the diffusion of conservative variables, all the other parameterizations (deep and shallow convection, radiation, subgrid scale orography, surface) being unchanged.

Seasonal global runs at various horizontal resolutions (between 25 and 200 km, in stretched and unstretched configurations) have been performed to validate the scheme against climatologies (ISCCP, CERES, GPCP) and to prove its stability for long time steps (1800s at 250km, 900s at 25km, 450s at 10km). Objective scores against observations (SYNOPT, TEMP) and analyses have been performed with a small positive impact on standard deviation of geopotential in the troposphere on North20 and South20 domains and a small negative impact in the Tropics (not shown). The temperature is increased in the Tropics at 200 hPa due to a decrease of water vapor (precipitation occurs now before saturation).

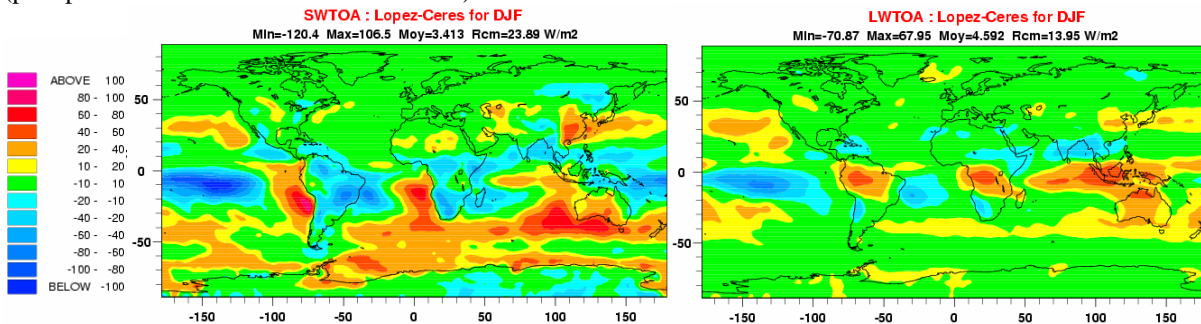


Figure 3: Comparison of the new scheme with CERES climatology for SW and LW net radiation at TOA with ARPEGE at operational resolution (T358C2.4) on DJF.

The impact on cloudiness (figure 4) is an increase of low level clouds at high latitudes and a decrease of low level clouds in the Tropics. There is still an important lack of marine stratocumulus (figure 3), but this problem will be addressed by current developments/validations made jointly with the GCM team on moist TKE scheme (Cuxart, Bougeault, Redelsperger, 2000) and a parametrization of entrainment at the top of PBL (Grenier and Bretherton,

2001). Medium clouds are significantly reduced at high latitudes. Cirrus are higher and more important in the Tropics. The liquid and solid water contents are increased below 900 hPa. Above the amount of ice water content is similar and the amount of liquid water content is significantly reduced in the upper troposphere according to the new partition function (figure 1a).

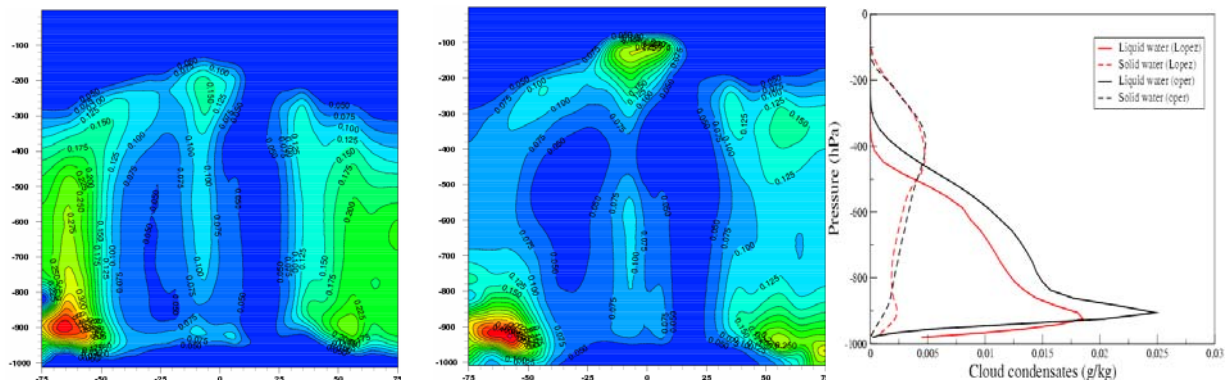


Figure 4: Zonal mean cloudiness with the operational (left) and the Lopez (middle) schemes. Global mean liquid and solid specific humidities for the two schemes (right). Data are computed with fifteen ARPEGE 96h forecasts over the period 11-25/02/2005.

The impact on precipitation is a significant reduction of the extreme amounts of precipitation, particularly above highest mountains. The global amount of total precipitation is slightly reduced, between 0.1 and 0.2 mm/days on average over the globe. The cumulated amount of precipitation is smoother spatially, with more precipitation on the leeward mountains and less on the windward mountains (figure 2b), both aspects being beneficial according to the current model biases. These differences are illustrated on figure 5 which represents the cumulated total precipitation between 6 and 30h ALADIN forecast on a case study with the operational and the new schemes. The comparison with SYNOP observations over Corsica proves that the amount of precipitation was strongly overestimated in the reference and more realistic with the new scheme.

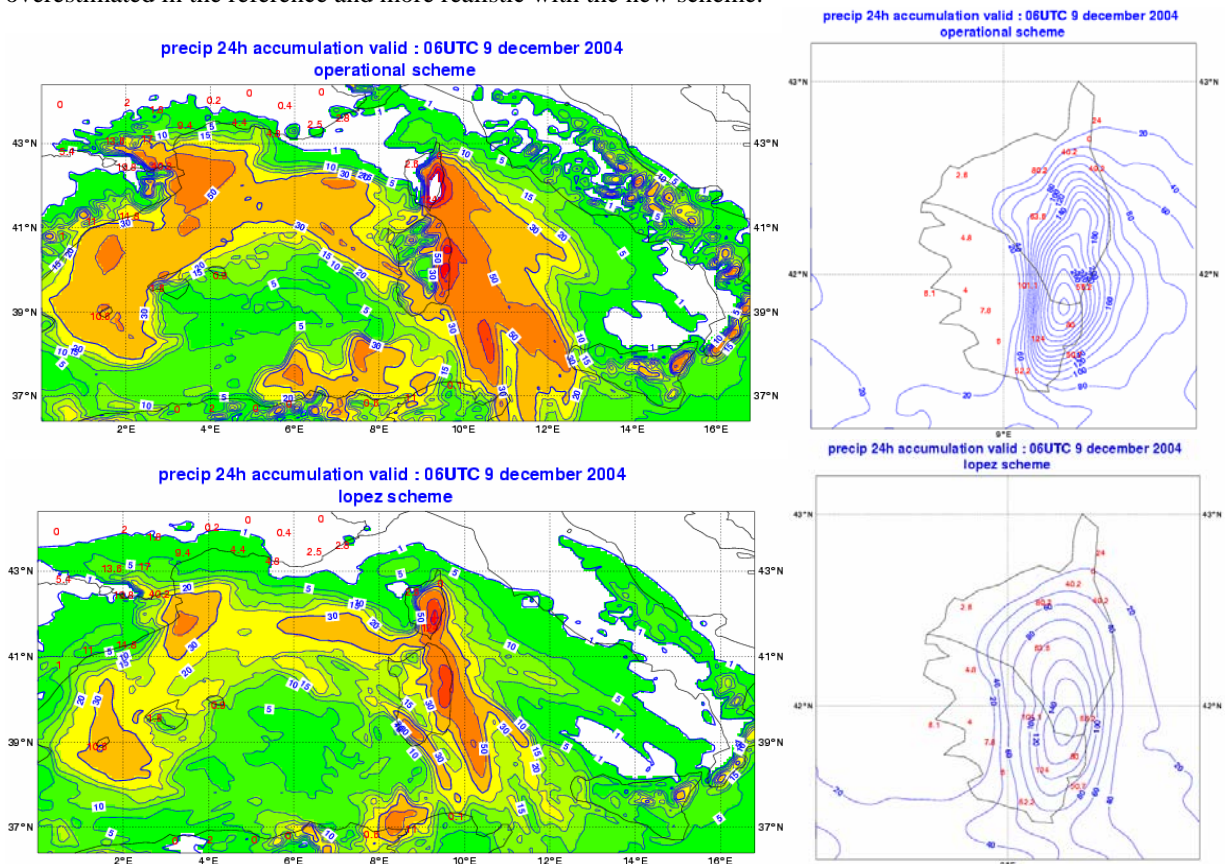


Figure 5: Cumulated precipitation between 6 and 30h forecast obtained from 30h ALADIN forecasts with the operational (top) and Lopez schemes (bottom) starting the 8<sup>th</sup> December 2004 at 00h UTC on the western Mediterranean Sea (left) and over Corsica (right). SYNOP observations are in red.

## VI) Conclusions and perspectives

The Lopez's large scale cloud and precipitation scheme has been implemented in last research version of ARPEGE and ALADIN models. Some improvements have been performed mainly on the treatment of precipitating water in relation with evaporation and collection processes. The scheme has been tuned to improve comparison with climatologies. The vertical diffusion of conservative variables was found necessary to cure stability problems, but a whole moist turbulence would be preferable (in work). Preliminary validations have been done in forecast mode with objective scores, comparison to climatologies and cases studies. The main improvements are a small increase of low level clouds at high latitudes, a smoother spatial precipitation field and a better repartition of precipitation over orography. The validation will continue and focus on 4D-Var assimilation experiments. Some sophistications would be interesting such as a better treatment of the precipitation melting and a separation of precipitating water in rain and snow, but the priority is likely the implementation of a moist turbulence scheme taking into account the prognostic liquid and ice water contents, a work made jointly with the ARPEGE GCM team.

## References

Website for the on-line documentation: <http://www.cnrm.meteo.fr/aladin/MODELES/EXT/Physics/index.html>

Bazile, E., 2005: Interactive mixing length and modification of the exchange coefficients for the stable case. Newsletter ALADIN 27.

Bougeault, P., 1985: A simple parameterization of the large-scale effects of cumulus convection. *Mon. Wea. Rev.*, 113, 2108-2121.

Bougeault, P. and J.-F. Geleyn, 1989: Some problems of closure assumption and scale dependency in the parameterization of moist deep convection for numerical weather prediction. *Meteorol. Atmos. Phys.*, 40, 123-135.

Cuxart, J., P. Bougeault, and J.-L. Redelsperger, 2000: A turbulence scheme allowing for mesoscale and large-eddy simulations. *Quarterly Journal of the Royal Meteorological Society*, Vol. 126 pp. 1-30

Fowler, L., D. and D., A. Randall, 1996: Liquid and Ice cloud microphysics in the CSU general circulation model. Part I, II and III. *J. Climate*, 9, 499-529 / 530-560 / 561-586.

Geleyn, J.-F., C. Girard and J.-F. Louis, 1982: A simple parameterization of moist convection for large-scale atmospheric models. *Beitr. Phys. Atmos.*, 55, 325-334.

Geleyn, J.-F., 1987: Use of a modified Richardson number for parameterising the effect of shallow convection. *J. Met. Soc. Japan*, Special 1986 NWP Symposium Issue, 141-149.

Geleyn, J.-F., 2003: Physical parameterisations in ARPEGE and ALADIN. Internal CNRM notes.

Gérard, L., 2005: Adaptations to ALADIN of the Lopez microphysical package. *ALADIN Newsletter*, 27, 131-134.

Grenier, H. and C. S. Bretherton, 2001: A moist PBL parameterization for large-scale models and its application to subtropical cloud-topped marine boundary layers. *Mon. Wea. Rev.*, 129, 357-377.

Kessler, E., 1969: On the distribution and continuity of water substance in atmospheric circulation. *Atmos. Meteor. Monograph*, Vol. 32, 84 pp.

Lopez, P., 2002: Implementation and validation of a new prognostic large-scale cloud and precipitation scheme for climate and data-assimilation purposes. *Q. J. R. Meteorol. Soc.*, 128, 229-257.

Louis, J.-F., 1979: A parametric model of vertical eddy fluxes in the atmosphere. *Boundary-layer Meteorol.*, 17, 187-202.

Louis, J.-F., M. Tiedke and J.-F. Geleyn, 1981: A short history of the operational PBL-parameterization at ECMWF. *ECMWF Workshop Proceedings on «Planetary boundary layer parameterizations»*, 25-27 November 1981, 59-79.

Ricard, J.-L. and J.-F. Royer, 1993: A statistical cloud scheme for use in an AGCM. *Annales Geophysicae*, 11, 1095-1115.

Smith, R. N. B., 1990: A scheme for predicting layer clouds and their water content in a general circulation model. *Q. J. R. Meteorol. Soc.*, 116, 435-460.

Troen, I. And L. Mahrt, 1986: A simple model of the atmosphere boundary layer; sensitivity to surface evaporation. *Bound.-Layer Meteorol.*, 37, 129-148.

Xu, K.M. and D. Randall, 1996: A semi-empirical cloudiness parameterisation for use in climate models. *J. Atmos. Sci.*, 53, 3084-3102.

# Preliminary tests with the use of separate prognostic treatment of cloud water and ice in Hirlam

Karl-Ivar Ivarsson  
Swedish Meteorological and Hydrological Institute  
S-601 76 Norrköping Sweden

## 1 Introduction.

Cloud condensate is very small droplets of water and of very tiny ice crystals in clouds. Correct amounts of cloud ice and cloudwater are important in atmospheric models since the precipitation release and the both shortwave and longwave radiation depend on the size and type of cloud condensate. Here, cloud ice and cloud water are both defined as particles of such small size that the falling speed ( sedimentation) could be neglected.

Larger ice or liquid water particles are regarded as hydro meteors and thus participating in the precipitation release. In the present Hirlam reference version (6.3.5), the partition of cloud condensate into a liquid part and a ice part is determined by the temperature only. This is an easy and strait-forward way, but there are disadvantages as well. One is that the evolution of clouds and systems of clouds can not be simulated in a realistic way. Mixed phase clouds normally form as liquid water. Ice crystal then grow by water deposition and then fall out as precipitation. At the same time, supercooled water droplets evaporate and thus become smaller or disappear. This process is often called the Bergeron-Findeisen process, and is driven by the difference between the saturation pressure over ice and water. Another one is that the amount of ice and water in the cloud can not be predicted in a realistic way. For instance, if a cloud becomes warmer, some cloud ice is forced to melt and becomes supercooled water. Occasionally, there are events with supercooled rain from clouds with only supercooled water, which are not possible to predict without a prognostic treatment of cloud water and ice.

A parameterization of prognostic scheme of content of ice and water is described in this paper. Some details of the parameterization is given in section 2, and tests with the scheme is evaluated in section 3. There are a short discussion and some conclusions in section 4 and section 5 contains a reference list.

## 2 Description of the parameterization.

### 2.1 General

This parameterization has be implemented in the framework of Hirlam 5.1.4, with some updates to a more recent versions. The code has only been implemented in the current Hirlam version of the Rasch-Kristjansen scheme (RK-scheme) see Rasch and Kristjansen, (1998) for details. Technically, cloud ice has been introduced as an extra scalar, in a similar way as turbulent kinetic energy was introduced for the turbulence parameterization.

### 2.2 Parameterization of the transformation from cloud water to cloud ice

The most important part of parameterization is the growth of cloud ice crystals by water deposition. This parameterization closely follows the one suggested by Rotstayn et al, (2000) for spherical ice crystals. The change of the cloud ice (  $\Delta q_i$  ) for each timestep can be expressed as

$$\Delta q_i = \min(q_w, C(2/3c_{vd}\Delta t + q_{i0}^{\frac{2}{3}})^{\frac{3}{2}} - q_i) \quad (1)$$

Here,  $q_i$  = cloud-ice content ,  $q_w$  cloud-water content ,  $C$  = cloud fraction,  $\Delta t$  = time step and  $q_{i0}$  = initial ice-crystal mass. ( $10^{-12}$  kg).  $c_{vd}$  is given by

$$c_{vd} = 7.8 \frac{(N_i/\rho)^{\frac{2}{3}}(e_{sw}/e_{si} - 1.)}{\rho_i^{\frac{1}{3}}(A_2 + B_2)} \quad (2)$$

$N_i$  is the ice crystal number concentration, given by  $10 \exp(12.96(e_{sw}/e_{si} - 1.) - 0.639)$  , which is 1 % of the concentration given by Meyers et al (1992).  $\rho$  is the density of the air,  $e_{sw}$  and  $e_{si}$  is the water vapor pressure with respect to water and ice respectively and  $\rho_i$  is the density of ice. The value of 700 is used here.  $A_2$  is given by

$$A_2 = \frac{L_s}{K_a T} \left( \frac{L_s}{R_v T} - 1 \right) \quad (3)$$

$L_s$  is latent heat of sublimation,  $K_a$  is the thermal conductivity of air (0.024),  $R_v$  specific gas constant for water, and  $T$  is temperature.  $B_2$  is computed as

$$B_2 = \frac{R_v p T}{2.21 e_{si}} \quad (4)$$

Here,  $p$  is pressure. Two different assumptions about the in-cloud spatial distribution of cloud-ice and cloud-water where tested by Rotstayn et al. One with ice and water totally separated, one with ice and water completely mixed. The relation above is derived for the latter assumption. Here, the in-cloud spatial distribution is assumed to be as follows:

1. One part containing all cloudwater but also cloud-ice with a fraction of  $(1 - f_{ice})C$
2. A second part with only cloud-ice with a fraction of  $f_{ice}C$
3. The concentration of cloud-ice is assumed to be the same in both fractions

Here,  $f_{ice}$  is the part of the cloud condensate that is ice ( $q_i/(q_i + q_w)$ ) . The in-cloud spatial distribution is chosen to let the mean relative humidity used in Eq (8) be consistent with the assumption that there is saturation with respect to water in the mixed-phase part and with respect to ice in the cloud-ice part. This distribution should probably be related to the size of the gridbox, but that should make the parameterization more complex. By this assumption the fraction of cloud containing only cloud-ice increases as the amount of cloud-ice increases. Eq. (1) becomes

$$\Delta q_i = \min(q_w, (1 - f_{ice})C(2/3c_{vd}\Delta t + q_{i0}^{\frac{2}{3}})^{\frac{3}{2}} - (1 - f_{ice})q_i) \quad (5)$$

### 2.3 Parameterization of precipitation release by the Bergeron-Findeisen process

When clouds-ice crystals grow and reach a critical size, they are assumed to fall out as precipitation. A typical time scale for ice crystals to reach that size is computed as a precipitation release by the Bergeron-Findeisen effect. (PBF) This parameterization is based on the ideas described in Hsie el al, (1980) and in Lin el al, (1983). This time-scale  $\Delta t_{bf}$  is computed as

$$\Delta t_{bf} = \frac{1}{8} q_i D_{crit}^2 \frac{e_{sw}/e_{si} - 1}{A_2 + B_2} \quad (6)$$

Eq (6) is also based on the growth of spherical ice crystals. The average ice crystal is assumed to be half-way in time to reach that critical size. Thus,  $(q_i + \Delta q_i) \min(1, 0.5\Delta t_{bf}/\Delta t)$  is assumed to be transformed from cloud ice to precipitation each timestep.  $\Delta q_i$  is computed by Eq (5). Technically, the term  $(q_i + \Delta q_i)/\min(1, 0.5\Delta t_{bf})$  is transported to the routine for cloud-micro physic (FINDMCNEW) .

## 2.4 The cloudcover calculation

The calculation of cloudcover follows the original code based on Slingo but with some minor changes. It is based on relative humidity, ( $RH_{mix}$ ) which is a mixture of saturation with respect to water ( $RH_w$ ) and ice ( $RH_i$ ). This mixture is only temperature dependent in the original code. Here, it is dependent on the actual value of  $f_{ice}$  and of the total amount of cloud condensate.

$$RH_{mix} = \alpha RH_{start} + (1 - \alpha) RH_{cloud} \quad (7)$$

where  $\alpha$  is set to unity if there is no cloud condensate and a linear transition to zero when the cloud condensate is larger than a critical value. The critical value is set to  $1/300 * (f_{ice} * q_{si} + (1 - f_{ice})q_{sw})$ .  $q_{si}$  and  $q_{sw}$ .  $RH_{start}$  is computed as  $\beta RH_w + (1 - \beta)RH_i$  where  $\beta$  is set to unity above -35 C, and to 0.25 below -69, and a linear transition in between. The values 1/300, -35, -69 and 0.25 are chosen in such way that parameterization should be not too far from some cirrus-parameterizations found in the literature e.g. Heymsfield et al., (1995) or Zurovac-Jevtic, (1999), but without making the parameterization unnecessarily complicated. It is also consistent with the assumption that mixed-phase clouds in the the beginning only contains cloudwater.  $RH_{cloud}$  is just a linear function of  $f_{ice}$ :

$$RH_{cloud} = (1 - f_{ice})RH_w + f_{ice}RH_i \quad (8)$$

## 2.5 Other important modifications

The fraction of ice used in the radiation scheme is only temperature dependent in the reference version. Here, it is replaced by  $f_{ice}$ . The relative humidity used in the condensation routine is computed in the same way as  $RH_{mix}$ . The convective cloud condensate which is computed in the convection scheme should also be divided into a liquid part and an ice part. The same should also be done for the change of the total condensate that is computed in the stratiform condensation scheme. Also here,  $f_{ice}$  is used, which is an easy way, but a weak part of the parameterization and will be discussed later.

# 3 Test results

## 3.1 0-D tests

“0-D tests” are simulations with just a single gridbox in this context. They have been used to study the two new parameterizations, the one of the transformation from cloud water to cloud ice, and the parameterization of PBF. One example of such tests are seen in figure 1. To the left is the evolution of the cloud condensate amount and the fraction of cloud ice if only the transformation from cloud water to cloud ice using Eq ( 5) is considered. The same evolution is seen to the right, when also the PBF is included. In all experiments,  $f_{ice}$  are zero in the beginning and the amount of cloud condensate is set to 3% of value of  $q_{sw}$  in all simulations. The cloud fraction is assumed to be 0.5, and the threshold diameter for ice-crystals to become precipitation is 0.5 mm.

The ice crystal concentration is only 1% of the value proposed by Meyers et al (1992). The reason for using that low value is to prevent the amount of cloud ice to get unrealistically high in the 3-D runs. Here, the opposite seems to be the case, at least for -35 C. Homogeneous freezing of cloud drops is an important process for temperatures lower than about -33 C, (Heymsfield and Miloshevich, 1993) and that is not taken into account here. It is also seen that including the PBF, the increase of cloud-ice is suppressed, which seems to be realistic.

## 3.2 3-D tests

Our operational Hirlam version have been run for a cold winter period, ( Jan 14 - 29 1999) and then the same version, but with separated prognostic equation for cloud water and cloud ice based on the parameterizations described in this paper. This two runs are called C22 and i22 respectively. The operational version is based on the framework of Hirlam-5.1.4, but with some updates from later versions. The RK-scheme is used

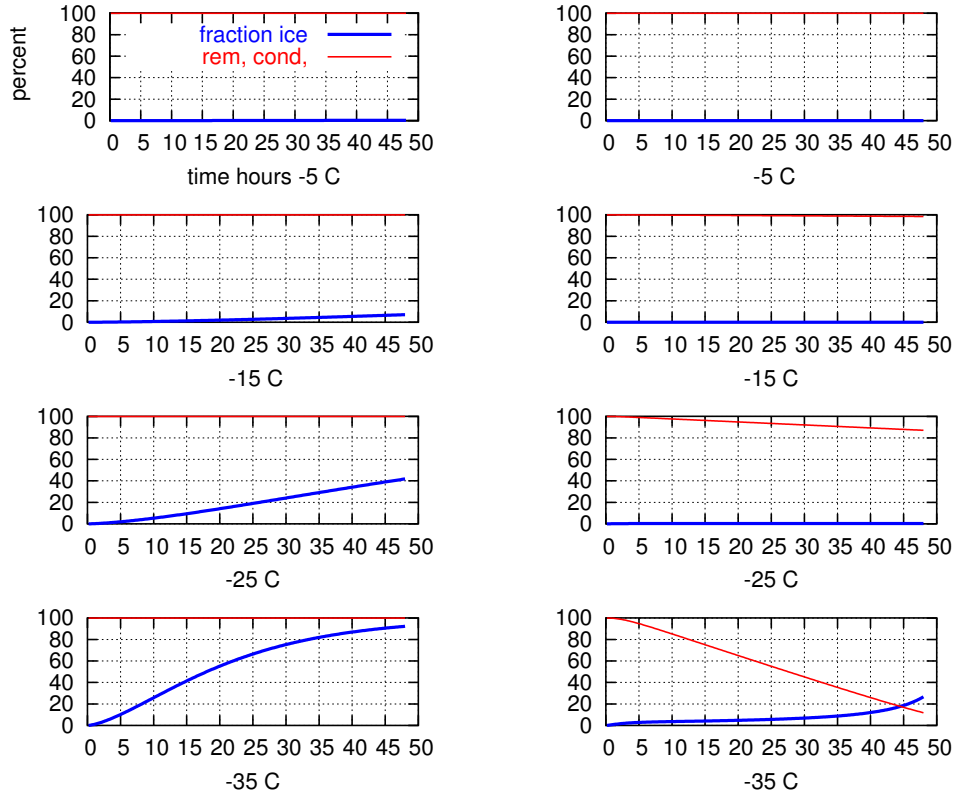


Figure 1: Time evolution of the fraction of ice for -5, -15 , -25 and -35 C. The red curve is the remaining amount of cloud condensate, and the blue is  $f_{ice}$ .

together with the Kain-Fritsch convection scheme. The area contains 306 x 306 gridpoints and 40 vertical levels. It covers mainly the North Atlantic, Europe, western Russia and a part of the Arctic sea. Semi-Lagrangian advection is used and a timestep of 10 minutes. The horizontal resolution is 0.2 degrees (22km). An analysis cycle length of 6 hours is used and the analysis technique is 3-DVAR. The verification result for the surface parameters is seen in figure 2.

It is basically the same for both runs, there are some small differences that one might notice anyway. The mean 2-meter temperature is a little bit higher in i22. A more detailed analysis shows that the temperature is generally colder in the northern part of the domain and warmer in the southern part than C22. The reason for the differences is not clear. One hypothesis is that a smaller amount of cloud-water in i22, (figure 4), makes the clouds more transparent for both longwave and shortwave radiation. The outgoing radiation is more important in the northern part and this leads to a cooling, but in the southern part in shortwave radiation is more important and thus the net result is a warming.

The verification result for upper air data is seen in figure 3. 3. The main difference between the runs is that the relative warming seen in i22 in the lowest part of the troposphere is compensated by a cooling between 700 and 300 hPa. The higher relative humidity in i22 is probably a second effect of this cooling. The reason for the cooling is not clear. Other differences are small. The mean fraction of ice,  $f_{ice}$  for different temperatures are seen in figure 4. The fraction of ice is generally somewhat higher than what is prescribed in the reference run, where it is assumed that  $f_{ice}$  increases linearly from zero at 0 C to unity at -40. Is not clear what the “truth” should be. Different studies give different result, and the variation of  $f_{ice}$  might also be dependent on the season, the type of weather regime and of the location. The prescribed relation is rather close to that found by Intrieri et al. But Bower et al. (1996), found much more cloud-ice

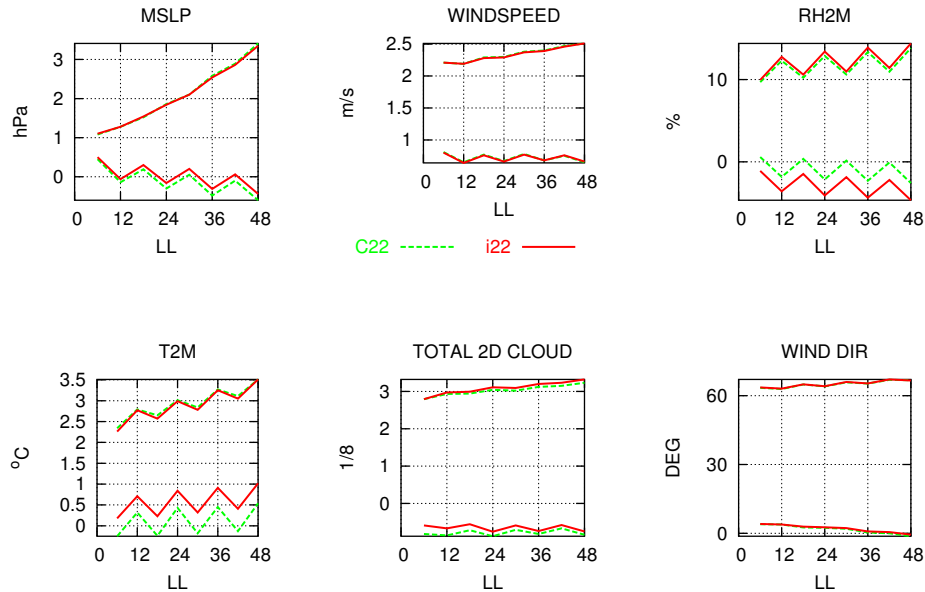


Figure 2: Verification result for European Ewglam stations for some surface parameters and different forecast lengths. C22 is the operational version i22 is with the new parameterization

in frontal stratiform clouds, but less in deep convective clouds. Bower et al., included also large ice particles (precipitation), thus giving higher  $f_{ice}$ , so those results are difficult to compare with the ones here.

A case study have been done for testing the parameterization for a rare weather event over Denmark and southern Sweden in January 15 1987. Then, supercooled drizzle and supercooled rain was reported for most weather-stations over that area. In this case the precipitating cloud was near the 925 hPa level, and the temperature inside the cloud was -10 to -13 C. It is clear that this cloud had no or very little cloud ice. However, the modeled cloud contained mostly cloud ice, so for this particular case the cloud ice content was far too high. But one have to bear in mind that this was an exceptional case.

Beesley et al (2000) compared the forecasted  $f_{ice}$  in the ECMWF model with observations over the Arctic region in November and December of 1997. The ECMWF model assumes a temperature-dependent partitioning of cloud condensate between water and ice, with a parabolic distribution of  $f_{ice}$  from zero at 0 C to unity at -23 C. A much larger fraction of liquid water clouds was observed than the ECMWF model predicted. This study indicates that assuming that  $f_{ice}$  increases linearly from zero at 0 C to unity at -40 might not be to far from “reality”, but there are rather large uncertainties in the measurements, both regarding the partition between ice and water and between cloud ice and precipitation.

## 4 Discussion and conclusions

Two versions of the Hirlam model have been run for a cold 15-day period in winter. One, using the standard way of determine the fraction of cloud condensate that is ice,  $f_{ice}$  based on a temperature dependent relation. A separate prognostic scheme for cloud water and ice have been used in the other one. The verification shows a near neutral impact of the forecast performance. There is a cooling in the upper part of the troposphere and also near the ground in the arctic region compared to the reference run. But there is a warming near the ground at southern latitudes. It is assumed that this might be caused by higher cloud ice content and lower could water content. The total cloud condensate content is nearly the same as in the reference run. (not shown). The fraction of cloud condensate that is ice is higher in experimental run. It is not clear if the contents of cloud ice and water are realistic or not, since this is difficult to validate. Satellite pictures could

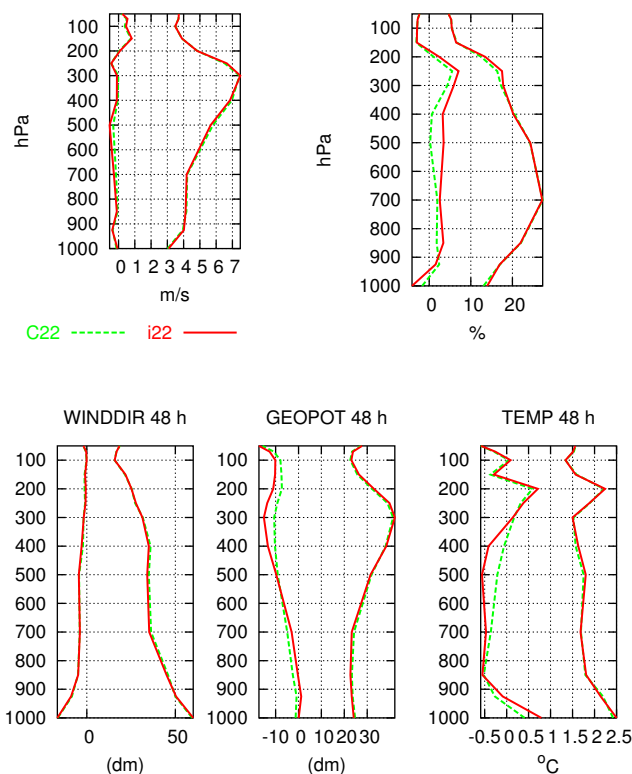


Figure 3: Verification result for European Ewglam sounding stations for 48 hour forecasts. C22 is the operational version i22 is with the new parameterization.

be used to validate this, but no such studies have been done yet.

The parameterization used here could be improved by a better use of the existing parameterization of the precipitation release. Thus, it is possible to determine how much of the cloud ice and how much of the cloudwater that should be transformed into precipitation. Here, this partition is just set to  $f_{ice}$ , and sensitivity studies indicate that this is the main reason for the high content of cloud ice, which in this test is suppressed by the use of a low ice crystal concentration. Also, the convective cloud condensate is partitioned in this simple way, and this is probably not the most realistic approach. Another question is how to initialize the ice fraction  $f_{ice}$ . Here, the prescribed temperature relation in the reference run is used. Different crystal habits for different temperatures are not considered, but may be of importance. It would also be important to test this parameterization in a more recent version of the Hirlam model, and also to use a more recent version of the RK-scheme.

## 5 REFERENCES.

Beesley et al 2000

'A comparison of cloud and boundary layer variables in the ECMWF forecast model with observations at Surface Heat Budget of the Arctic Ocean (SHEBA) ice camp.' *Journal of geophys. res.*, 105, NO. D10, 12,337-350

Bower K. N. et al 1996

' A parameterization of the ice water content observed in frontal and convective clouds.' *Q.J.R. meteorol. Soc.* 122 1815-1844.

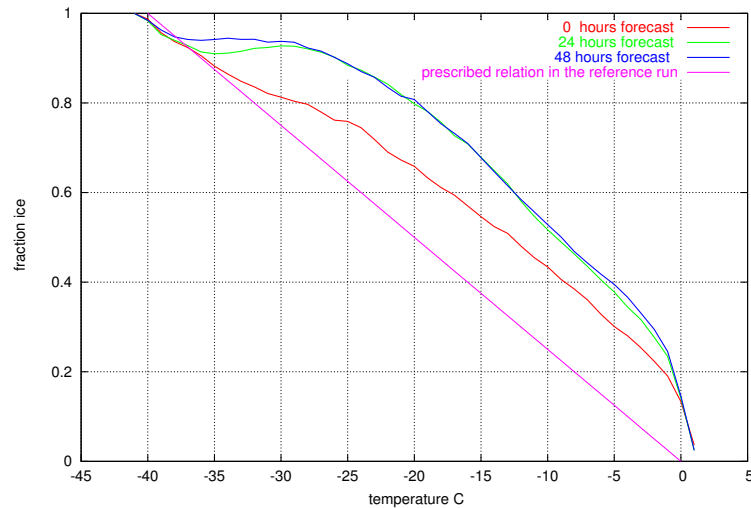


Figure 4: The fraction of the cloud condensate that is ice for different temperatures and forecast lengths, compared to the prescribed temperature dependent relation in the reference run.

Heymsfield, A.J., and L.M. Miloshevich 1993.	'Homogeneous ice nucleation and supercooled liquid water in orographic wave clouds.' <i>J. Atmos. Sci.</i> , 50, 2335-2353.
Heymsfield, A.J., and L.M. Miloshevich 1995.	'Relative humidity and temperature influence on cirrus formation and evolution: observations from wave clouds in FIRE II.' <i>J. Atmos. Sci.</i> , 41, 846-855.
Hsie et al 1980:	'Numerical simulation of ice-phase convective cloud seeding.' <i>J. Appl. Meteor.</i> 19 1950-1977
Lin et al 1983:	'Bulk parameterization of the snow field in a cloud model. ' <i>J. Appl. Meteor.</i> 22 1065-1092.
Meyers et al 1992	'New primary ice-nucleation parameterization in an explicit cloud model. ' <i>J. Appl. Meteor.</i> 31 708-721.
Rasch P.J. and Kristjansson J.E. 1998	' A comparison of the CCM3 model climate using diagnosed and predicted condensate parameterizations. ' <i>Journal of Climate</i> , p 1587 -1614
Rotstayn et al 2000:	'A Scheme for calculation of the liquid fraction in mixed-phase stratiform clouds in large scale models. ' <i>Mon. wea. rev.</i> , Vol 128 p 1070-1088.
Zurovac-Jevtic, D., 1999.	'Development of a cirrus parameterization scheme: Performance studies in HIRLAM.' <i>Mon. Wea. Rev.</i> , Vol 127, 470-485 .

# Parameterization of Convection in the Global NWP System GME of the German Weather Service

*Dmitrii Mironov<sup>†</sup> and Bodo Ritter*

German Weather Service, Offenbach am Main, Germany  
(dmitrii.mironov@dwd.de, bodo.ritter@dwd.de)

In this note, recent results concerning the parameterization of convection in the global numerical weather prediction (NWP) system GME (Majewski et al. 2002) of the German Weather Service (DWD) are briefly described. GME utilises the well-known Tiedtke (1989) mass-flux convection parameterization scheme that contains only minor modifications as compared to its original release. With the ultimate goal to improve the representation of atmospheric convection in numerical models, in GME in particular, the work at DWD over the last one and a half year proceeded along two lines. (i) An analytical study is performed with the aim to better understand what we actually do when applying mass-flux convection schemes, that were initially developed for NWP systems with coarse horizontal resolution (300 to 200 km), in the present-day resolution (50 to 5 km) global and limited-area NWP systems. To this end, the fundamentals of the mass-flux modelling framework are briefly recollected and a number of assumptions that stand behind the current mass-flux convection schemes are critically considered. The analogy between budget equations for the second-order statistical moments of fluctuating fields derived in the mass-flux modelling framework and in the ensemble-mean modelling framework with Reynolds averaging are examined. These exercises help elucidate the essential physics behind the mass-flux approach and the meaning of various disposable parameters of mass-flux schemes. They help address a key question as to which assumptions behind the mass-flux parameterization schemes should be reconsidered and relaxed. (ii) Several modifications in the existing GME mass-flux convection scheme are tested through a series of numerical experiments. The aim of this exercise is to improve the GME performance as much as possible without major changes in the existing convection scheme, i.e. keeping the framework of the traditional mass-flux approach. This purpose is served by tuning/ revising convective trigger function, formulation of entrainment and detrainment, and the way convective precipitation is generated and evaporated.

Figure 1 illustrates the GME performance in the Tropics. The diurnal cycle of surface precipitation in the Rondônia area, Brazil, in February is simulated with GME, using the GME binary operational in March 2004 and the 1999 GME analysis stored in the DWD data bank for the model initialisation. The GME output is compared with the output from the two versions of ECMWF IFS (Bechtold et al. 2004) and with observational data from the 1999 Large-Scale Biosphere-Atmosphere Experiment (LBA) wet season campaign (Silva Dias et al. 2002). Observations demonstrate a strong diurnal cycle of surface precipitation that is dominated by convection. As Fig. 1 suggests, the GME performance is not unsatisfactory, although some problems are readily apparent. In particular, a too early onset of strong day-time precipitation and a too early precipitation maximum are predicted. The night-time precipitation maximum seen in data is missing in the GME output. The ECMWF IFS shows a similar performance, except that the night-time precipitation maximum is simulated slightly better with the ECMWF IFS 25R4.

---

<sup>†</sup>Corresponding author address: Deutscher Wetterdienst, AP2003, Kaiserleistr. 29/35, D-63067 Offenbach am Main, Germany.

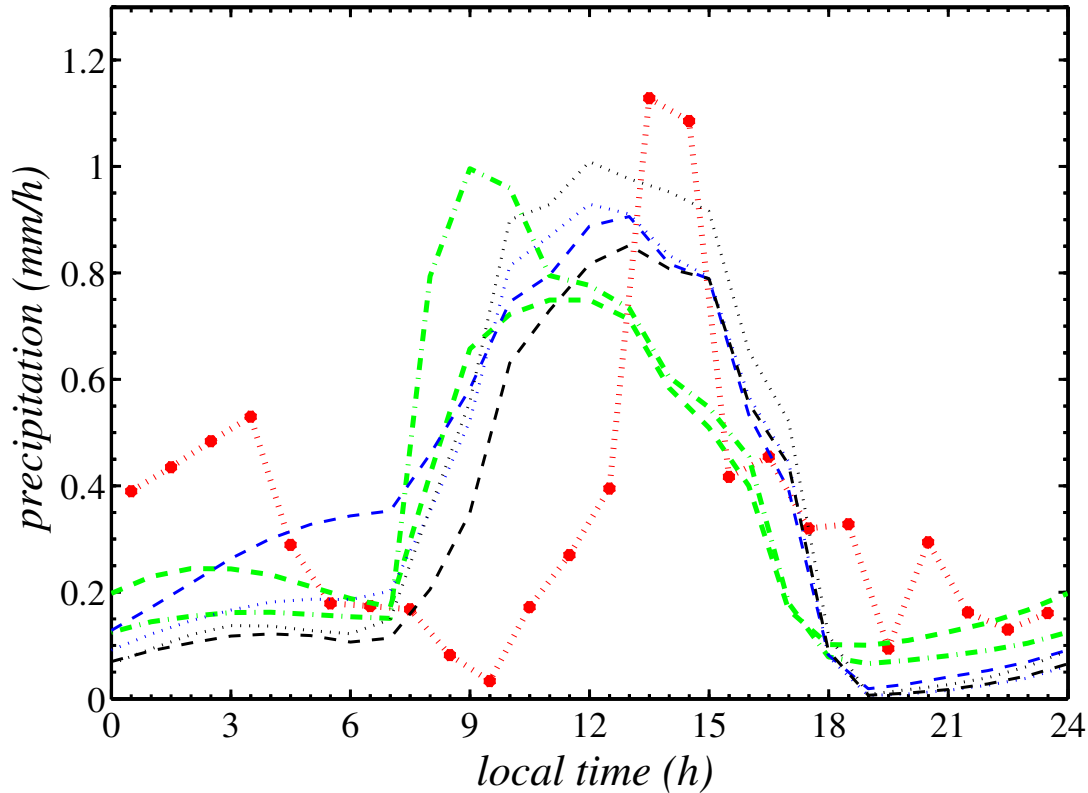


Figure 1. Diurnal cycle of surface precipitation in the Rondônia area. Midnight at Rondônia corresponds to ca. 4:30 UTC. Red heavy dotted curve shows the LBA 1999 observational data. Green heavy dot-dashed curve and green heavy dashed curve show the 24–72 hour (local time) T511 ECMWF forecasts performed with the 25R1 and 25R4 versions, respectively, of the ECMWF IFS. The ECMWF results are obtained by means of averaging over February 2002 and over a lat-long rectangle whose corners’ co-ordinates are 7.7 S 74.1 W, 1.8 S 65.0 W, 4.0 S 60.5 W, and 13.8 S 71.7 W. Thin curves show the GME results obtained by means of averaging over the period from 29 January to 28 February 1999 and over the  $10^\circ \times 10^\circ$  lat-long square (2 S to 12 S, 63 W to 73 W). Thin dashed curves show the 4–28 h forecast initialised at 00 UTC (blue) and the 16–40 h forecast initialised at 12 UTC (black); thin dotted curves show the 28–52 h forecast initialised at 00 UTC (blue) and the 40–64 h forecast initialised at 12 UTC (black). The 00 UTC GME curves show total precipitation, whereas the 12 UTC GME curves show convective precipitation only.

Further test runs are performed to look at the GME performance in mid-latitude. Numerical experiments reveal problems with the precipitation timing in mid-latitudes similar to those in the Tropics. In most cases, convection is triggered too early leading to a premature day-time precipitation maximum. Furthermore, convection in mid-latitudes is typically too active.

In an attempt to better understand the reason for the above deficiencies an analytical study of the mass-flux modelling framework is performed. A consideration of basic assumptions that stand behind the current mass-flux parameterizations suggests that many of them are too restrictive. These are, first of all, the assumptions that (a) convection is quasi-stationary (no

time-rate-of-change terms in the mass-flux equations), and that (b) in a triple decomposition of a quantity in question (vertical velocity, temperature, humidity) into the contributions from updraughts, from downdraughts, and from the so-called environment, a mean over the environment is equal to a mean over the entire grid box. The assumption (a) deprives a convection scheme of memory. As a result, a scheme responds to external forcing practically instantaneously, leading to a premature initiation of convection and an erroneous diurnal cycle. The assumption (b) actually means that the area covered by convective updraughts and downdraughts is small as compared to the size of the grid box. This assumption is justified, to a good approximation, for the horizontal grid size of order 200-300 km, but is less justified if the grid size is of order 50 km typical of the present-day global NWP systems, not to mention the limited-area NWP systems whose grid size falls below 10 km. Then, there is no wonder that the current mass-flux convection schemes are too active, most notably, in mid-latitudes. A wealth of DWD experience with GME and with the limited-area NWP system LM (Steppeler et al. 2003) strongly suggests that the above is indeed the case. It is notable that the fact that the assumption (b) is invalidated as the resolution of the atmospheric model is increased was pointed out already by Tiedtke (1988, page 21). Unfortunately, little caution has been exercised in numerous subsequent applications, where the Tiedtke (1989) scheme and similar mass-flux convection schemes have been applied without regard for their limits of applicability.

The analogy between the mass-flux and the ensemble-mean (i.e. Reynolds-averaged) budget equations for the second-order statistical moments of fluctuating fields is examined. An analysis of the scalar variance equations has been performed by de Rode et al. (2000) and Lappen and Randall (2001). They found, among other things, that the sum of the lateral entrainment and detrainment rates in the mass-flux equation corresponds to the inverse scalar-variance dissipation time scale in the ensemble-mean equation. We extend the analysis of de Rode et al. (2000) and Lappen and Randall (2001) to examine the budgets of the vertical-velocity variance and of the vertical scalar flux.

We find that the term with the entrainment and detrainment rates in the mass-flux budget of the vertical-velocity variance describes the combined effect of dissipation and of pressure redistribution. A similar term in the mass-flux budget of the scalar flux is the destruction term that describes the pressure effects. This is in apparent contradiction with the interpretation of the entrainment-detrainment term in the mass-flux budget of the scalar variance, where it describes the scalar-variance dissipation. This shows the inherent limitation of the mass-flux models, at least as they are currently used in the NWP systems. Since the scalar-variance dissipation, the velocity-variance dissipation, the pressure redistribution and the pressure gradient-scalar covariance depend on the mean flow variables in very different ways, it seems very difficult, if not impossible, to describe all the above effects in terms of only two quantities, the rates of lateral entrainment and detrainment.

A positive outcome of the above analytical exercise is that it suggests an improved formulation for the rates of turbulent entrainment and detrainment. Using the second-order closure ideas as to the parameterization of the pressure-scalar covariances in convective flows (e.g. Zeman 1981, Mironov 2001), an extended formulation for the rates of turbulent entrainment  $E_u$  and detrainment  $D_u$  in convective updraughts is derived (details of the derivation will be reported in the subsequent papers). It reads

$$(E_u, D_u) = M_u \left[ (\epsilon, \delta) + C_B a_u^2 (1 - a_u)^2 \frac{g}{\bar{\theta}} \frac{\theta_u - \bar{\theta}}{(M_u/\bar{\rho})^2} \right] = M_u \left[ (\epsilon, \delta) + C_B \frac{g}{\bar{\theta}} \frac{\theta_u - \bar{\theta}}{(w_u - \bar{w})^2} \right]. \quad (1)$$

Here,  $g$  is the acceleration due to gravity,  $w$  is the vertical velocity,  $\theta$  is the potential temperature,  $M_u$  is the convective mass flux,  $a_u$  is the fractional area coverage of convective updraughts,

$\rho$  is the density, and  $C_B$  is an dimensionless constant. A subscript “u” refers to convective updraughts. An overbar denotes a grid-box mean. The first term in brackets on the right-hand side of Eq. (1) corresponds to the original Tiedke (1989) formulation, where  $E_u$  and  $D_u$  are set proportional to the updraught mass flux  $M_u$  through the constant fractional entrainment  $\epsilon$  and detrainment  $\delta$  rates (their dimensions is  $\text{m}^{-1}$ ). The second term in brackets accounts for an important dependence of  $E_u$  and  $D_u$  on the potential-temperature (buoyancy) difference between the updraught and the environment.

A series of GME runs are performed to test the extended entrainment/detrainment formulation (1). By and large, the GME performance in mid-latitude is positively affected in that convective activity is slowed down. The amount of convective precipitation, that is typically overestimated, is reduced and the initiation of convection is somewhat delayed. The GME performance in the Tropics is, however, not improved as the suppression of convective activity is somewhat too strong. The result is not conclusive and further testing is required.

Several other modifications in the existing GME mass-flux convection scheme have been tested two of which are mentioned here. (i) Suppressing convective precipitation in favour of grid-scale precipitation has a neutral or a slightly positive impact on the GME performance in mid-latitudes. However, the performance in the Tropics is slightly deteriorated. (ii) A modified formulation for the trigger-function is developed. Potential temperature and specific humidity of a convective test parcel is determined by means of averaging over the updraught source layer that extends from the first model level above the underlying surface to the cloud base. A zero-order approximation to the cloud base height is found using a test parcel that originates from the first model level above the surface. In this way, the test parcel properties are less dependent on the vertical resolution than the original Tiedtke (1989) formulation currently used in the GME convection scheme. The proposed formulation involves only marginal additional computational cost (it requires only one additional call to a routine that computes the cloud base height). Other trigger-function formulations proposed to date (e.g. Kain 2004) may be somewhat more physically plausible, but they are computationally expensive as they involve an iterative procedure to determine the updraught source layer. The proposed modifications in the trigger-function formulation has a slightly positive impact on the GME performance. Convective activity is slowed down. A day-time precipitation maximum in the Tropics is slightly shifted towards late afternoon, i.e. towards the time it should occur according to the observations.

An overall conclusion is that the performance of the GME mass-flux convection scheme leaves much to be desired, but is not entirely unsatisfactory. The performance will deteriorate as the horizontal resolution is increased. To avoid this requires major changes in the GME convection scheme. In all likelihood, the same is true for most (if not all) other mass-flux convection schemes used in global and limited-area NWP systems. Minor “cosmetic” changes within the existing mass-flux framework will hardly improve the representation of convection. A notable advance requires that a number of basic assumptions behind the mass-flux schemes be reconsidered and relaxed, and advanced formulations for various components of convection schemes be developed. A step forward in this direction is the extended entrainment/detrainment formulation given by Eq. (1). In a long-term prospective, a unified convection-turbulence scheme based on the second-order closure ideas seems to be an attractive alternative. Such scheme should account for non-local features of convective mixing and should treat all sub-grid scale mixing processes in a unified framework. Work along this line is initiated at DWD.

*Acknowledgements.* We thank Peter Bechtold of ECMWF for providing results from the ECMWF IFS forecasts, and Michael Buchhold, Thomas Hanisch, Erdmann Heise, Detlev Majewski, Werner Wergen and other colleagues at DWD for discussions and helpful suggestions.

## References

- [1] Bechtold, P., J.-P. Chaboureau, A. Beljaars, A. K. Betts, M. Köhler, M. Miller, and J.-L. Redelsperger, 2004: The simulation of the diurnal cycle of convective precipitation over land in a global model. *Quart. J. Roy. Meteorol. Soc.*, **130**, 3119–3138.
- [2] Kain, J. S., 2004: The Kain-Fritsch convection parameterization: an update. *J. Appl. Meteorol.*, **43**, 170–181.
- [3] Lappen, C.-L., and D. A. Randall, 2001: Toward a unified parameterization of the boundary layer and moist convection. Part I: A new type of mass-flux model. *J. Atmos. Sci.*, **58**, 2021–2036.
- [4] Majewski, D., D. Liermann, P. Prohl, B. Ritter, M. Buchhold, T. Hanisch, G. Paul, W. Wergen, and J. Baumgardner, 2002: Icosahedral-hexagonal gridpoint model GME: description and high-resolution tests. *Mon. Weather Rev.*, **130**, 319–338.
- [5] Mironov, D. V., 2001: Pressure-potential-temperature covariance in convection with rotation. *Quart. J. Roy. Meteorol. Soc.*, **127**, 89–100.
- [6] Silva Dias, M. A. F., S. Rutledge, P. Kabat, P. L. Silva Dias, C. Nobre, G. Fisch, A. J. Dolman, E. Zipser, M. Garstang, A. O. Manzi, J. D. Fuentes, H. R. Rocha, J. Marengo, A. Plana-Fattori, L. D. A. Sá, R. C. S. Alvalá, M. O. Andreae, P. Artaxo, R. Gielow, and L. Gatti, 2002: Clouds and rain processes in a biosphere-atmosphere interaction context in the Amazon Region. *G. Geophys. Res.*, **107**(D20), 8072, doi:10.1029/2001JD000355.
- [7] Steppeler, J., G. Doms, U. Schättler, H. W. Bitzer, A. Gassmann, U. Damrath, and G. Gregoric, 2003: Meso-gamma scale forecasts using the non-hydrostatic model LM. *Meteorol. Atmos. Phys.*, **82**, 75–96.
- [8] Tiedtke, M., 1988: *The Parameterization of Moist Processes. Part 2: Parameterization of Cumulus Convection*. Meteorological Training Course, Lecture Series, European Centre for Medium Range Weather Forecasts, Reading, UK, 78 pp.
- [9] Tiedtke, M., 1989: A comprehensive mass flux scheme for cumulus parameterization in large-scale models. *Mon. Weather Rev.*, **117**, 1779–1800.
- [10] Zeman, O., 1981: Progress in the modelling of planetary boundary layers. *Ann. Rev. Fluid Mech.*, **13**, 253–272.

## Testing bulk parameterization of microphysics in ALARO 10

Tomislav Kovacic  
DHMZ, Croatia  
kovacic@cirus.dhz.hr

### Summary

The most recent development in Meteo France is a high resolution (<10 km) model, AROME. Its prototype is based on ALADIN non-hydrostatic dynamic core and physics parameterisations from Meso-NH. At the same time a project ALADIN-2 is under way. One of its subprojects is ALARO 10, a hydrostatic counterpart of AROME, to be used on the 10 km scale with longer time step. In short terms it can be described as ALADIN hydrostatic dynamic core and physics parameterisations from Meso-NH plus parameterisation of convection.

For microphysics a bulk parameterisation is used with five water species, these are: cloud water, cloud ice, rain, snow and graupel. This scheme is used for precipitation on resolved scales. For convective precipitation Kain-Fritsch-Bechtold parameterisation is used.

The first results with ALARO 10 prototype revealed a dependency of precipitation amounts coming from microphysical scheme on time step. With longer time steps there is more precipitation than with shorter ones. To cure this problem a time splitting for microphysical scheme was introduced in the model. The microphysical scheme for each vertical column is calculated several times for one time step of the model. This is controlled by number of iterations of microphysics, so the time step for microphysics is given as  $MPSTEP = TSTEP / NITER$ , where  $MPSTEP$  is a time step for microphysics,  $TSTEP$  is a time step of the model and  $NITER$  the number of iterations.

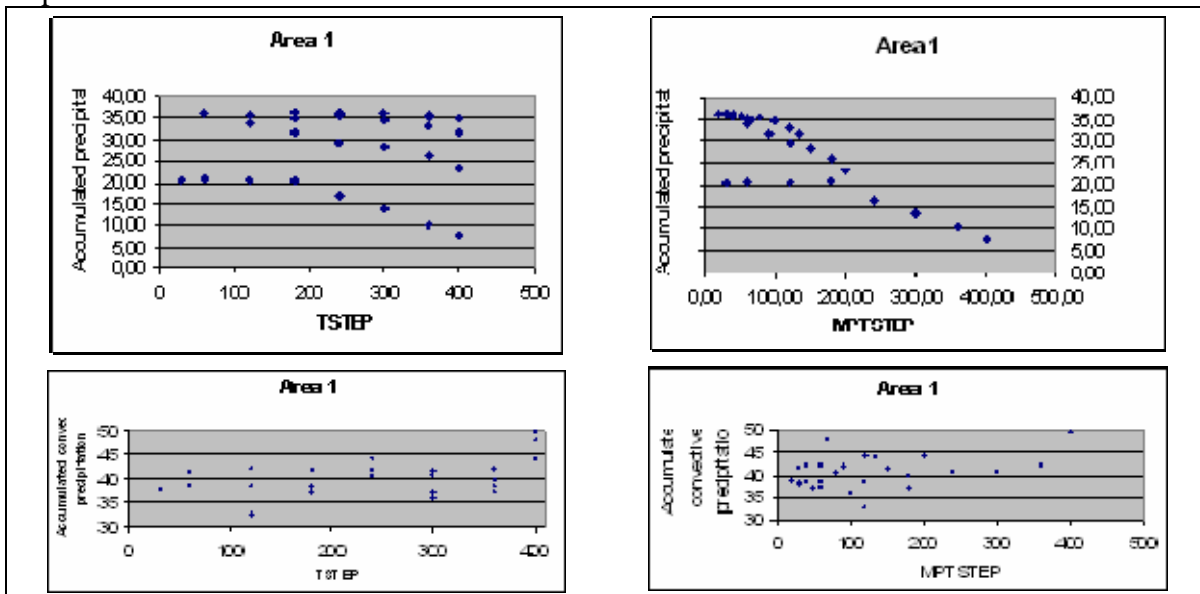


Figure 1: Gard case, area 1. Scatter plot of dependency of maximal amount of accumulated precipitation on time step and number of iterations. Upper row is for precipitation coming from microphysical scheme, lower row is for precipitation from convective scheme.

The effect of iterations of microphysics was studied on flood case in south of France. The flood took place in the Gard department on 2002-09-08. This case was used to test AROME, too. Initial time for ALARO 10 run was 2002-09-09, 12 UTC. A number of 12 hours runs

were done with various combinations of time steps and numbers of iterations. Time steps used were: 30, 60, 120, 180, 240, 300, 360 and 400 s, and numbers of iterations were: 1,2,3,6 and 9, but not all on each time step.

The results for maximal amounts of precipitation in two separate areas of precipitation are shown on figures 1 and 2. In upper rows is precipitation from microphysical scheme and in lower rows from convective scheme. For each time step several runs were done with different numbers of iterations. On the left side, in both figures, over each time step there is several points with higher and higher amount of precipitation, corresponding to increasing number of iterations. The lowest points on scatter plots correspond to one iteration, or no iterations, first one over it is for two iterations and so on. Dependency of maximal amount of precipitation on time step for microphysics is shown on the right sides of figures. Points over one time step for microphysics are from different time steps of the model.

Precipitation are 1 is in Gard department. It is dominated by convective precipitation. Dependency on time step and number of iterations is shown in upper left corner of Fig. 1. Lowest points, no iterations of microphysics, show what was known from the first tests of ALARO 10, that amount of precipitation is growing with shorter time step. About time step 200 s it stops growing and remains mainly constant. We can say that it converges to the finite value as time step is going to lower values. Other points form a separate group with values converging to the same value for each time step. We can say that irrespective of time step the amount of precipitation converges to the same value when number of iterations is growing. The problem is that this with iteration and without them there are different value to which amounts of precipitations are converging. The same can be seen on the upper right side of Fig. 1, where two branches of points can be noticed. In the lower row of the Fig. 1 scatter plots for convective precipitation are shown. No dependency on time step or number of iterations can be seen on them.

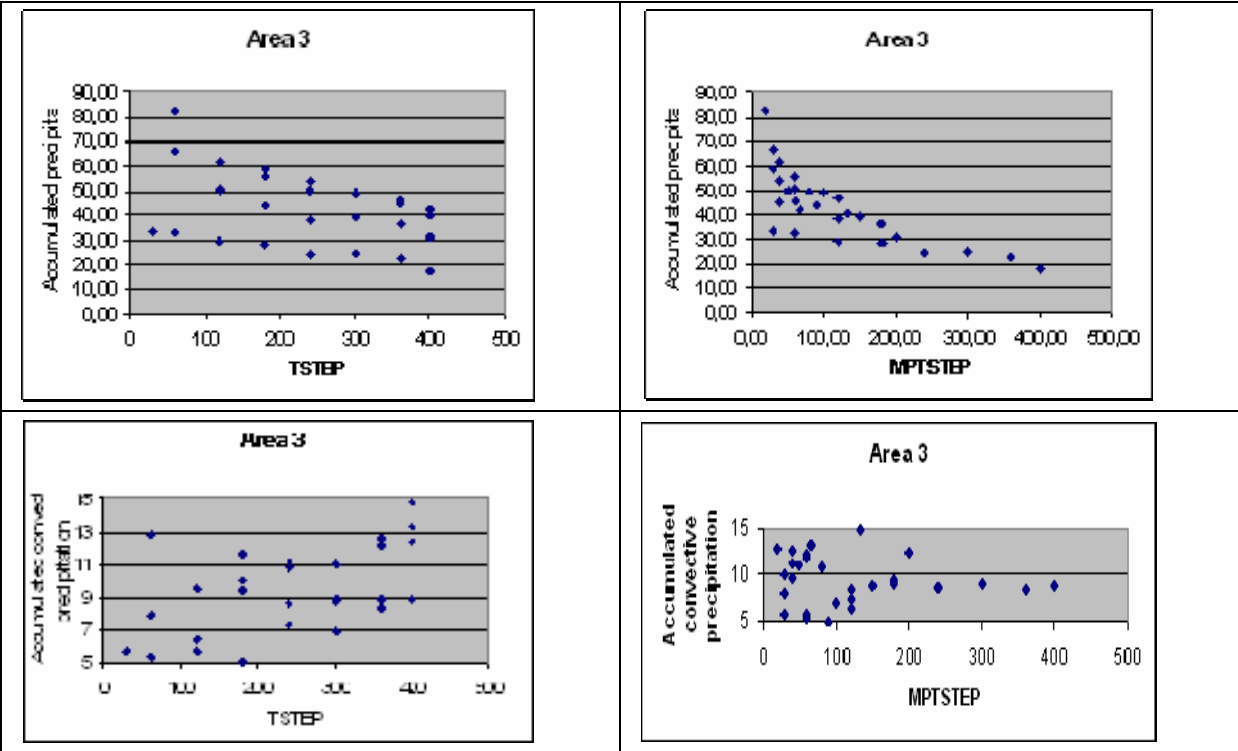


Figure 2: Same as Fig. 1, only for area 3.

Other precipitation area, noted number 3, is connected to the frontal system approaching southern France from the west. In this area more precipitation is coming form resolved precipitation, that is from microphysical scheme than from convection. Results are

shown on Fig. 2. On the upper left scatter plot the dependency on time step is shown. Lowest points, corresponding to no iterations of microphysics, show convergence to a finite value as time step is shorter. Again, for each time step amount of precipitation is converging with growing number of iterations (the spacing between points is diminishing), but limiting value is dependant on time step. These limiting values are not converging to one value, because there is a point, coming from TSTEP= 60 s and NITER= 3, which gives a southern jump in precipitation amount. Without this point we could say that limiting values are slowly converging to finite value, but again different from that achieved without iterations. Convective precipitation in this area is slightly dependent on time step. It is increasing with increasing time step.

After testing bulk parameterization of microphysics in ALARO 10 on one case following conclusions can be drawn:

- The amount of precipitation increases with decreasing time step, and for converges for both studied areas of precipitation.
- Iterations of microphysics, or time splitting, doesn't converge always, and when it does it is not the same value of amount of precipitation as when time step is decreasing without iterations of microphysics.
- More cases have to be studied to reach final conclusion.

# Use of reflectivity to validate Hirlam

Irene Sanz, J.A. García-Moya

INM – Madrid, Spain.

## ABSTRACT

Nowadays, one of the main concerns in the validation and verification of numerical prediction models is the verification of the precipitation. This variable is more difficult to verify than the rest of one because of the precipitation has a high variability in space and time. To do it, one suitable parameter is the reflectivity. At INM, a model used to simulate radar reflectivities (Radar Simulation Model, RSM) is running, thanks to it, it is possible to get simulated and observed reflectivity with the same resolution and compare them.

In this paper, RSM has been used in a case of a convective severe thunderstorm that took place in the Eastern part of Spain in 2001. Forecast fields of Hirlam with three different resolutions and actual files of radar network have been needed for this work. Several images obtained for this case will be presented.

## 1.INTRODUCTION.

Most of the meteorological variables observed are verified at INM, in special the surface variables, such as pressure at sea surface level, 2meter temperature, 10meters wind, cloud cover and 2 meter moisture. Nevertheless, there is one variable that is not verified, the precipitation. .

Precipitation verification is more complicated than the rest of the variables because of the high variability of precipitation in space and in time. For this reason it's necessary look for parameters related with the precipitation and with homogeneous horizontal and vertical distribution.

A valid parameter to help the verification and validation of Hirlam is the reflectivity. There are actual reflectivity measurements of radars in a short period of time in several heights of the atmosphere.

A good tool to verify the precipitation could be Radar Simulation Model (RSM), because thanks to it, it is possible to obtain simulated reflectivity and compare it with actual reflectivity obtained from radar network.

## 2.HIRLAM MODEL.

Hirlam at INM is running in the multiprocessor supercomputer Cray-X1. Thanks to it, it is possible to run higher horizontal resolutions for Hirlam, reaching 0.16 degrees and 0.05 degrees. The version used of Hirlam is 6.1.2. and the forecast fields covers hours from 00 to 72 every hour. The features of three experiments used in this work are shown in the table below.

<i>Horiz. resol.</i>	<i>lat x lon</i>	<i>Vertical levels</i>	<i>Area coordinates</i>				<i>South Pole</i>	
0.20	194 x 100	31	50.0 N	66.5 W	15.5 S	30.0 E	-90.0	0.0
0.16	582 x 424	40	32.18 N	46.5 W	35.5 S	46.46 E	-35.0	-15.0
0.05	366 x 272	40	10.75 N	15.0 W	10.7 S	15.25 E	-49.5	-6.0

Table 1. Features of Hirlam experiments

The areas of these experiments are represented in the figures in red points, in the case 0.2 degrees (Figure 1) and enclosed by the blue line in the others figures.

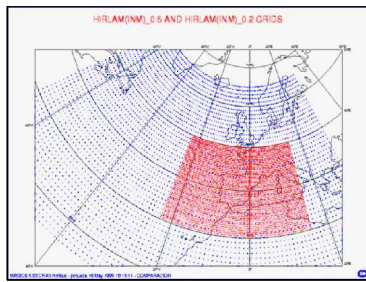


Figure 1. area 0.2 deg.

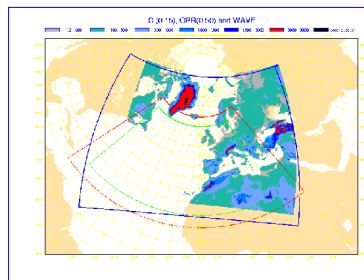


Figure 2. area 0.16 deg.

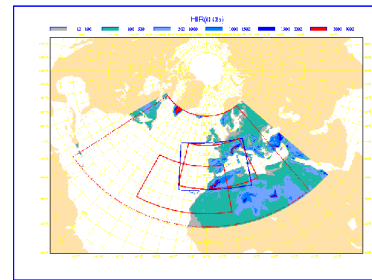


Figure 3. Area 0.05 deg.

### 3.RADARS AT INM.

Radar network at INM is formed by 13 radars located all over Iberian Peninsula plus one in Canary Island. All radars can work in two different modes of action, normal mode and Doppler mode. The radius of action and the resolution of radars depend on the mode. In the Normal Mode, the radius of action is 240 Km and the resolution is  $2 \times 2 \text{ Km}^2$  and in the Doppler Mode the radius of action is 120 Km and the resolution is  $1 \times 1 \text{ Km}^2$ .

There are 20 elevation angles and for each elevation angle the radar covers 360 degrees. In next table these angles are shown.

Elevation angles																			
0.5	1.4	2.3	4.1	5.0	5.9	6.8	7.7	8.6	9.6	10.7	12.0	13.4	14.9	16.6	18.4	20.4	22.6	25.0	

Table 2. Elevation angles.

Radar images are obtained every 10 minutes. Then, these images are processed in Regional Radar Centres where orographic filters are applied to them. After that, the polar coordinates (PPI) are turned into cartesian coordinates (CAPPI), so that products obtained from Regional Radar Centres are CAPPI's or vertical sections. The main features of these reflectivity products are:

a) PPI (Plan Position Indicator): it's a product created in the lowest angle. It's a flat image, so it is useless to visualize the three dimension structure. Data can be obtained in normal mode and in Doppler mode and they are available every 10 minutes.

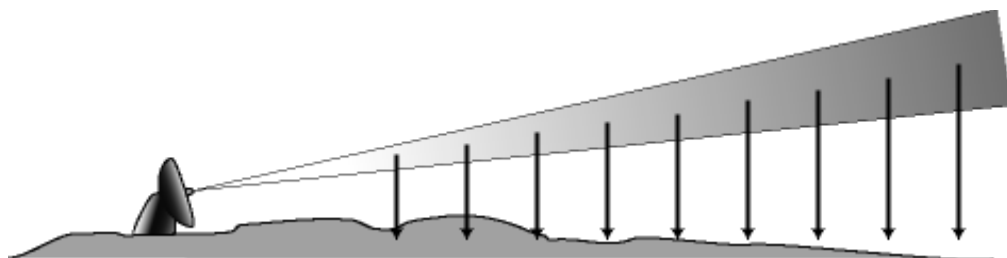


Figure 4. PPI projection

b) CAPPI (Constant Altitude Plan Position Indicator): it's a vertical section that represents the values on a horizontal plane. Data can be obtained only in normal mode every 10 minutes. There are 12 CAPPIs and each of one has a height over sea surface level that is equal for all radar except the CAPPI 1 where this height depends on the radar. The heights of the Cappi's are represented in table 3.

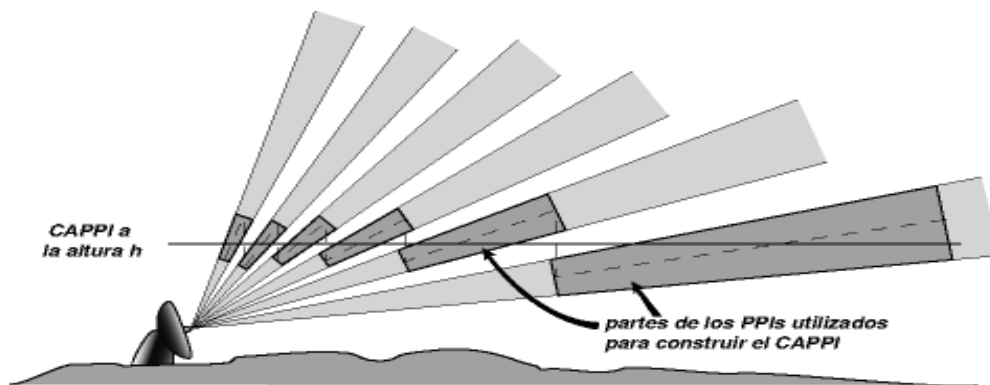


Figure 5. CAPPI projection

<b>CAPPI 1</b>	<b>(1000-2100) m</b>	<b>CAPPI 7</b>	<b>7500 m</b>
<b>CAPPI 2</b>	<b>2500 m</b>	<b>CAPPI 8</b>	<b>8500 m</b>
<b>CAPPI 3</b>	<b>3500 m</b>	<b>CAPPI 9</b>	<b>10000 m</b>
<b>CAPPI 4</b>	<b>4500 m</b>	<b>CAPPI 10</b>	<b>12000 m</b>
<b>CAPPI 5</b>	<b>5500 m</b>	<b>CAPPI 11</b>	<b>14000 m</b>
<b>CAPPI 6</b>	<b>6500 m</b>	<b>CAPPI 12</b>	<b>16000 m</b>

Table 3. Heights of CAPPI's.

#### 4. RADAR SIMULATION MODEL.

RSM uses forecast files of Hirlam and actual files of radar to simulate radar reflectivities. Then these files are converted into images getting two different images (the actual and the simulated ones). Both of them can be compared to obtain the relation between them.

To obtain these images, the RSM calculates simulated and observed reflectivity at the same resolution as the Hirlam forecast fields. The observed reflectivity is computed converting radar data (which are in ASCII format) into Hirlam grid.

In this work, this model has been used with three resolutions. The figures show the images obtained by RSM and the actual image obtained by radar network.

#### 5. CASE OF STUDY.

On the night of October the 10<sup>th</sup> in 2001 there was a convective situation associated with a severe supercell over Southeast of Iberian Peninsula (around Murcia and Alicante). This caused important damages in areas around Murcia and Alicante because of the size of kernels hail. Heavy rain in a short time took place. There aren't references about tornados or intense winds in surface in this date.

Radar and sounding data from Murcia are available. At first, the storm was located about 30-50Km away from this radar, and then it moved 120 Km towards the northeast. This situation lasted about 2 hours.

During the day and the previous, in middle-upper levels there was a CUT-OFF over Cadiz Gulf area (in the Southwest of the peninsula). As a consequence of it, a lot of cloudy bands appeared in the north of Africa which swept over South and Southeast of Spain, apart from this, convective cells in the Southern Mediterranean coast area were developed.

In surface level the peninsula was influenced by high pressure located on southern French coast and by a wide area of low pressures over Alboran Sea. This gave rise to a flow from the East that brought humidity to the eastern part of the peninsula from the Mediterranean coast.

From satellite images we can see how the cell was developing between 21 and 22 pm (at these hours was the convection was more important).

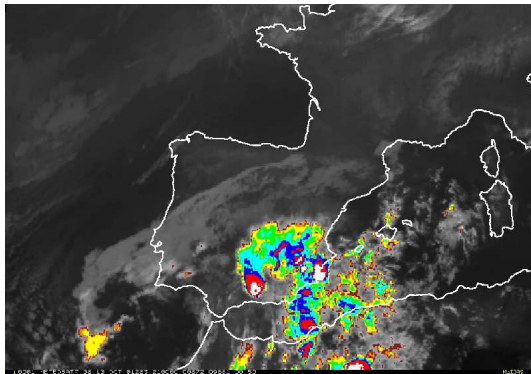


Figure 6. IR satellite image (21:00)

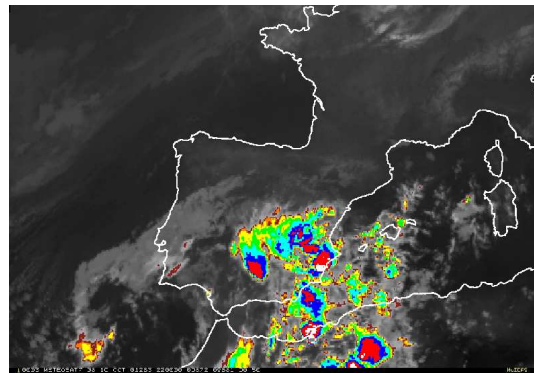


Figure 7. IR satellite image (22:00)

Enhance images: Temperatures range from  $-32^{\circ}\text{C}$  and changes in colour are each  $-4^{\circ}\text{C}$ : red, with limits between  $-56^{\circ}\text{C}$  and  $-59^{\circ}\text{C}$ , white between  $-60^{\circ}\text{C}$  and  $-63^{\circ}\text{C}$  and grays between  $-64^{\circ}\text{C}$  and  $-67^{\circ}\text{C}$ .

To study this case we used Murcia's radar data. The resolution of the radar data is  $2 \times 2 \text{Km}^2$ . Murcia radar is at 1270 metres over SSL. The lower exploration is made at 0.5 degrees of elevation so at 35 Km. of distance this beam is raised at 100-200 meters over the high of the radar and at 120 Km. this is at 1600-1700 meters. Therefore the convective structure was located between 1400 and 3000 meters over SSL.

The pictures below show the actual images obtained by Murcia radar, in them the shift of the cell towards the northeast can be seen.

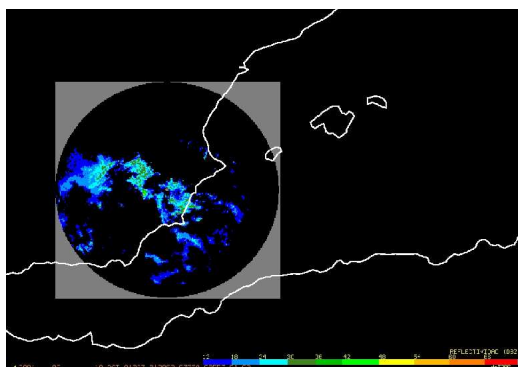


Figure 8. actual radar image (21:00)

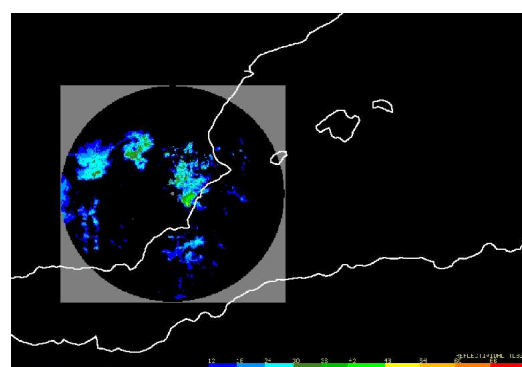


Figure 9. Actual radar image (22:00)

The vertical profile obtained at 22 pm. is shown in Figure 10. The heights of these CAPPIS are: Capi1=1800m, Capi3=2500m, Capi5=5500m and Capi8 = 8500m. There is a echo's movement in vertical and in lower levels the structure of image has the shape of a hook.

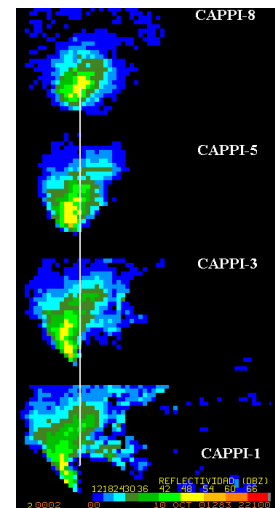


Figure 10. Vertical profile

## 6.RESULTS.

RSM has been used in the case of study to simulate reflectivities at three resolutions. Three different figures are shown for each resolution. The simulated and observed reflectivity obtained by RSM and the actual radar images are plotted in the following figures. Note that simulated and observed reflectivity images have the same resolution, whereas the resolution of the actual radar image is 2x2 Km<sup>2</sup> (because RSM uses radar files obtained in normal mode). The scale represents reflectivity in dBZ. Figures obtained from RSM are plotted using Metview (white background) and the figures obtained directly from radar network are plotted using McIDAS (black background).

In this case of study we have files of Hirlam from 00 of 10<sup>th</sup> October to 12 of 11<sup>st</sup> October (36 hours) every hour, but we only have six files of Murcia radar (between 21 of 10<sup>th</sup> October and 02 of 11<sup>st</sup> October), so the comparison between simulated reflectivity and observed reflectivity done for these hours.

The minimum value of reflectivity is -30.0 dBZ and the maximum value is 72 dBZ. In the images only positive values are represented.

The reflectivities obtained from RSM and the actual reflectivity are plotted in pictures below. The difference between the actual and the observed image is due to the change of resolution.

The main results obtained for each resolution are shown by Figs. 11-20 at the next page:

## 7.CONCLUSIONS

The use of RSM to validate mesoscale Hirlam is better when the horizontal resolution of Hirlam is more similar to the resolution of radar (2x2 Km<sup>2</sup>). In the three experiments used in this work both reflectivities (simulated and observed) have been obtained and in the third case, with 0.05 degrees of resolution the images of simulated reflectivity are closer to the actual one.

RSM can be useful for nowcasting when it is operational at INM. To achieve this, it is necessary to use parallel programming, due to the long run times with one processor.

This model is expected to be operational at the end of this summer.

**A. 22 Km resolution (0.2 degrees).**

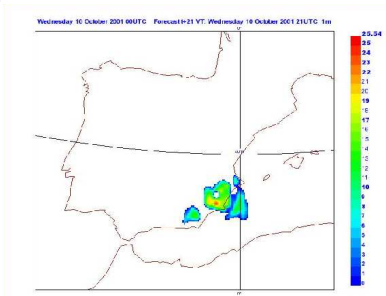


Figure 11. Simulated reflectivity (21:00)

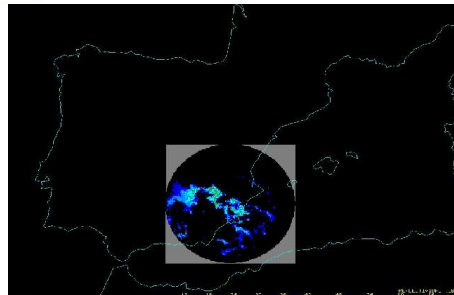


Figure 13. Actual radar image (21:00) 2x2Km²

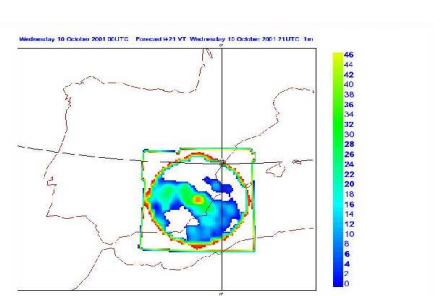


Figure 12. Observed reflectivity (21:00)

**B. 16,6 Km resolution (0.16 degrees).**

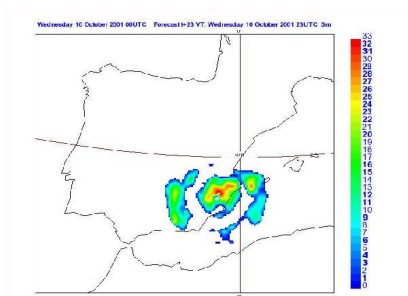


Figure 14. Simulated reflectivity (23:00)

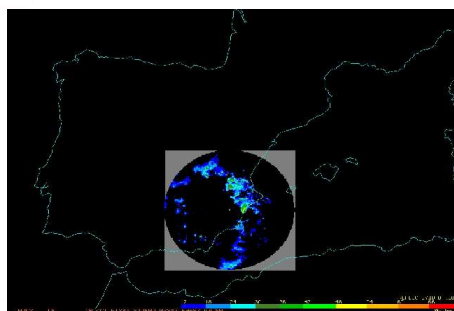


Figure 16. Actual radar image (23:00) 2x2Km²

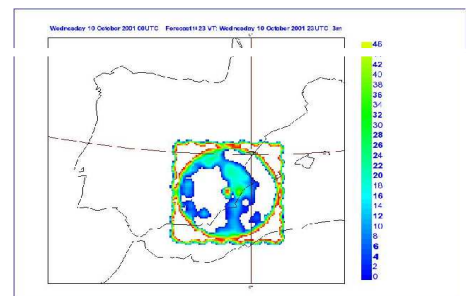


Figure 15. Observed reflectivity (23:00)

The cell moving towards Northeast can be seen in the following sequence of figures:

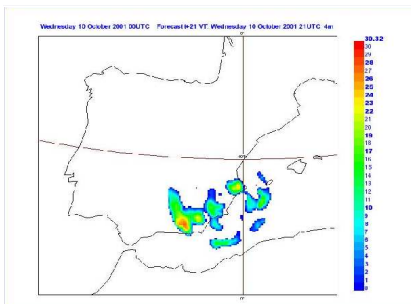


Figure 17. (21:00)

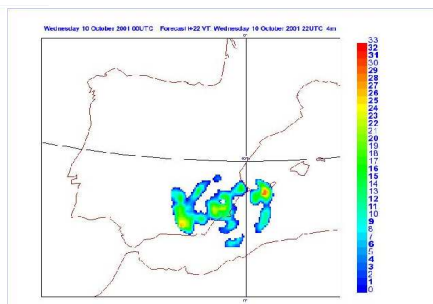


Figure 19. (22:00)

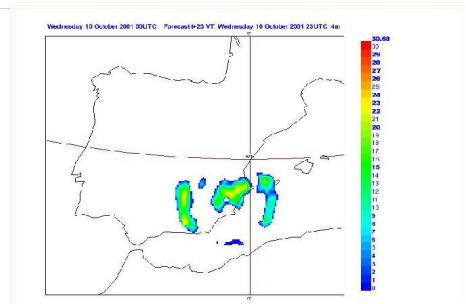


Figure 18. (23:00)

**C. 5,5 Km resolution. (0.5 degrees)**

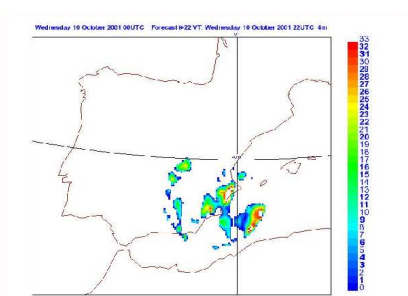


Figure 20. Simulated reflectivity (22:00)

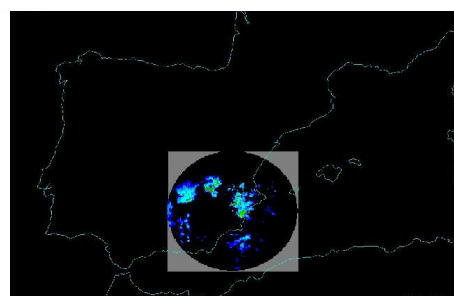


Figure 22. Actual radar image (22:00) 2x2Km²

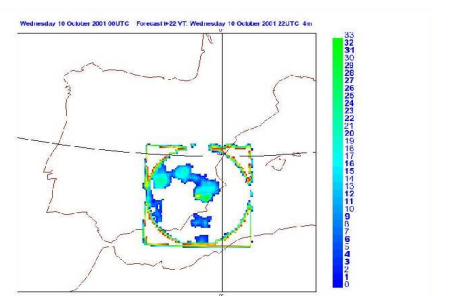


Figure 21. Observed reflectivity (22:00)

# Satellite Data in the Verification of Model Cloud Forecasts: a convective case in summer 2003 seen from NOAA satellites

Christoph Zingerle  
Finnish Meteorological Institute  
christoph.zingerle@fmi.fi

## 1 Introduction

Satellite measurements form a vast source of observational atmospheric data. This Data is suitable for verification of cloud forecasts produced by numerical weather prediction (NWP) models, especially where conventional observations are sparse. For an inter-comparison of model and satellite, radiative transfer models (RTM) can be utilized to simulate the outgoing radiation at the top of the atmosphere for a given atmospheric profile (Morcrette 1991). Such RTM is used in this study to calculate radiances from HIRLAM forecasts. A convectively active period during July 2003 is studied, comparing simulated radiation from the model to NOAA AVHRR satellite observations.

## 2 Methodology and material

### 2.1 Methodology

To use satellite data in the verification of the cloud forecasts, the model output and the satellite's radiance measurement have to be turned into comparable quantities.

Satellite instruments measure, within a certain band of wavelength, radiance arriving at the top of the atmosphere. For the detection of clouds, the parts of the infrared spectrum of the Earth is employed where the atmosphere is transparent for radiation (atmospheric window region). An important window region can be found at  $11\mu m$ . All the radiation arriving at a satellite instrument, sensible in this band of wavelength, is assumed to originate either from solid or liquid particles in the atmosphere or from the Earth's surface.

NWP models forecast the atmosphere's behavior. The structure of the atmosphere, together with the surface parameters, is responsible for the transfer of radiation (RT) to space. RTM can be employed to simulate what a satellite instrument measures when looking at particular atmospheric profiles. The comparison between such a simulation and the satellite observation enables a judgement on the coupled parameterized processes in the model (Morcrette 1991).

#### 2.1.1 The radiative transfer model

RTTOV 8.5 (Saunders & Brunel 2004) is applied to simulate outgoing radiances of atmospheric profiles, forecasted by the HIRLAM, for two NOAA AVHRR infrared channels. RTTOV uses profiles of T, q, clw, cli, cf,  $O_3$ , handles clear and cloudy multilevel radiances, multi-phase cloud fields (water/ice/mixed) and it has a consistent random overlap scheme (Räisänen 1998). In addition, RTTOV allows to choose between 4 effective diameter schemes for ice particles and 2 crystal aggregates.

## 2.2 Forecast model

48 hour forecasts have been produced at ECMWF for the days from July 15th to 21st with HIRLAM version 6.2.5. The domain covers the region of Scandinavia at a horizontal resolution of  $0.2 \times 0.2$  deg ( $\sim 22$  km), the vertical discretization is 40 levels and boundary conditions are taken from the ECMWF model. Analysis, initialization and forecast were run in a 3-hourly cycle. In this first case study, only the forecast starting on July 15th at 06 UTC has been considered, as the first two days of the period were most active in terms of convection. For verification a sub-region, covering Finland, has been chosen.

## 2.3 Satellite data

The observational data used for the case study originates from the AVHRR instrument on four NOAA polar orbiting satellites. The two infrared channels in the atmospheric window region have a central wavelength of  $10.8\mu m$  ( $10.3 - 11.3\mu m$ ) and  $12\mu m$  ( $11.5 - 12.5\mu m$ ) and a resolution of 1 km at sub satellite point. The time gap between the satellites passes over the target area is highly irregular and varies from 1/2 to 6 hours.

To match the very high resolution satellite data with the HIRLAM grid, a simple up-scaling has been performed based on following two assumptions:

- the model grid values represent the mean of the grid-box,
- neighboring satellite pixels tend to have similar properties.

Each calibrated pixel of the AVHRR image is assigned to a particular model grid-box, according to the navigation information (Fig. 1). The number of satellite pixels in a grid-box varies between 50 and  $\sim 400$ , depending on the satellite viewing angle. A simple arithmetic mean is calculated from all pixels assigned to a grid-box. The very high resolution structure of the satellite image is lost, while the general features, important for the verification process, are preserved.

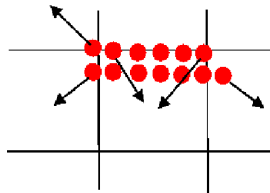


Figure 1: Re-sampling scheme used for up-scaling satellite pixels to the model grid.

## 3 Results

Standard verification scores at the time of satellite over-passes are calculated for the area of Finland, RMS-error and correlation coefficient are plotted in figure 2. A clear daily cycle is found: RMSE is much lower during night than during day, correlation is significantly higher during night. This is mainly due to the clear sky nighttime conditions observed practically over the entire area of Finland. The satellite receives radiation originating from surface and not much modified by the atmosphere while there are no clouds in the model either and the radiative transfer is calculated on clear conditions. Convection, however, is a phenomenon known to be hard to forecast in pattern and intensity. This fact is also mirrored in worse scores during the day and especially during the afternoon, when convection is strongest.

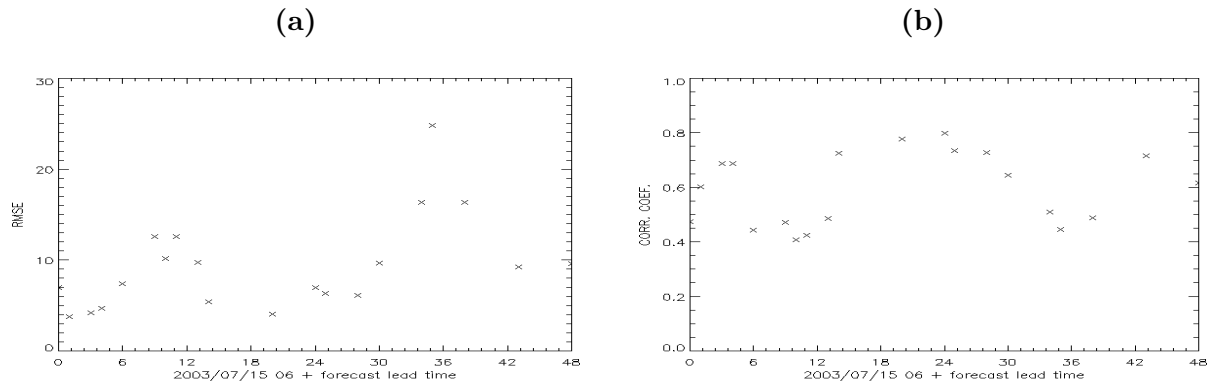


Figure 2: 2003/07/15 06 UTC - 2003/07/17 06 UTC, (a) RMS-error, (b) correlation coefficient for all available fc/obs-pairs.

Figure 3 indicates a strong underestimation of convection by the model. In the late afternoon, the satellite (Fig. 3 b) observed a much lower temperature than was simulated from predicted model profiles (Fig. 3 a). The difference is, in the center of the convective cell, bigger than 45 K, whereas in cloud-free areas of the domain the model is capable of simulating the surface temperature within  $\pm 5$ K (Fig. 3 c). As the scatter-plot in figure 3 d shows, the hot pixels (cloud free during day) in the satellite image are well predicted by the model and the difference to observations is small. Observations of cold brightness temperatures are not well simulated by the model.

However, the model indicates weak convective activity in the right place (low pattern error).

## 4 Conclusions and further work

The reasons for the clear underestimation of the BT in the model are multi-fold. About 1/2 of the BT-error can be explained by the RTM's high sensitivity to cloud-fraction. Only a small error in the representation of cloud fraction in the input profiles can cause huge errors in the calculation of the BT. It will be subject of a further study, how realistic the cloud-fraction in the HIRLAM model under convective conditions is. The other 1/2 of the BT-error can be caused by the convective scheme. It looks like convection cannot grow higher than a certain level, which might have different reasons. One is the entrainment of air into the convective cell, another could be the tropopause being too low in the model.

Figure 3(a) and (b) indicate, that there is some agreement in the pattern of convection and the main reason for bad scores during afternoon is a big intensity error. To divide these two sources of error, an entity based verification method should be applied to this, and several other cases.

The low temporal resolution of NOAA polar orbiting satellites and their irregularity is a clear disadvantage in verifying convective activity predicted by a NWP. Continuous observations are provided by METEOSAT satellites and should be implemented in further studies.

## 5 Acknowledgement

Thanks to Carl Fortelius, who supplied the forecasts run at ECMWF. The work is funded by EUMETSAT in the frame of a research fellowship (Verification of NWP cloud fields against satellite and/or SYNOP clouds).

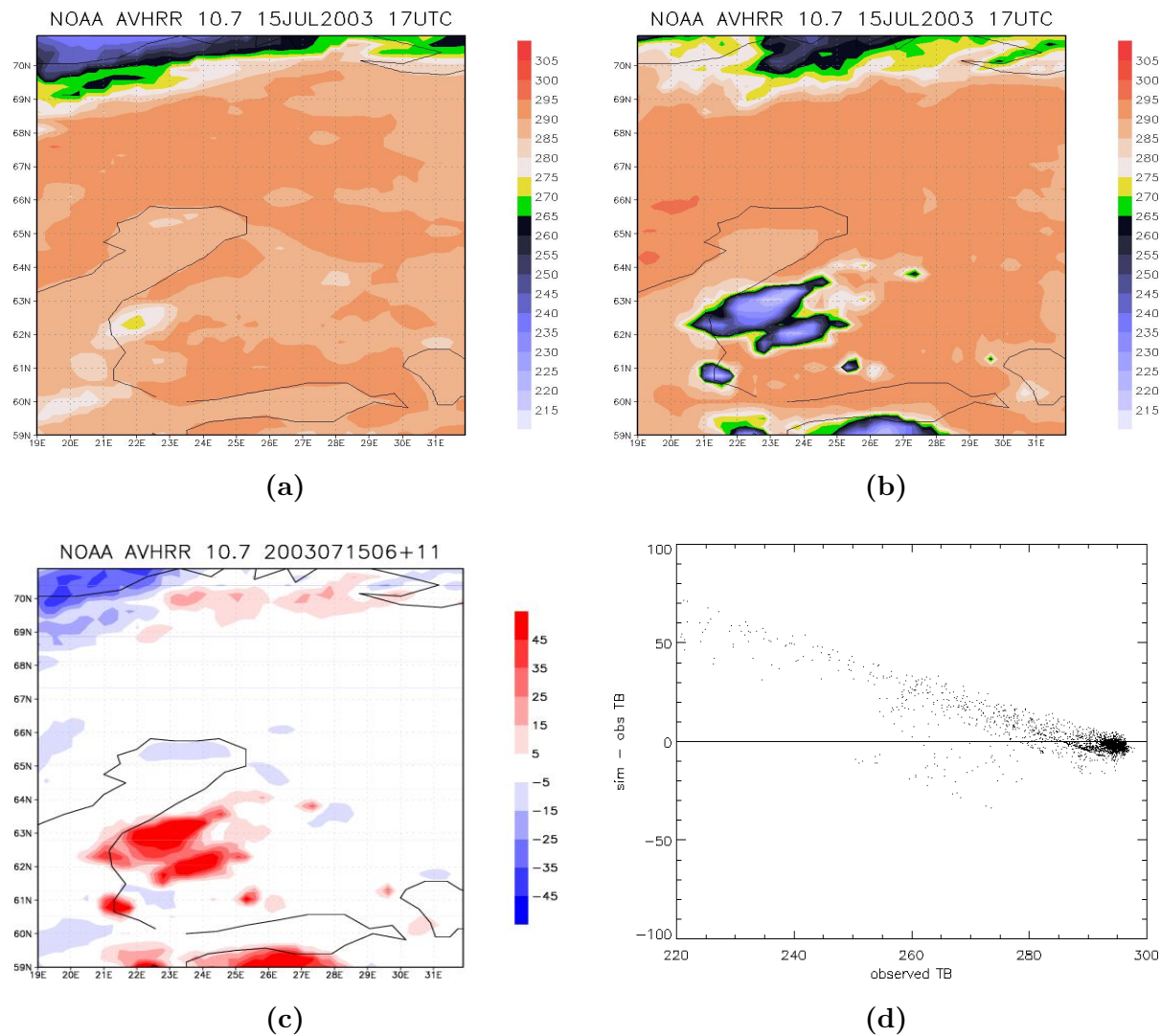


Figure 3: (a) Simulated model brightness temperature (BT), (b) observed satellite BT, (c) difference plot (fc - obs), (d) scatter-plot obs / (fc - obs).

## References

- Morcrette, J.-J. (1991). Evaluation of model-generated cloudiness: Satellite-observed and model-generated diurnal variability of brightness temperature. *Monthly Weather Review* **119**, 1205 – 1224.
- Räsänen, P. (1998). Effective longwave cloud fraction and maximum-random overlap clouds: A problem and a solution. *Monthly Weather Review* **126**, 3336 – 3340.
- Saunders, R. & Brunel, P. (2004). Rrtov-8.5 user guide. *EUMETSAT SAFNWP* <http://www.metoffice.gov.uk/research/interproj/nwpsaf/rtm/> p. 46.

# Precipitation and temperature forecasts in two HIRLAM versions

Kalle Eerola  
Finnish Meteorological Institute

## 1 Introduction

The concept of RCR (Regular Cycle with the Reference) was created in the HIRLAM project to give a higher status to the HIRLAM reference system. According to it, FMI (Finnish Meteorological Institute) runs operationally a suite called RCR, which is as close as possible to the reference system. In this way the reference system is run regularly and verified on daily basis, which allows to learn more about its strong and weak points. Because the results of RCR runs are archived at ECMWF, testing of new developments is also convenient, as the control run for new experiments is available and the same observations and boundaries as RCR can be used.

All new developments must be carefully tested different meteorological conditions and at different seasons before they are accepted. In this paper we compare precipitation and temperature forecasts of two HIRLAM versions, 6.3.5 (H635) and RCR, in early autumn conditions. The setup of experiment H635 resembles as much as possible that of RCR: it has the same area, the same resolution in the horizontal and vertical and it uses the same boundaries and observations as RCR. Especially it is worth mentioning, that it uses the same forecast frame boundaries from ECMWF as RCR, thus being very close to operational system.

The main developments included in H635 after RCR are described by Eerola (2005) and references there, and are not repeated here. An exception from that list is, that by mistake the smoothed orography is not used in our present H635 experiment.

The time of this experiment covers September 2004. Thus the comparison represents the behavior of the system in late summer/early autumn conditions.

## 2 Monthly accumulated precipitation forecasts

In this chapter we look at the monthly accumulated precipitation amounts in Scandinavia. September 2004 was very rainy in Finland. The observed precipitation amount was everywhere above normal and in large parts of Finland it rained more than double the normal.

Figure 1 shows the accumulated monthly precipitation from experiments RCR (left panel) and from H635 (right panel). In both cases the monthly accumulated precipitation has been computed as a sum daily precipitation of the second day of forecasts, ie. +24-+48-hour forecasts. Over the Scandinavian mountains the precipitation amounts are very similar. When looking at Finland we see that H635 produces more rain than RCR, especially in the southern and central parts of Finland. The maximum amount exceeds 140 mm at the southern coast and 110 mm is exceeded in many parts of the country. When comparing to observed precipitation (not shown),

H635 fits better to it. Observed precipitation amount of 140 mm is exceeded in south-eastern corner of Finland and 110 mm in several locations in Central Finland.

If we look at the structure of precipitation pattern, we see that H635 produces a smoother pattern of accumulated precipitation. Especially this is true over the Scandinavian mountains and in Sweden, where a lot of small-scale structures are seen in the RCR experiment. Figure 2 shows only the convective part of the monthly accumulated precipitation. Here we see clearly that the structure in H635 is smoother. In principle, there are two modifications (in addition of smoothed orography, which was not used here) in H635, which should give smoother structures: physics-dynamics coupling (Martinez, 2004) and Tanguay-Ritchie semi-Lagrangian correction in temperature equation (McDonald, 2002). It is difficult to say, which is more important in this case.

The large scale precipitation amounts in RCR and H635 are rather similar (not shown). On the other hand, Figure 2 also reveals that H635 produces more convective precipitation. Thus the increase of total precipitation in H635 compared to RCR is a mainly due to the increase in convective part during this late summer/early autumn period.

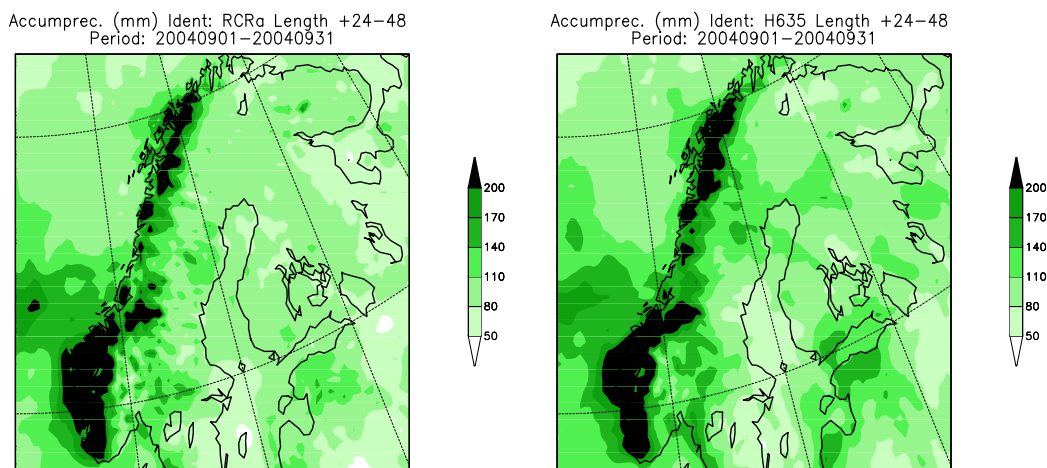


Figure 1: *Monthly accumulated total precipitation for Scandinavia from RCR (left panel) and H635 (right panel). The accumulated precipitation is computed from daily precipitation of the second day of forecasts (+24-+48 hours).*

### 3 Temperature forecasts

Figure 3 shows the verification scores of two-meter temperature and two-meter relative humidity as a function of forecast length for the EWGLAM stations for September 2004. Only forecasts starting at 00 UTC analysis are taken into account in order to get information about the diurnal cycle. We can see that at nighttime (+24 and +48 hours forecasts) the negative bias of about one degree, present in RCR, has almost totally disappeared: H635 is almost unbiased. At day time the negative bias, present in RCR, is decreased, but not totally disappeared in H635.

RCR has a clear positive bias in the two-meter relative humidity. This has almost totally disappeared in H635. Partly this is due to the decreased temperature bias.

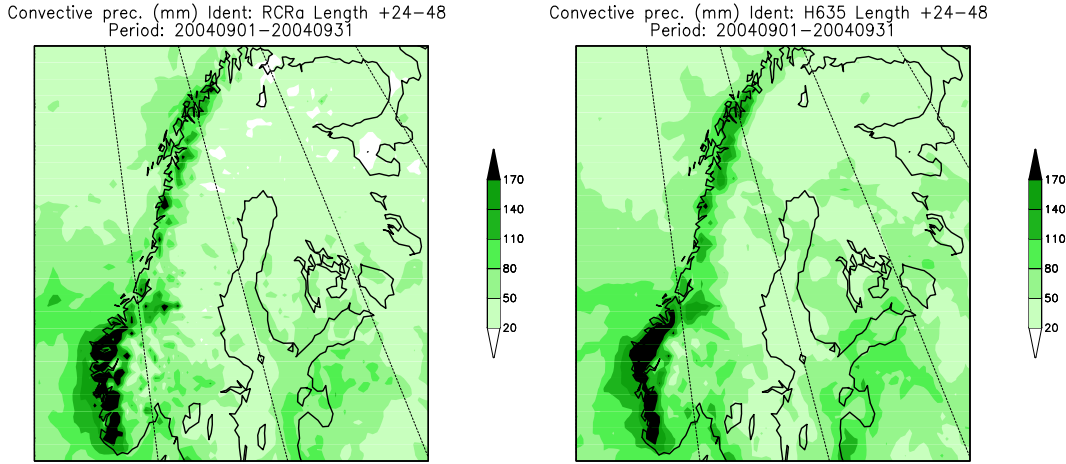


Figure 2: As Figure 1, but for convective part of the precipitation. Note that scale in this figure is different than in Figure 1

Eerola (2005) has described the geographical distribution of the bias in two-meter temperature and relative humidity. The figures are not repeated here, but the main conclusions of that paper were:

- During nighttime the negative bias in the two-meter temperature (too cold night temperatures) of RCR is clearly reduced almost everywhere in the experiment H635. In the Eastern Europe there is now even positive bias over quite a large area.
- The day-time bias is negative (too cold day temperatures) in both models over the European continent. However, the bias is clearly reduced in experiment H635 as compared to RCR.
- Both models are rather good in the Southern Europe and the improvements are therefore smaller in H635.
- The improvements in the two-meter temperature are reflected in improved relative humidity forecasts.

Thus there are remarkable improvements in temperature and relative humidity in H635 when compared to RCR. Concerning cloudiness, it is difficult to compare directly observed and modeled cloudiness. Eerola (2005) concludes that cloudiness in H635 is reduced as compared to RCR. The decreased cloudiness helps to give higher, more correct day-time temperatures.

## 4 Concluding remarks

In this study we first compared the monthly accumulated precipitation forecasts of RCR to HIRLAM beta-version H635. It appeared that H635 produces more precipitation in Finland than RCR, and is more close to observations one than RCR. Also the accumulated precipitation field is smoother in H635 than in RCR. The increase in precipitation is mainly due to the increase of convective precipitation.

## Verification against observations EXP: RCRa H635

Time: 2004090100 - 2004093018 Domain: EWG Forecast from 00

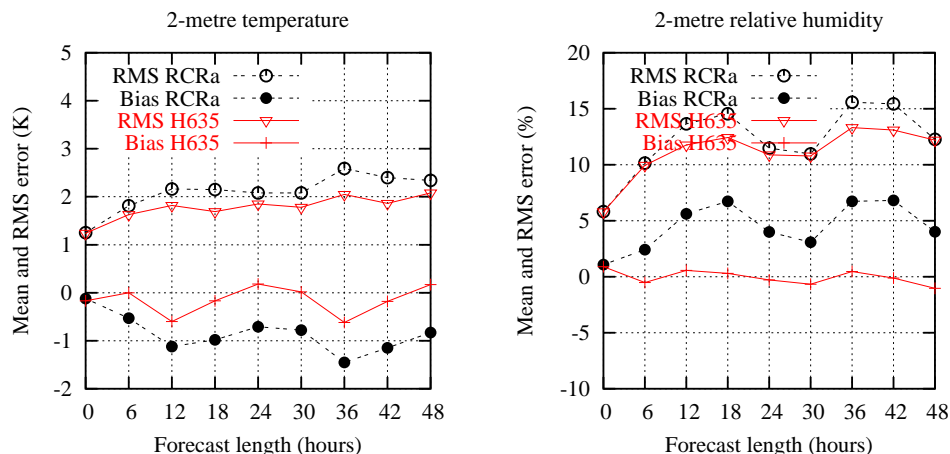


Figure 3: The verifications scores (bias and rms) of two-metre temperature and two-metre relative humidity for experiments RCR and H635 as a function of forecast length in September 2004. The verification is done against EWGLAM stations and only forecasts starting at 00 UTC analysis are taken into account.

Also two-metre temperature forecasts are better in H635. Especially the night temperatures are much closer to observations, but there are improvements also in day temperatures.

The current results may be compared to those presented by Järvenoja (2005). He compared RCR and the meso-beta-scale operational model at FMI, called MBE. The MBE model differs from RCR only in the horizontal resolution: RCR has a resolution of 22 km, while MBE uses resolution of 9 km. In summer conditions Järvenoja (2005) gets very similar results as the present study: increased precipitation and improved two-metre temperatures in the sense that the negative bias has significantly decreased. The possible explanation in both cases is the decreased cloudiness. An open question is why the improved horizontal resolution in MBE and several meteorological corrections in H635 produce similar improvements in the summer/early autumn conditions.

## References

- Eerola, K., 2005: Verification of Hirlam version 6.3.5 against RCR in autumn conditions. *HIRLAM Newsletter*, **47**, xx–xx.
- Järvenoja, S., 2005: A new meso-b-scale hirlam at fmi. *HIRLAM Newsletter*, **47**, xx–xx.
- Martinez, I., 2004: Final version of the physics-dynamics coupling. *HIRLAM Newsletter*, **46**, 37–47.
- McDonald, A., 2002: Changes to the HIRLAM needed for finer grids? *HIRLAM Newsletter*, **42**, 9–17.

# What can a LAM-NWP system tell us about the atmospheric water cycle

Carl Fortelius, Finnish Meteorological Institute

## 1 Introduction

The BALTEX regional reanalysis project (Fortelius et al., 2002) was carried out jointly by the Finnish (FMI) and Swedish (SMHI) national meteorological services as an ECMWF special project with the objective to carry out high resolution data assimilation around the Baltic drainage basin (Fig. 1) over one year (Sept. 1999-Oct. 2000) during the BALTEX main experiment BRIDGE (Bengtsson 1998), and thereby to promote the use of assimilation products in regional climate system research. A specific objective is to produce gridded fields of all components needed to close the energy and water cycles, with a spatial resolution of approximately 22 km and a temporal resolution of one to six hours. The computational domain is shown in Figure 1. More details are given on the project home page, which is linked to the BALTEX web site <http://w3.gkss.de/baltex/>.

## 2 The assimilation system

The forecast model is based on Hirlam level 4, but grid-scale condensation and precipitation are parameterized according to Rasch and Kristjansson (1998), and convection according to Kain and Fritsch (1998), whereas surface and soil processes are treated as in the Rossby Centre climate model as described by Bringfelt et al., (2001).

Boundary conditions at the lateral edges of the domain are specified using analyses from the ECMWF, updated every 3 hours, and interpolated linearly in time to every time step of the forecast model.

The analysis of atmospheric variables is performed using 3DVAR, employing six-hourly cycling. The observations consist of surface data from reporting weather stations, ships and drifting buoys, and upper air data from radio soundings and reporting aircraft. The analyzed atmospheric state is filtered with respect to gravity waves using a diabatic digital filter to get a balanced initial field for the prognostic model.

On land surfaces, only the snow-cover is analysed based on observations, while the temperature and moisture in the soil and vegetation are described by the soil-model. Analogously, the numerous inland lakes in Scandinavia are described with a separate lake model (Ljungemyr et al. 1996). The surface temperature (SST) and ice evolution in the Baltic Sea are described with a coupled ice-ocean model (Gustafsson et al. 1998), forced by the atmosphere-model via fluxes of heat and water vapour, and relaxed towards the observed SST-distribution. Elsewhere, analysed SST and ice distributions from the ECMWF are used.

## 3 Water balance of the Baltic drainage basin

Barring chemical reactions, the amount of water substance in any volume can change only by fluxes through the boundaries of the volume. For a column of air, these fluxes consist of precipitation ( $P$ ), phase transitions at the surface (evaporation, dew formation et. c.,  $E$ ), and horizontal transports through the lateral boundaries. The net effect of these transports is given by the convergence of the vertically integrated horizontal flux of water vapour and cloud condensate ( $C$ ). In most cases the contribution from

the cloud condensate is so small as to be entirely negligible. Symbolically we may write:  $W = C + E - P$ , where  $W$  stands for the rate of change of water substance within the atmospheric column.

All the terms in this equation are easily obtained from the BALTEX reanalysis data. Terms  $E$  and  $P$  are included in the model output as accumulated within each forecast. Term  $W$  is readily computed by taking the difference of appropriate model states. Term  $C$  is often evaluated using the state variables of surface pressure, wind and specific humidity, (e.g. Fortelius, 1995). This method is cumbersome and usually inaccurate, since many numerical approximations of derivatives and integrals are involved. A much simpler approach is to evaluate  $C$  as a residual term in the budget equation. If this is done in such a way, that all the remaining terms in the equation refer to the same forecast, i.e. the change predicted by the model for a given period is compared to the accumulated precipitation and evaporation during the same period, then the residual is actually equivalent to the accumulated flux convergence as given by the forecast model during the same period.

Fig. 2 illustrates the atmospheric water budget of the Baltic drainage basin from September 1999 through September 2000, as given by the BALTEX reanalysis system. The graphs present 30-day running means based on hours 6 - 12 of four forecast cycles each day. For the basin as a whole (top panel) precipitation (Heavy solid line) dominates over evaporation (dashed line) except for shorter periods during spring and autumn. The deficit (surplus), indicated by the line at the edge of the grey shading, is nearly balanced by convergent (divergent) flux of water vapour flux (the unmarked edge of the same grey shading) so that the rate of change (not shown) is usually small. Averaged throughout the year, the region is clearly one of net imported water vapour.

Comparing the predicted rate of change of the water content to the one that may be deduced from analyses valid at the corresponding times sheds some light on the reliability of these results. The black shaded area shows the difference between these tendencies, which is seen to be small in magnitude compared with either  $E - P$  or  $C$ . Nevertheless, positive values, indicating excessive accumulation of water in the forecasts, prevail in winter, while the opposite is true in summer. The pattern is consistent with the systematic error of the surface pressure (not shown), reflecting the tendency of the model to spuriously accumulate mass in the region during winter and disperse mass during summer.

Conditions over the land fraction of the drainage basin (middle panel) are similar to those prevailing over the total basin. This is not surprising, as most of the area is covered by land. It is interesting to note, that even the land-part of the basin may serve as a net exporter of water vapour on a monthly time scale. This happens in September 1999 and in May 2000, and again in September 2000.

Over the Baltic Sea itself (Fig. 2, bottom panel), conditions look rather different from those over the continental parts. Precipitation and evaporation both follow a similar annual cycle, but the former is more variable on a monthly time scale. Hence sometimes one and sometimes the other dominates the scene, and periods of net import and export of water vapour follow each other at irregular intervals throughout the year without any obvious annual cycle.

## 4 Precipitation

The verification of precipitation forecasts in general is made difficult by the huge variability of precipitation in time and space. In general a large number of in situ measurements is needed to estimate the average precipitation over a model grid box. A network of radars provides virtually continuous observations, but obtaining accurate estimates of the precipitation at the surface using radars alone is very problematic. The BALTEX Radar Data Centre combines corrected rain gauge data with radar measurements over the catchment basin of the Baltic Sea. These data were used for verification of the predicted precipitation. Products and methodologies of the BALTEX Radar Data Centre (BALTRAD) are described in Michelson et al. (2000). The data used here consists of gridded consecutive 12-hourly precipitation sums with a horizontal resolution of 2 km. For the purpose of this study, the BALTRAD data are transformed by box-averaging to the HIRLAM-grid having a grid length of 22 km.

Figure 3 shows time series of 7-day running mean precipitation totals over the rectangular area shown in Fig. 1. This area was chosen mainly because of the high quality of the radar network there. As before, the model output consists of hours 6-12 of four forecast cycles each day. The correspondence

between the two totally independent estimates is quite remarkable on all time scales, and the linear correlation coefficient is as high as 0.95. Even for half-daily precipitation sums (not shown), the linear correlation coefficient between the two estimates is as high as 0.91. Annual totals differ by only 6mm for BALTRAD and 788 mm for HIRLAM, so the difference is definitely within the observational uncertainty.

Although important, the total amount is only one aspect of precipitation. It is also important how the precipitation is distributed in space and time. Fig. 4 shows frequency-histograms of semi diurnal precipitation in different seasons for all (22 by 22 km) grid-boxes within the control area. The main features of the observed distributions, including their seasonal changes, are well reproduced by the reanalysis products, especially in spring and summer. In autumn and winter the occurrence of weak precipitation is overpredicted by the system at the cost of cases with no precipitation at all (note that the leftmost columns in Fig. 4 have been divided by a factor of 10 for greater readability).

## 5 Conclusions

The BALTEX regional reanalysis project has demonstrated that data assimilation using a modern limited area numerical weather prediction system is a feasible way to determine the essential features of the energy and water cycles of the Baltic drainage basin.

## 6 References:

- Bengtsson, L., 1998: Interrim memorandum of understanding for the conduct of BRIDGE 1999-2001 in frame of BALTEX. Int. BALTEX Secr., GKSS Forschungszentrum, Geesthacht, Germany, 58 pp.
- Bringfelt, B., J. Räisänen, S. Gollvik, S. Lindström, L. P. Graham and A. Ullerstig, 2001: The land surface treatment for the Rossby Centre Regional Climate Model-version 2. *SMHI Reports of Meteorology and Climatology*, textbf98, SMHI, 40 pp. (Available from the Swedish meteorological and hydrological institute, SE-601 76 Norrköping, Sweden)
- Fortelius C. 1995: Inferring the diabatic heat and moisture forcing of the atmosphere from assimilated data. *J. Clim.*, **8**, 224-39.
- Fortelius, C., U. Andrae, and M. Forsblom, 2002: The BALTEX regional reanalysis project. *Boreal Environmental Research*, **7**, 193-201.
- Gustafsson N., L. Nyberg. and A. Omstedt, 1998: Coupling of a high-resolution atmospheric model and an ocean model for the Baltic Sea., *Mon. Wea. Rev.*, **126**, 2822-2846.
- Kain, J. S. and M. J. Fritsch, 1998: Multiscale convective overturning in mesoscale convective systems: Reconciling observations, simulations and theory. *Mon. Wea. Rev.*, **126**, 2254-2273.
- Ljungemyr P., N. Gustafsson and A. Omstedt, 1996: Parameterization of Lake thermodynamics in a high resolution weather-forecasting model. *Tellus*, **48A**, 608-621.
- Michelson D.B., T. Andersson, J. Koistinen, C. G. Collier, J. Riedl, J. Szturc, U. Gjertsen, A. Nielsen and S. Overgaard, 2000: BALTEX Radar Data Centre Products and their methodologies. *SMHI Reports Meteorology and Climatology*, **90**, 76 pp. (Available from the Swedish meteorological and hydrological institute, SE-601 76 Norrköping, Sweden)
- Rosen, R., 1999: The global energy cycle. In: Browning K.A. and Gurney R.J. (Eds.): Global energy and water cycles. Cambridge University Press, 292 pp.
- Rasch, P. J., and J. E. Kristjansson, 1998: A comparison of the CCM3 model climate using diagnosed and predicted condensate parameterizations. *J. Climate*, **11**, 1587-1614.
- Undén, P., L. Rontu, H. Järvinen, P. Lynch, J. Calvo, G. Cats, J. Cuxart, K. Eerola, C. Fortelius, J. A. Garcia-Moya, C. Jones, G. Lenderlink, A. McDonald, R. McGrath, B. Navasques, N. Woetman Nielsen, V. Odegaard, E. Rodriguez, M. Rummukainen, R. Room, K. Sattler, B. Hansen Sass, H. Savijärvi, B. Wichers-Schreur, R. Sigg, H. The, A. Tijn, 2002. HIRLAM-5 scientific Documentation, HIRLAM-5, c/o Per Undén SMHI, S-601 76 Norrköping, Sweden. Available electronically: <https://hirlam.knmi>

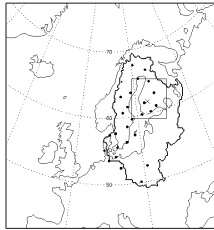


Figure 1: Domain of the BALTEX regional reanalyses. The black dots and the cross indicate the sites of weather radars.

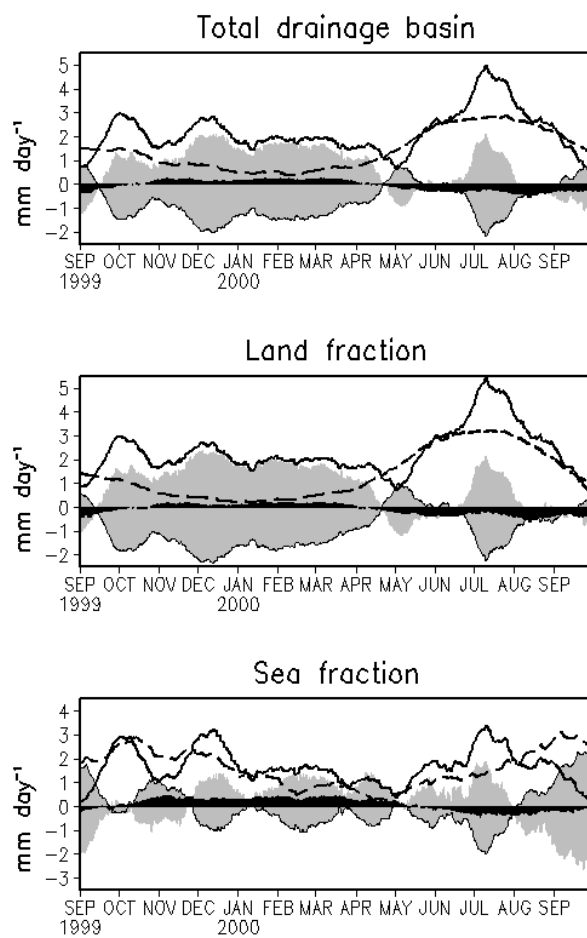


Figure 2: Terms in the atmospheric water budget over the drainage basin of the Baltic Sea. Graphs represent 30-day running means based on forecast hours 6-12 of four forecast cycles each day. Precipitation and evaporation are shown as heavy solid and dashed lines, respectively, and the difference between evaporation and precipitation is shown by the solid line at the edge of the grey shaded band. The unmarked edge of this band shows the net convergence of lateral water transport in the atmosphere. The black shaded band gives the bias of the predicted rate of change of the atmospheric water content relative to the analysed one.

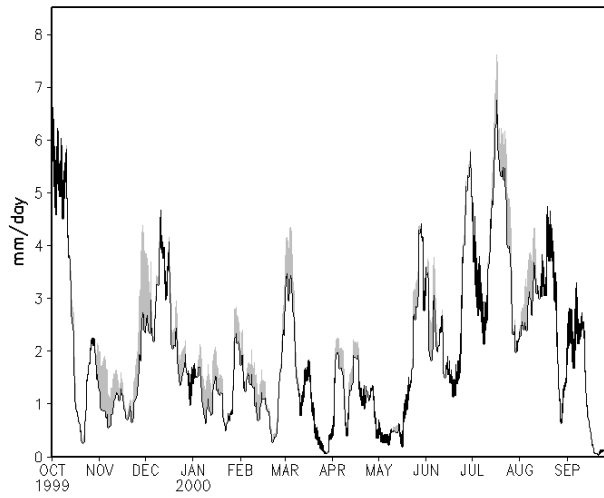


Figure 3: Areal 7-day running mean precipitation totals for the rectangular area shown in Fig. 1. The solid line shows precipitaitoin retrievals from the BALTEX Radar Data Centre. Grey and black shading, respectively indicate positive and negative differences between the BALTEX reanalysis system and the BALTRAD retrieval. Model results refer to hours 6-12 of four forecasts each day.

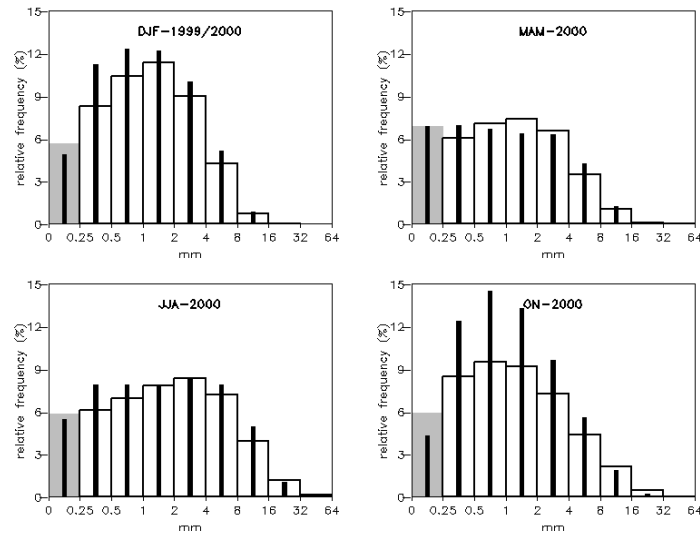


Figure 4: Relative frequency distributions of semi diurnal precipitation totals for all grid-boxes within the rectangular control area in Fig. 1. The thin black columns refer to the BALTEX reanalysis system, while the wide unfilled columns show precipitation retrievals from the BALTEX Radar Data Centre. Different panels refer to different periopds, as indicated by the letters and numbers. The leftmost columns have been divided by 10 for greater readability.

## **Convective indexes calculated from HIRLAM output.**

Anna Kanukhina

The Russian State Hydrometeorological University (RSHU), Faculty of Meteorology,  
Meteorological Forecasting Department

### **Abstract**

Forecasting possibility of convective phenomena arising time, place and type was estimated with the aid of calculated convection indexes. To calculate these parameters HIRLAM (High Resolution Local Area Model) forecast and analysis files have been processed. Six indexes chosen for study were divided into 3 groups. Indexes from the first diagnostic group estimate atmospheric stability state. There's a parameter having triggering function for convection arising. Third group gives information on possible convective phenomena type. Analyses and calculations are done for June 29,2000; June 19,2001; November 21-23, 2001; July 03-03,2002; July 16-20, 2003.

### **Introduction**

Strong convective events have a short time of development. Existing observation network not always allow registering these mesoscale processes in time. Modern NWP models give prognostic data with high temporal and spatial resolution. That's why forecasting possibility of dangerous phenomena arising time, location and behavior was studied on base of HIRLAM output.

### **Data and method**

The data used are HIRLAM analyses and forecasts with a horizontal resolution of 22 km and 31 levels. Forecast files correspond to 6,12,18,24 and 30 prediction hours. On base of HIRLAM forecasts, fields and profiles of convection indexes were calculated, and then areas of phenomena possible arising were picked out. Received results were compared with observations: HIRLAM analyses files, radio sounding at exact points, synoptic maps as surface observations. The area of interest is North West of Russia and most part of Scandinavian Peninsula. Mostly summer days during few years were taken to study convective indexes and they were divided into 3 groups. The first group is formed by cases with thunderstorms, showers; atmosphere energy characteristics showed high possibility of convection arising. They are June 29,2000, June 19,2001, July 03-06,2002. The second group are cases without thunderstorms or other evident convective phenomena but the atmosphere is unstable and ready for convection development what may be determined by convection characteristics( July 16-20,2003). The third group includes cases with thunderstorms but convective parameters don't indicate clear atmospheric instability (November 21-23, 2001). Visual analysis of indexes' fields and profiles, scattering graphs, correlation coefficients are base for results discussion.

The following data are necessary for indexes calculations: temperature field on the ground and temperature distribution with altitude, its variation with time; the same for dew point temperature; wind field and wind profile and its variation, at least up to the surface 500 hPa; surface pressure tendencies; humidity characteristics. Derived convective parameters and their combinations indicate favorable conditions for the development of dangerous phenomena, and help to locate it.

### **Indexes used for analysis**

Numerous studies [Calas *et al.* 2000, Ducrocq *et al.* 1998, Riosalido *et al.* 1998, S n si *et al.* 1998, Stensrud *et al.* 1997] devoted to convection indexes helped to compose indexes ensemble for the analysis. These indexes may be divided into 3 main groups:

1. diagnostic parameters characterizing the atmosphere preparedness for convection development ( $\Gamma$ , C, MOCON);

2. predicting value which indicate whether the phenomena will arise or not ( $\chi$ ), Index of Falkovich A.I. (Rusin, 1996).
3. indexes helpful for phenomena type and intensity estimation (CAPE, HEI).

a) The equivalent static stability index,  $\Gamma_e$ , is used (Rusin, 1996). The traditional method namely comparison of the actual and adiabatic (saturated adiabatic) lapse rates, is not convenient.

$$\Gamma_e = \frac{\theta \cdot (\theta_{eU} - \theta_{eL})}{\theta_e \cdot \Delta Z}, \quad (1)$$

“U” and “L” denotes upper and lower boundary of the layer respectively.

- If  $\Gamma_e > 0$ , the atmosphere is stable;
- if  $\Gamma_e = 0$ , the atmosphere is neutral;
- if  $\Gamma_e < 0$ , the atmosphere is unstable.

The index  $\Gamma_e$  is calculated for every layer between standard isobaric surfaces, the lowest level being the ground surface. The index is represented as non-dimensional

$$\Gamma = \frac{\Gamma_e}{\bar{\gamma}}. \quad (2)$$

Here  $\bar{\gamma}$  is the value of long – standing average vertical temperature gradient for the particular layer taken as ,0.65 °/100 m .

b) MOCON (moisture convergence) for quantifying the low level moisture supply and lifting process.

$$\text{MOCON} = -\nabla_{Hh} \cdot (rV) = -r\nabla_H \cdot V - V \cdot \nabla_H r \quad (3)$$

Where  $r$  is the mixing ratio at 2 m and  $\mathbf{V}$  is the wind velocity at 10 m above ground level. The MOCON sign is closely related to that of the convergence field, so that areas of positive MOCON values depict areas of low-level wind convergence.

c) energy helicity index EHI is

$$\text{EHI} = \text{CAPE} \cdot H. \quad (4)$$

The larger this index, the more severe convective phenomena can develop. The helicity of relative motion H is estimated from the following formula

$$H = \vec{V}_{\text{rel}} \cdot \text{rot} \vec{V}_{\text{rel}}, \quad (5)$$

d) The available convective potential energy is denoted as CAPE

$$\text{CAPE} = \int_0^{z_h} g \cdot \frac{\theta_e - \bar{\theta}_e}{\theta_e} dz, \quad (6)$$

e) To judge with a degree of confidence the convection development, Falkovich’s index of the convective instability is used that is

$$\chi = \frac{\Delta Z_{KHC} - \Delta Z_3}{\Delta Z_3}, \quad (7)$$

where  $\Delta Z_{KHC}$  is the thickness of the convectively unstable layer,  $\Delta Z_3$  is the thickness of the locking layer. The top of the locking layer is the altitude which air has to reach as it is lifted up from the initial level in order to receive positive buoyancy. If  $\chi \geq 0$ , convection will develop, since the atmosphere is convectively unstable. If  $\chi < 0$ , only a shallow layer of convection is possible.

g) generalized index of convection development possibility C shows atmospheric circulation type also:

$$C = \left[ (\Gamma - \Omega) \sqrt{\Gamma^2 + \Omega^2} \right] e^{-\Omega \Gamma}, \quad (8)$$

where  $\Omega$  is circulation parameter. If  $C \leq 0$ , convective disturbances are possible.

## Results

Checkout of work process was done at example of a convective case on 23.11.2001 at airport Kyardla (Estonia) when fast Cb development was accompanied with strong vertical air motions. The airport is not supplied with sounding station but different convective events were observed at neighboring stations (showers, thunderstorms, Cb). Calculated indexes' profiles and fields are shown at the picture 1. Atmospheric statical instability index and generalized parameter  $C$  are negative at model levels 27-29 which correspond to 850-950 hPa layer. This status is favorable for convection development and fits the theory. Falkovich's index  $\chi$  is close to zero at 29-30 model levels (900-1000 hPa) but above mentioned parameters are positive here and where they are positive –  $\chi$  is negative. Negative Falkovich's index indicates strong convection development impossibility but shallow convective systems are probable to arise. It could be explained by exact locality of  $\chi$  usage and insufficiency of available spatial resolution.  $C$  and  $\Gamma$  keep negative values within 850-950 hPa layer even at 6, 12 and 24 h forecasts (picture 1). Usefulness of land or sea surface temperature including at initial data was under question for  $C$ ,  $\Gamma$ ,  $\chi$  values. Calculations showed little change of values only not indexes' signs. Correlation coefficients calculated for all indexes and days were averaged and plotted at the picture 2.

As it could be seen from scattering diagrams (pictures from presentation) and  $C$ ,  $\Gamma$  fields (pictures in presentation) their isolines repeat the form of each other. That's why it is worth to use only  $C$  parameter as containing information on statical atmospheric instability and circulation type too. 6 and 12 h forecasts of  $C$ ,  $\Gamma$  fields are very close to analysis data. Forecasts for the longer time lead to loss of isolines structure, minimum and maximum values changing and instability area shearing. Atmospheric statical instability index and generalized parameter  $C$  have the best correlation between analysis data and 6 and 12 h forecasts comparing to all other parameters (picture 2). Visual comparison of surface charts and convective indexes' fields calculated by analysis for the same date showed the following: CAPE values clearly indicate locations of possible strong convective events; positive MOCON areas pick out regions of moist convection and help to estimate its intensity. Positive HEI values are associated mostly with Cb clouds. Atmospheric instability areas become smaller with increasing of forecasting period from 12 h till 24 h and their location is displaced as convection inhibition demonstration.

During June 16-20, 2003 strong or frequent convective events were not observed over considered region. Indexes' fields showed low or close to zero values of CAPE and MOCON. HEI values were variable and don't allow to find a regularity.  $C$  and  $\Gamma$  analysis fields were positive mostly. Even Falkovich's parameter field don't indicate locations of possible convection arising. But rare convective events were observed in reality.

As example of case when indexes showed atmospheric instability, and dangerous weather phenomena were not registered is November 22-24, 2001. CAPE, MOCON and HEI fields allowed to indicate showers band from Finish Gulf till Ural mountains. Parameters  $C$ ,  $\chi$  and  $\Gamma$  gave not so clear information and did not pick out this showers' band.

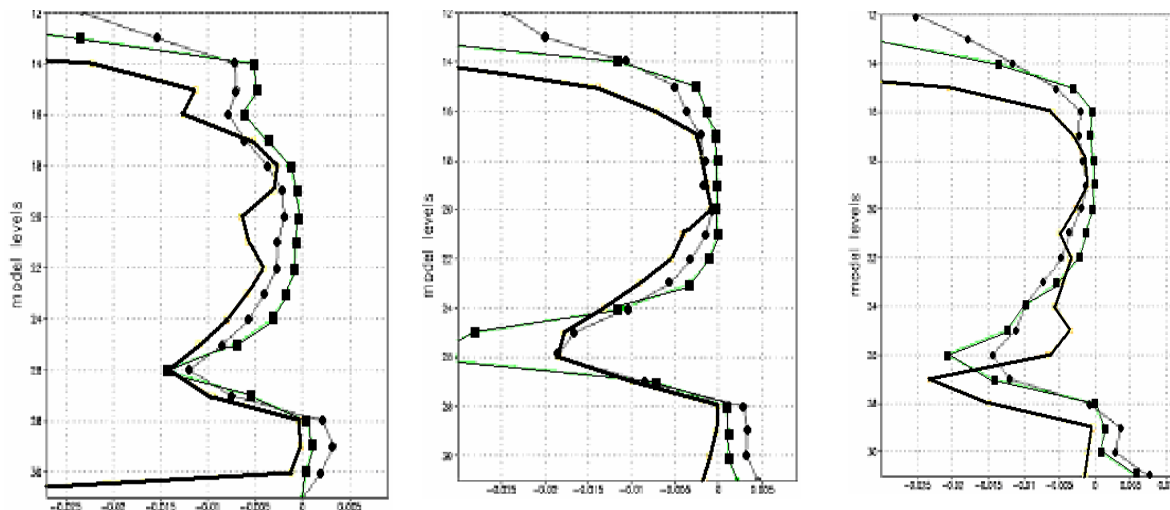
## Summary.

Values of Falkovich's index calculated by forecast data differed appreciably from values calculated by analysis files, and even 6 h  $\chi$  forecast didn't show results rather good on 22 km resolution. The same could be said analysing HEI values. Reasonable information are shown by CAPE and MOCON fields but for forecasting period not longer than 12 h. Statical stability index and generalized parameter  $C$  had the best correlation between analysis and forecast data, valid forecast period is about 24 h.

Convective indexes calculations may be considered as tool for effectiveness estimation of convection parameterization schemes or spatial resolution changing within NWP models.

### Acknowledgments

Many thanks to Prof. Tarakanov G.G.(RSHU) and Ekatherina Kourzeneva (RSHU), Laura Rontu (FMI) and Carl Fortelius (FMI) for giving valuable comments, guidance and encouragement.



C,  $\Gamma$ ,  $\chi$  profiles. Analysis data on 12UTC 23.11.2001.

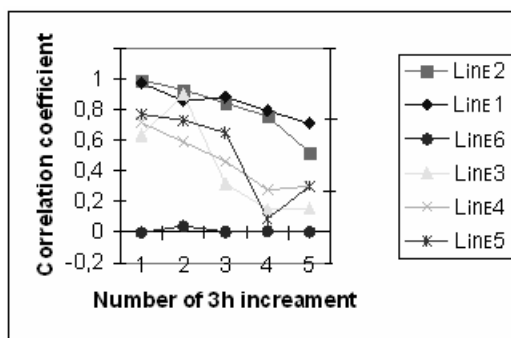
C,  $\Gamma$ ,  $\chi$  profiles. 12 h forecast from 23.11.2001 00:00UTC at 12UTC 23.11.2001 fc=12.

C,  $\Gamma$ ,  $\chi$  profiles. 24 h forecast from 22.11.2001 12:00UTC at 12UTC 23.11.2001 fc=24.



$\chi/1000$  line  
C\*100 line  
 $\Gamma$  line

Picture 1. C,  $\Gamma$ ,  $\chi$  profiles at airport Kyardla (Estonia) according to analysis data, 12 h forecast and 24 h forecast on 12UTC 23.11.2001.



Picture 2. Indexes' correlation coefficients (forecast and analysis)  
Line 1 –C, line 2 –  $\Gamma$ , line 3 –  $\chi$ , line 4 – CAPE, line 5 – MOCON, line 6 – HEI.

## References

1. Rusin I.N., Tarakanov G.G.,1996: Very shortrange forecasting, St.Petersburg, RSHU, 308 pp.
2. Gray M.E.B.,2001: The impact of mesoscale convective system potential-vorticity anomalies on numerical-weather- prediction forecasts// *Q. J. of the Royal Met. Soc.*, No. 571. January. Part A, 73- 89.
3. Calas C., Ducrocq V., Sényesi S. , 2000: Mesoscale analyses and diagnostic parameters for deep convection nowcasting. *Meteorol. Appl.* 7, 145-161.
4. Ducrocq V.,Tzanos D., Sényesi S. ,1998: Diagnostic tools using a mesoscale NWP model for the early warning of convection. *Meteorol. Appl.* 3, 329-349.
5. Improvement of techniques for early warning of convection. Project I.1,2001. Improvement of Nowcasting Techniques,Theme I:Strong Convection, *COST Action 78, Final report*, 37-66.
6. *HIRLAM Scientific Documentation, FIRST DRAFT, October 2001*, 31-36.
7. Riosalido R.,Carretero O.,Elizsga F. and Martin F., 1998: An experimental tool for Mesoscale Convective Systems (MCS) nowcasting. *Nowc. and V. Short R. Forec.. SAF Training Workshop*. 9-11 December.
8. Sényesi S., Ducrocq V., Rose-May Thepenier R.-M. and Calas C.,1998: MSG and the nowcasting of convective systems: Relevance of instability indices and other convection-related diagnostics. *Nowc. and V. Short R. Forec.. SAF Training Workshop*. 9-11 December.
9. Stensrud D.I., Cortinas I.V., Brooks H.E, 1997: Discriminating between Tornadic and Nontornadic Thunderstorms Using Mesoscale Model Output. *Weather and Forecasting*, September, Vol. 12, N 3, 613-632.
10. Tuduri E., Ramis C. , 1997: The Environments of Significant Convective Events in the Western Mediterranean. *Weather and Forecasting.*, June,Vol. 12, N 2, 294-306.
11. IFS Documentation Cycle CY25r1. Chapter 5 'Convection', Part IV: 'Physical processes', 2003, pp. 68- 71.

# The flood case 27–29 July 2004

SAMI NIEMELA

*Finnish Meteorological Institute, P.O.Box 503, FI-00101 Helsinki, Finland*

## 1 Introduction

The southern and central parts of Finland received very large precipitation amounts during 27–29 July 2004 due to a slowly moving low pressure system. This rain event caused flooding over large areas. Fig. 1a shows radar retrieved 12-hour accumulated precipitation amount valid at 12 UTC 29 July 2004. This illustrates that the low pressure system remained nearly stationary over Gulf of Finland. Consequently, the main precipitation area was located over Southern Finland and western part of the Gulf. At that time, the maximum precipitation amounts obtained were between 40–50 mm  $12\text{h}^{-1}$ . The reference HIRLAM, ran operationally at FMI with a horizontal resolution of 22 km (RCR starting from 12 UTC 27 July 2004), failed to produce such strong precipitation amounts as were observed during this two day period.

The objective of this study is to clarify the following questions. Can we make better precipitation forecasts just by reducing the grid size? Can we even simulate the structure of the precipitation event with meso- $\gamma$ -scale HIRLAM? In this study, we also compare the nonhydrostatic version of HIRLAM (Room, 2001) with the traditional hydrostatic HIRLAM. The different meso- $\gamma$ -scale model configurations are validated using data from FMI's radar network. Modelled radar reflectivities, which are computed by using the Radar Simulation Model (Haase and Fortelius, 2001), produced by non-operational experiments can be compared directly with observations. More detailed description of the study is presented by Niemela and Loridan (2004)

## 2 Experimental setup

Several experiments, both simulations and forecasts, are conducted in order to study the extreme precipitation event. FMI's operational forecasts (RCR and MBE with 22 and 9 km grid size, respectively) and one ECMWF forecast are also used in the evaluation. The analysis time of the operational HIRLAM forecasts is 12 UTC 27 July 2004, whereas ECMWF forecast started at 06 UTC 27 July 2004 (RCR's boundary field). Experimental forecasts with 5.6 km grid size, both hydrostatic (HH) and nonhydrostatic (NH), are made in order to study the effect of resolution on the precipitation forecast. The main differences to operational suites are the nonhydrostatic dynamics of NH and partly modified physical parameterizations in both HH and NH. The modifications in physics mainly involve changes in convection and condensation scheme (Straco, Sass, 2002) and turbulence scheme (CBR). These changes should be considered as tuning, which aims to make these schemes more applicable in higher resolution ( $\Delta x \leq 10$  km). The meso- $\gamma$ -scale HIRLAM simulations (HH and NH with MBE analyses as

boundaries), utilizing both 5.6 and 2.8 km grid size, try to find an answer to the second question, which was mentioned at the end of Section 1.

## 3 Results

### 3.1 Forecasts

Fig. 1 shows 12-hour precipitation amount [mm] accumulated during 36–48 hour forecast period (in ECMWF case 42–54 h). ECMWF model (panel b) is able to predict the location of the low pressure center fairly well. Consequently, the location of the main precipitation area is also well predicted. However, ECMWF seems to produce too much precipitation over the central parts of Finland.

Both operational HIRLAM forecasts, panels c and d, clearly misplace the low pressure center about 300 km to south-west from the observed location. Consequently, the areas with heaviest predicted precipitation are also located in wrong place. RCR underestimates the maximum precipitation by about 20–25 mm, whereas MBE creates maximum rainfall more close to observed one.

Both experimental forecasts (5.6 km grid size) also misplace the low pressure center (panels e and f). This is a clear example of how the forecasts, with small integration domain, are slaves of their lateral boundaries. NH produces similar precipitation distribution as MBE, whereas HH seems to overestimate the precipitation amount. The maximum precipitation amount produced by HH is clearly too strong.

Fig. 2 shows the time series of areal averaged 12-hour accumulated precipitation amount. On the average, coarser resolution ECMWF and RCR produce less precipitation than MBE, HH and NH. In this case, the precipitation amount produced by the higher resolution models are closer to radar observations (not shown). HH and NH behaves similarly than MBE and therefore do not bring any extra value to the average precipitation. However, HH and NH generate locally more intense precipitation rates compared to MBE, as shown in Fig. 1.

### 3.2 Simulations

Fig. 3 shows the instantaneous radar reflectivity fields from the model experiments (panels a–d) and the corresponding observations (panels e–f) valid at 12 UTC 29 July. Both hydrostatic experiments (a – 5.6 km and b – 2.8 km) create wide precipitation cells with strong reflectivity (>40 dBZ), which are not observed. However, nonhydrostatic results are more congruent with observations.

Fig. 4 presents frequency distributions of radar reflectivity from both model experiments and observations. All the distributions are gathered during the 54 hour simulations. Nonhydrostatic experiments with 5.6 and 2.8 km grid length represent the distribution of moderate and strong reflectivities (>24 dBZ) very well, whereas hydrostatic models clearly overestimate. The overestimation by HH is much more prominent with the 2.8 km grid size. The difference between NH experiments with different resolutions is smaller. It seems that the higher resolution NH slightly underestimates the amount of strong reflectivities (>32 dBZ) in general. However, both HH and NH, with the 2.8 km grid size, produce reflectivities over 48 dBZ ( $\approx 24 \text{ mm h}^{-1}$ )

in some grid cells. HH does it even with the 5.6 km grid size. Consequently, models produce locally too much precipitation ( $100\text{--}150\text{ mm }12\text{h}^{-1}$ , not shown). Such high values are about 2–3 times more than observed rainfall.

The amount of reactivities below 24 dBZ is clearly overestimated by all experiments. This basically means that the model creates wider precipitation areas with weak intensity compared to observations. One reason to overestimation can be seen from Figs. 3d and 3f. Models cannot resolve highly scattered, smallest scale convective precipitation cells (in panel f). Instead, they produce smoother precipitation fields with weak intensity (panel d).

## 4 Conclusions

During 27–29 July 2004 extreme precipitation event swept over southern and central Finland creating flooding over large areas. Operational forecast of FMI starting from 12 UTC 27 July 2004 failed to produce high precipitation amounts at right locations. Therefore, several model forecasts and simulations of this event has been conducted in order to study the possible additional value of meso- $\gamma$ -scale HIRLAM.

- Obviously, the location of the precipitation can not be improved just by reducing the grid size. If the outer model fails to produce the prevailing synoptic conditions, surely the inner model can not do any better. This just emphasize the important role of the high-quality synoptic-scale model as part of the meso- $\gamma$ -scale NWP system.
- However, the average precipitation amount can be increased, and in this case improved, by reducing the grid size from 22 to 9 km. By reducing the grid size from 9 km further to 5.6 km does not have such a big impact on the average (locally the impact is larger).
- Nonhydrostatic model combined with the Straco-scheme and the 5.6 km grid, can produce realistic reactivity distribution. However, models utilizing the 2.8 km grid size tend to produce too much precipitation. Hydrostatic model overestimates the amount of strong reactivities with both resolutions.

## References

- Haase, G. and C. Fortelius, 2001: Simulation of radar reactivities using Hirlam forecasts. HIRLAM Tech. Rep. 51, SMHI, S-601 76 Norrkoping, Sweden. Hirlam-5 Project, 22 pp.
- Niemela, S. and T. Loridan, 2004: The flood case 27–29 July 2004: added value of the meso- $\gamma$ -scale HIRLAM? *HIRLAM newsletter*, **46**, 48–58.
- Room, R., 2001: Nonhydrostatic adiabatic kernel for HIRLAM. Part I: Fundamentals of nonhydrostatic dynamics in pressure-related coordinates. HIRLAM Tech. Rep. 48, SMHI, S-601 76 Norrkoping, Sweden. Hirlam-5 Project, 25 pp.
- Sass, B. H., 2002: A research version of the STRACO cloud scheme. DMI Tech. Rep. 02-10, Danish Meteorological Institute, DK-2001 Copenhagen, Denmark. 25 pp.

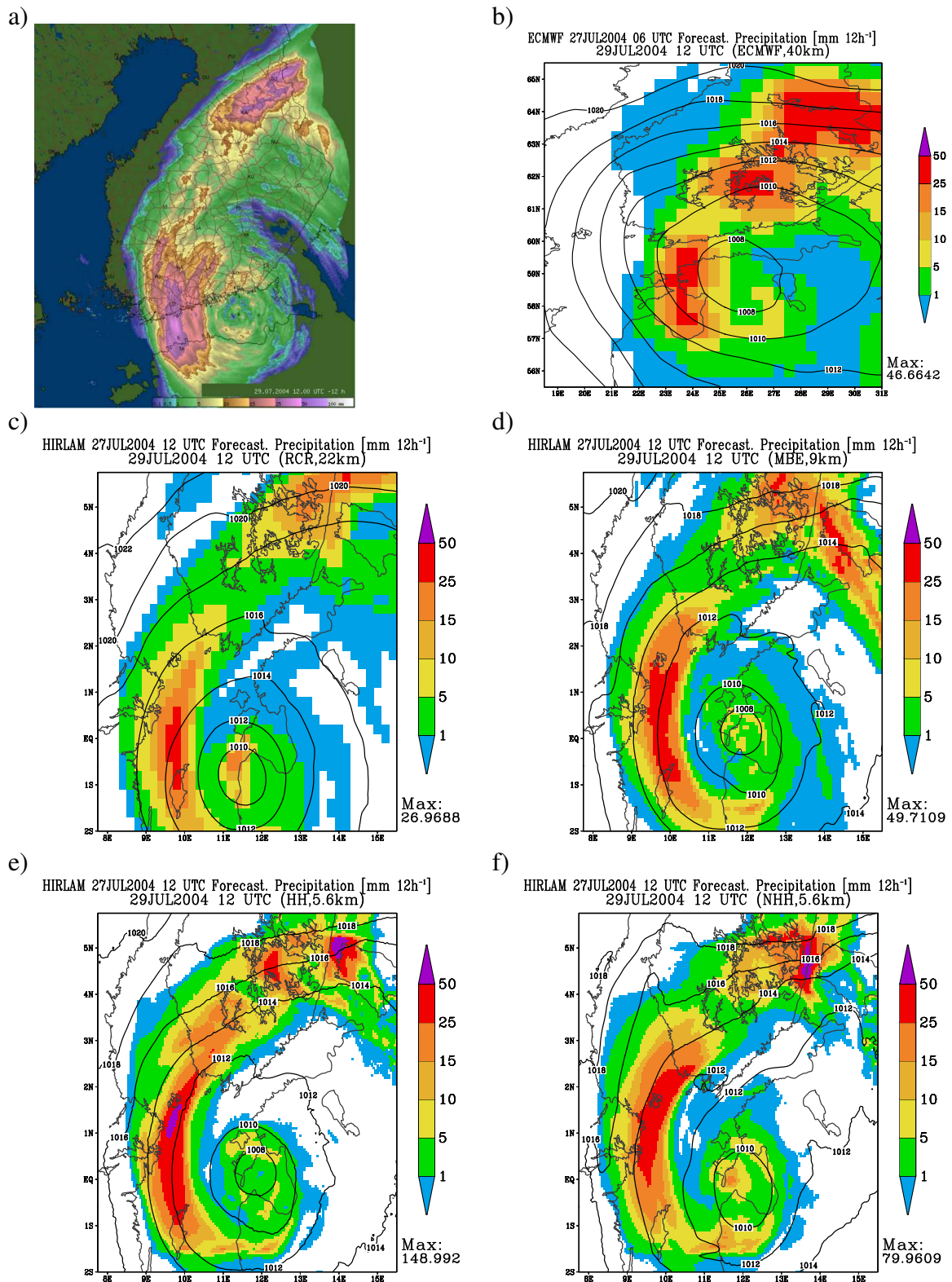


Figure 1: 12-hour accumulated precipitation [mm] and mean sea level pressure [hPa] valid at 12 UTC 29 July 2004. a) Observation retrieved from the FMI's radar network and the forecasts from b) ECMWF 40 km, c) RCR 22 km, d) MBE 9 km, e) HH 5.6 km and f) NH 5.6 km.

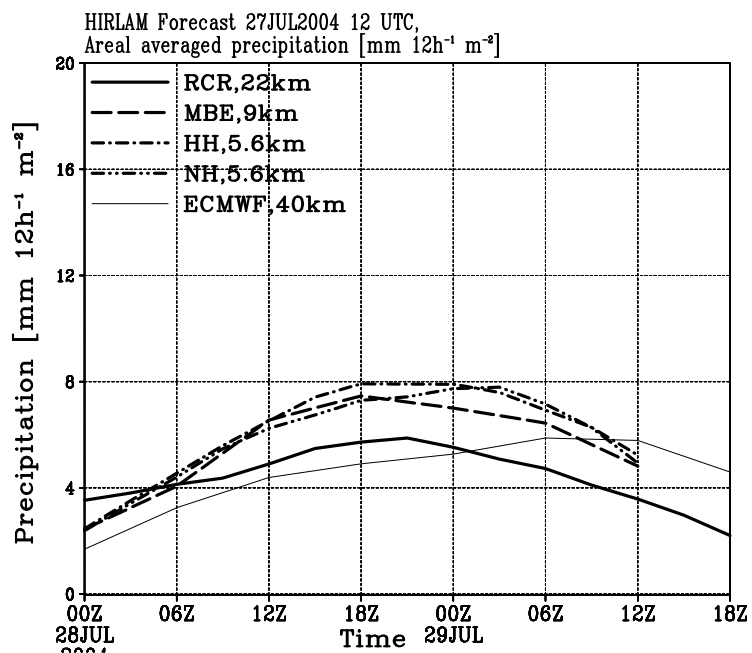


Figure 2: Time series of the areal averaged 12-hour accumulated precipitation [mm]. Forecasts averaged over the area seen in Fig. 1c: solid (thick) = RCR, 22 km, dashed = MBE, 9 km, dot-dashed = HH, 5.6 km, dot-dot-dashed = NH, 5.6 km and solid (thin) = ECMWF, 40 km.

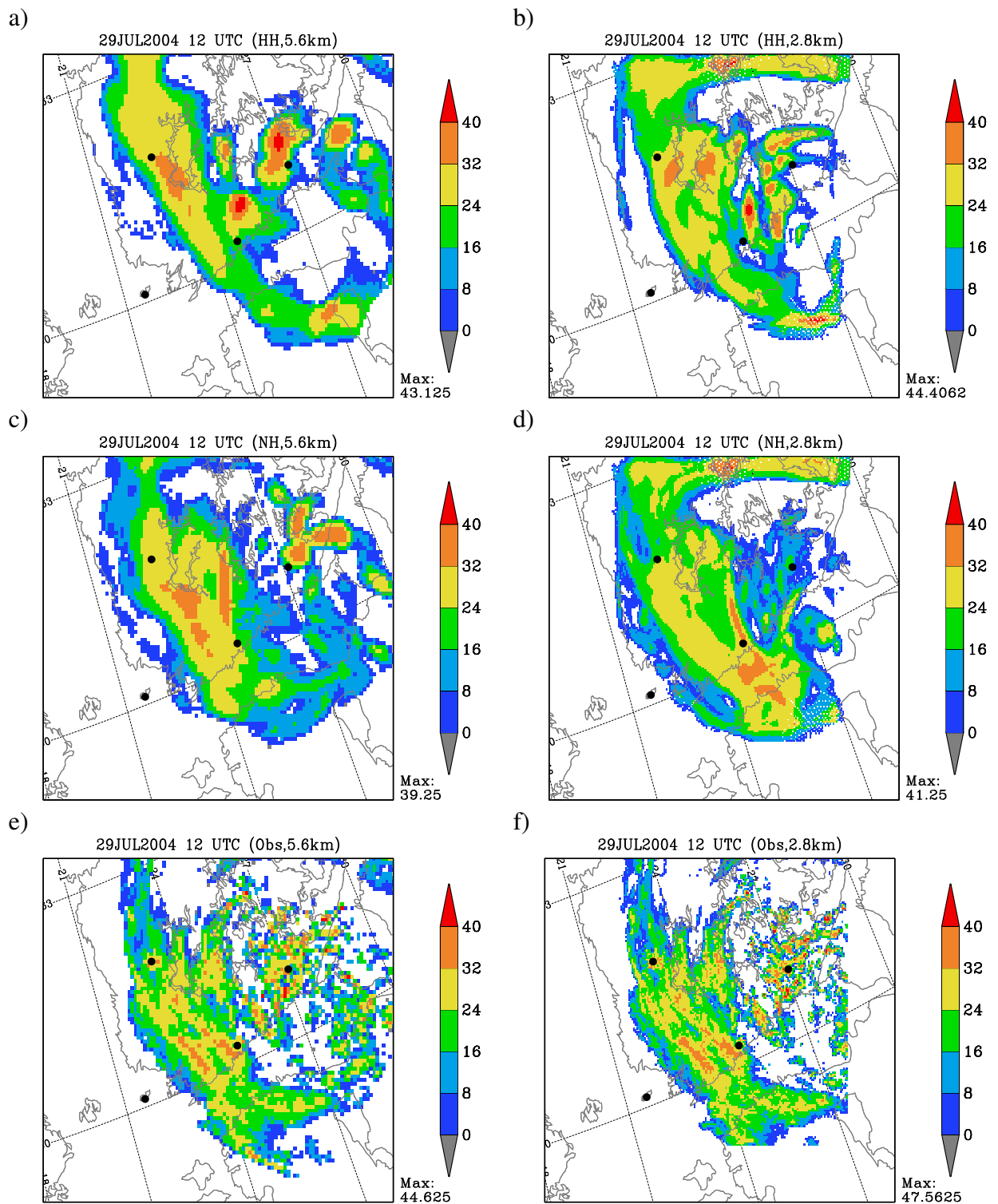


Figure 3: Composite of radar reflectivity [dBZ] fields after 48 hour simulation valid at 12 UTC 29 July 2004. a) HH, 5.6 km, b) HH, 2.8 km, c) NH, 5.6 km, d) NH, 2.8 km, e) radar observation, 5.6 km and f) radar observation, 2.8 km. The locations of the radars are marked with black dots.

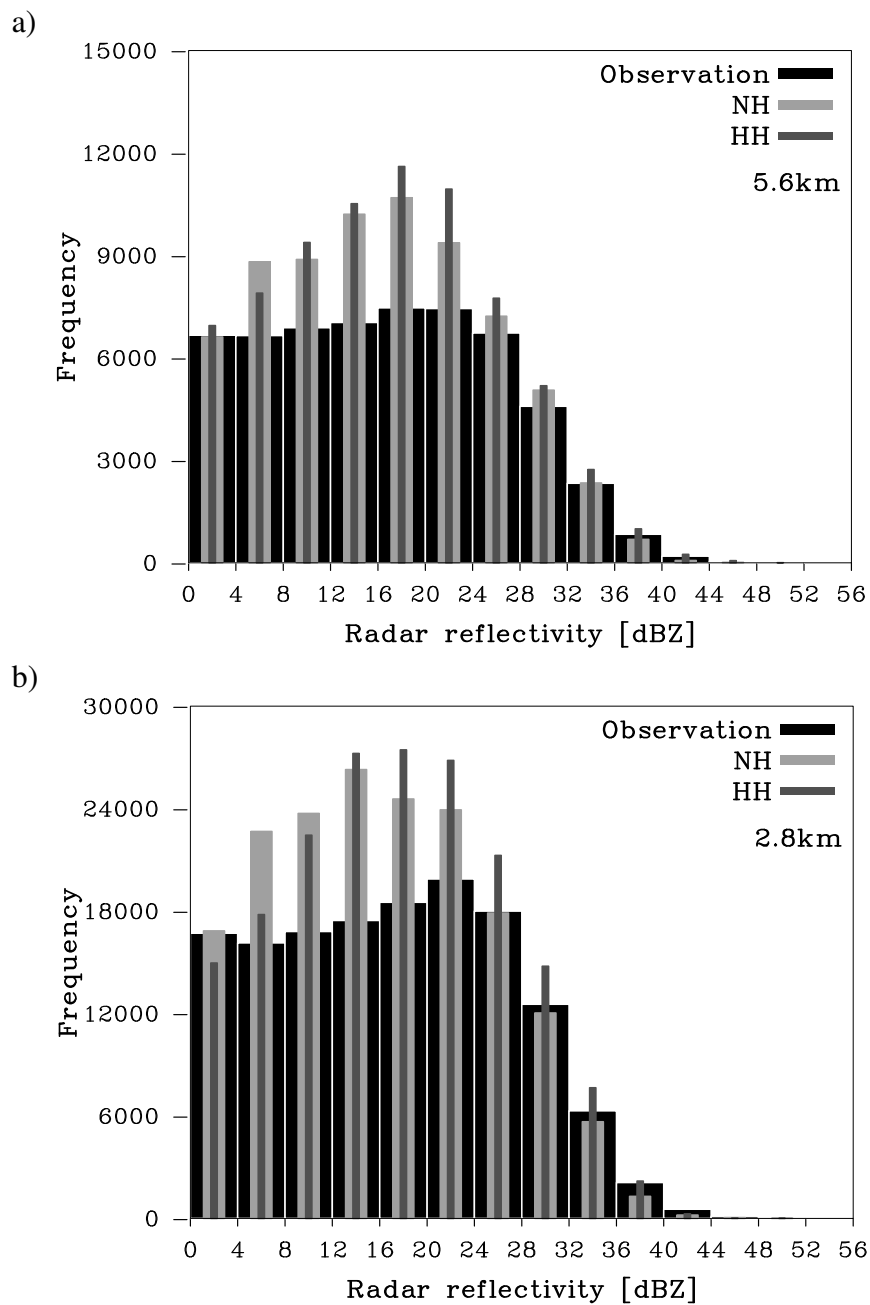


Figure 4: Frequency distributions of radar re ectivity [dBZ] produced by 54 hour simulations starting from 12 UTC 27 July 2004. Grid length is a) 5.6 km and b) 2.8 km. NH- and HH-experiments are represented with light gray and dark gray bars, respectively. Black bars represent dBZ-observations. The elevation of radar antenna is  $0.4^\circ$ . In this case re ectivity values below 0 dBZ are not meteorologically important and therefore those are omitted.

# Case study based on one dimensional model with Kain-Fritsch convection parameterization scheme

Paulius Jalinskas

Lithuanian Hydrometeorological Service, Lithuania

Vilnius University, Lithuania

paulius@meteo.lt

## 1 Introduction

The problem of convective parameterization is widely recognized by the modeling community to be a crucial component in obtaining successful numerical simulation and forecasts (Emanuel and Raymond, 1993). The major weight in this study is put on the Kain-Fritsch (KF) parameterization of convection, which is one of the most sophisticated convective schemes today. KF scheme is modified Fritsch and Chappell (FC) scheme, KF uses one-dimensional entraining/detraining plume cloud model (ODEDP), while FC - one dimensional entraining plume model (ODEP). In ODEDP is assumed that any mixture that becomes negatively buoyant detrains from the cloud while those mixtures that remains positively buoyant entrains into the cloud (Kain and Fritsch, 1993).

The convection scheme in HIRLAM (with few exceptions) takes its fundamentals from the KF scheme as well as single column version of SMHI Rossby Centre Regional Climate Model (RCA1D) where the physical parameterizations follow closely those in the operational version of the HIRLAM model at SMHI (Jones et al., 2004). RCA1D is tool to be used in this study to understand the different features of the KF scheme. Sensitivity studies are performed for the following features of the convection:

- Downdraft effect
- Precipitation fall-out rate effect
- The role of the different trigger functions

The deep convection case is utilized to analyze the impact of these features.

## 2 1-D experiments setup

All experiments are performed on RCA1D model with the deep convection case. 40 vertical levels are used in the standard RCA1D model setup. Deep convection case was designed from data collected at the Atmospheric Radiation Measurement (ARM) Southern Great Plains site during summer 1997 Intensive

Observing Period. The case is from 2330 UTC 26 June to 24 UTC 30 June 1997 (Julian Day 178 to 182) and was simulated by 2D cloud resolving model (2-D model results further called observations). This case features a weak precipitation event that occurred on Day 179 and a strong precipitation event on Day 180-181, which was mainly associated with a complex of thunderstorms that developed in south-east Kansas in the late evening of day 180 local time. This convective event was well captured by the ARM sounding array (Xie et al., 2002).

### 3 Results

The results from 1-D experiments with the deep convection case are described in this section. In the first experiment downdrafts were switched off. Downdrafts forms from falling precipitation and rain cooled air with following transport of colder air. Downdrafts have grate bearing on the stabilization of the boundary layer by convection. By switching off the downdrafts we can expect acceleration of cloud water detraining from cloud and growing precipitation amount (Fig. 1). The effect of switching off the downdrafts could be seen on lower percentage of total cloud cover between Julian Days 179-180. Furthermore it has an impact on amount of outgoing longwave radiation and total cloud water path (TCWP) between Julian Days 181-181.5 during strong precipitation event.

Different rates of cloud water conversion to precipitation were tested in another state of experiment. The amount of precipitation that will fall out from a layer in the cloud is a function of vertical velocity speed and the amount of condensate in the layer. A rate constant, which in the reference model is set to 0.03, determines the speed at which condensate fall out. This fall-out rate is main objective in this part of study. Two runs, one with faster (0.09) and one with near normal (0.02) rate are executed to investigate the importance of this empirically derived constant. The intuitively correct would be to have earlier precipitation in the case with higher fall-out rate compared to near normal fall-out rate (Fig.2). These results could be seen from Julian Day 179.5 to 180; later non-linear effects give more or less the opposite results in precipitation and total cloud cover timeseries (Fig. 2).

The next stage was to investigate the trigger functions, which are used in convective parameterization routines. Specifically, the trigger functions 1) estimates the magnitude of the largest vertical velocity perturbation from a source layer and 2) calculates the total amount of inhibition between the source layer and LFC (level of free convection). It is worth mentioning that if the condition for deep convection is not satisfied the scheme directly checks for shallow convection. Two types of triggers were studied: first - only relative humidity, second - only virtual temperature as trigger function. Both trigger functions act quite similar and both give produce peak of total cloud cover and total cloud water path between Julian Day 180.5 and 181 (Fig.3). This peak could be explained by shallow convection occurred exactly during this time in 1-D model run with only shallow convection turned on (not shown).

### 3.1 Conclusions

Downdrafts act as drying factor and indirectly affect surface radiation budget.

Precipitation fall-out rate is not a crucial factor for deep convection event.

Both relative humidity and temperature trigger function resulted increase of total cloud cover just before heavy rainfall event.

Kain-Fritsch scheme can reasonably forecast heavy precipitation event peak but still lacks occurrence in total cloud cover.

### References

- [1] Emanuel, K. A., and D. J. Raymond, Eds., 1993. *The representation of cumulus convection in numerical models*. Meteor. Monog., **46**, 246.
- [2] Jones, C. G., U. Willen, A. Ullesting and U. Hansson, 2004. *The Rossby Centre Regional Atmospheric Climate Model Part I: Model Climatology and Performance for the Present Climate over Europe*. Ambio, **33**, 199-210.
- [3] Kain, J. S. and J. M. Fritsch, 1993. *A one-dimensional entraining detraining plume model and its application in convective parameterization*. J. Atmos. Sci., **23**, 2784-2802.
- [4] Xie, S., and co-authors, 2002. *Intercomparison and evaluation of cumulus parameterizations under summertime midlatitude continental conditions*. Quart. J. Roy. Meteor. Soc., **128**, 1095-1135.

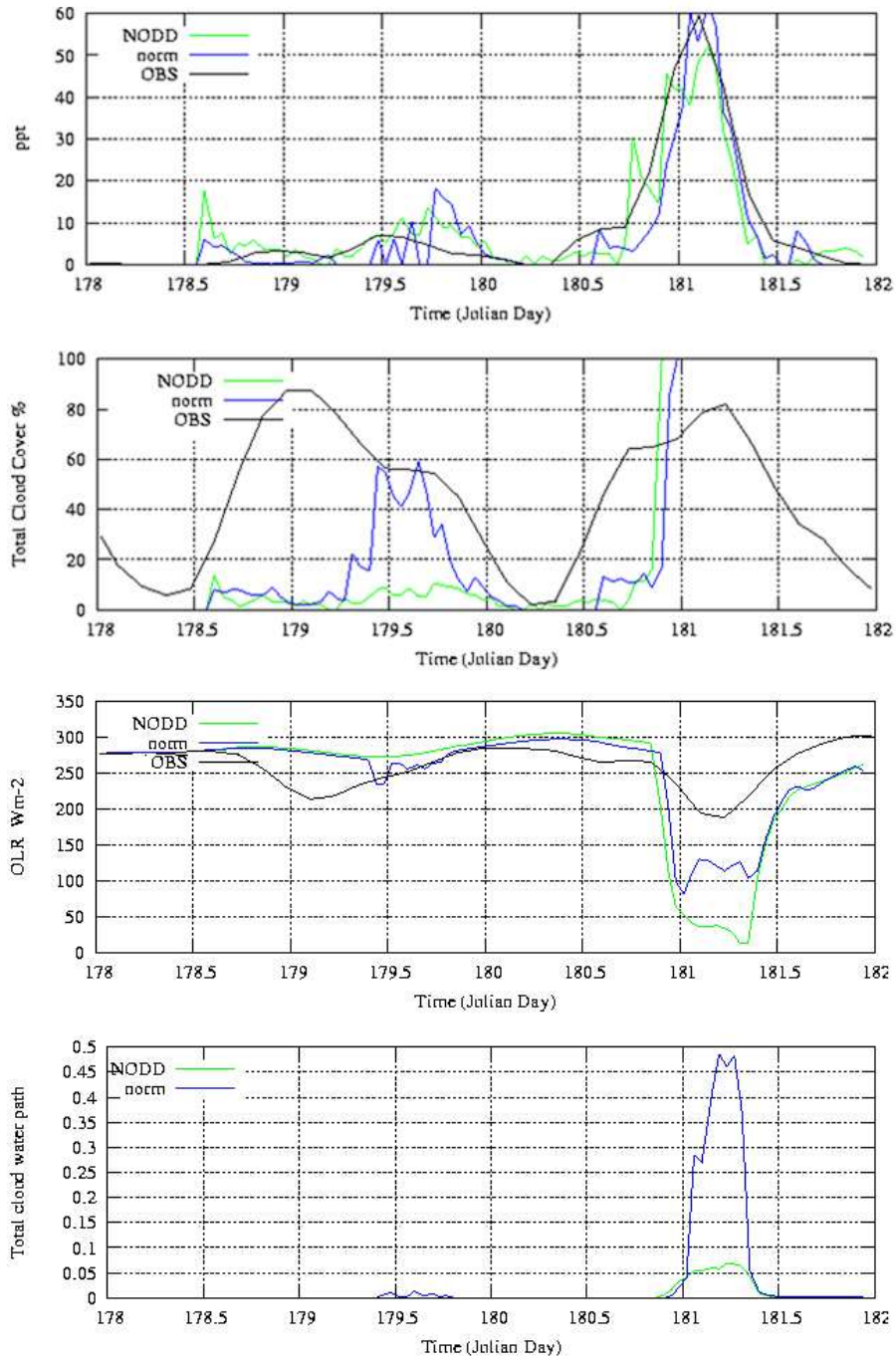


Figure 1: Precipitation (ppt) in mm/day and total cloud cover (%), outgoing long-wave radiation (OLR) in  $Wm^{-2}$  and total cloud water path in  $kg/m^2$  from RCA1D simulations with no downdrafts (NODD), with downdrafts norm and timeseries of observations (OBS)

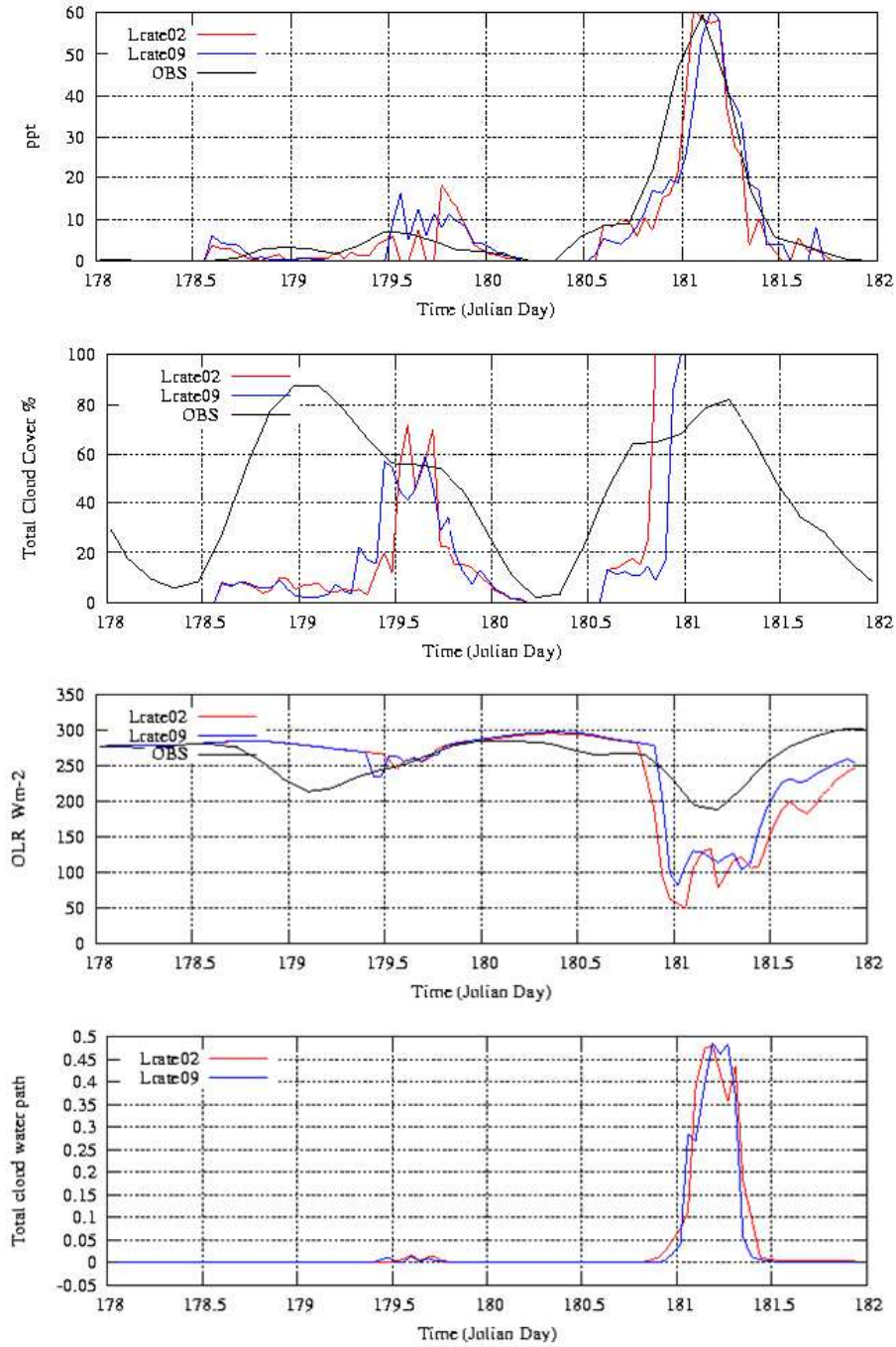


Figure 2: Precipitation (ppt) in mm/day and total cloud cover (%), outgoing long-wave radiation (OLR) in  $Wm^{-2}$  and total cloud water path in  $kg/m^2$  from RCA1D simulations with precipitation fall-out rate equal to 0.02 (Lrate02), 0.09 (Lrate09) and timeseries of observations (OBS)

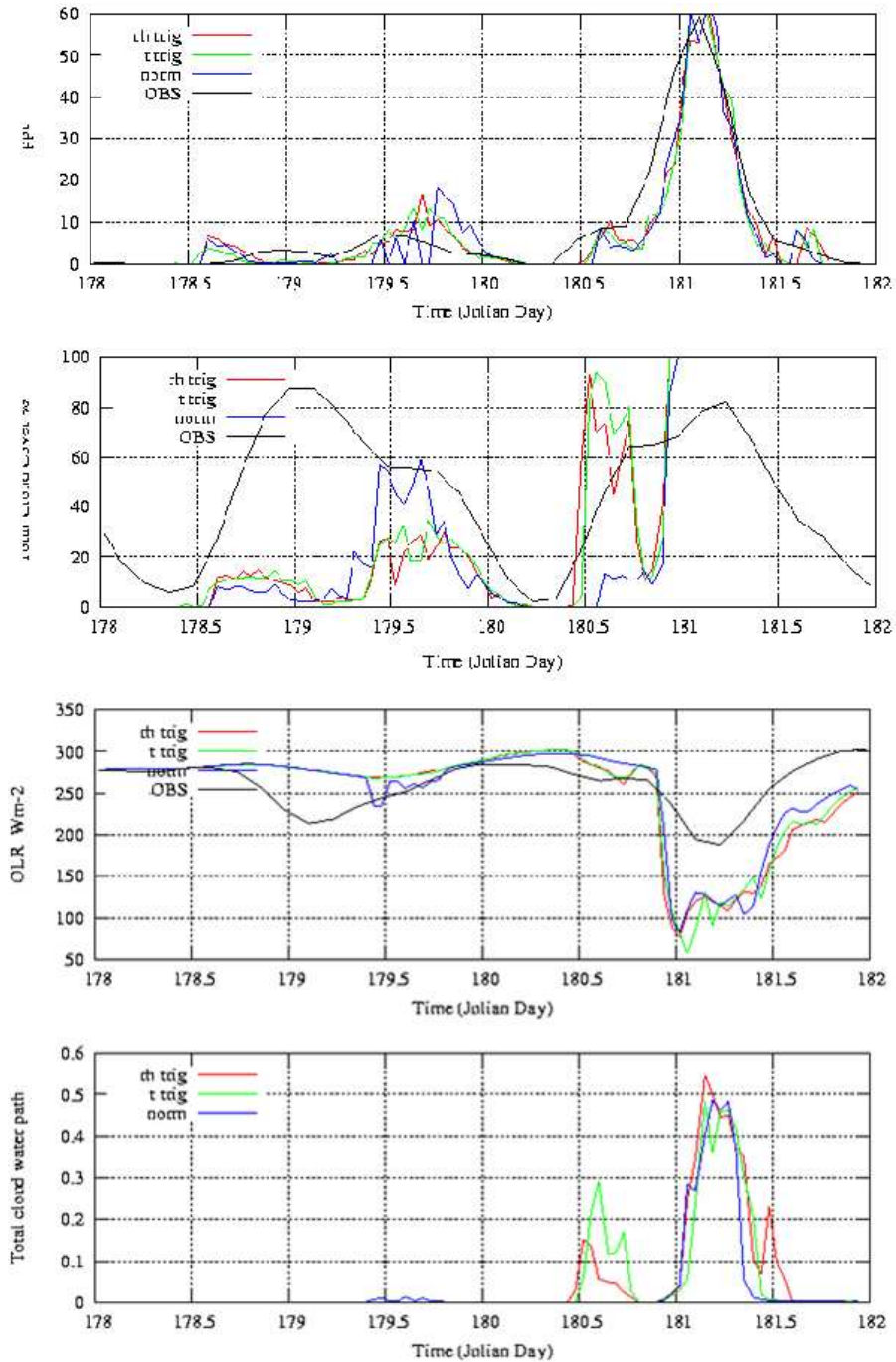


Figure 3: Precipitation (ppt) in mm/day and total cloud cover (%), outgoing longwave radiation (OLR) in  $Wm^{-2}$  and total cloud water path in  $kg/m^2$  from RCA1D simulations with only relative humidity (rh trig), only temperature (t trig) and both trigger functions (norm); timeseries of observations (OBS)

# Summary of the working group discussion on the representation of convection in high resolution numerical models

Dmitrii Mironov and Colin Jones

Excellent discussions of convection and turbulence parameterisation issues took place during the workshop. Among other things, an attempt was made to identify (i) at which resolution (horizontal grid size) of a numerical model of atmospheric circulation (NWP model, climate model) convection parameterisation (scheme) be switched off entirely, (ii) at which resolution a parameterisation of deep precipitating convection is no longer needed but a parameterisation of shallow non-precipitating convection should be kept, (iii) what are the key quantities that ensure consistency between convection scheme and other physical parameterisation schemes of an atmospheric model, (iv) which avenues of investigations (development strategies) are most fruitful.

There is an opinion nowadays that convection scheme can simply be switched off if a horizontal grid size of an atmospheric model is less than about 4 km. Such hope seems to be illusory. Even with a horizontal grid size of about 1 km, a convection parameterisation will be required. Although convective motions in most of the troposphere are going to be explicitly resolved, triggering of convection, the process that predominantly occurs through the boundary layer, remains at sub-grid scales and should therefore be parameterised. The question is whether a separate convection scheme should be kept, or the work performed by a convection scheme can be delegated to an extended turbulence scheme capable of describing non-local boundary-layer convection in a rational way. Most currently used turbulence schemes are unable to describe boundary-layer convection realistically.

Three resolution ranges are identified. With a horizontal grid size of order 2 km or less, no parameterisation of deep precipitating convection is required. However, a parameterisation of shallow non-precipitating convection, either as a separate scheme or as part of a non-local turbulence scheme, is required. With a grid size of order 10 km or greater, deep precipitating convection should be parameterised in one way or the other. The grid-size range from about 2 km to about 10 km is a “grey zone” where a deep convection parameterisation is still required but should be less active than it is in most currently used atmospheric models. It should be mentioned that the above grid-size thresholds are not grounded theoretically. They are based on practical experience of numerical model users and should be treated as rough tentative estimates.

As part of a very complex, strongly non-linear numerical modelling system, a convection parameterisation is intimately coupled with all other system components. Achieving harmony between a convection scheme and other parts of the system physics and numerics is a challenge. The first priority task is to make a convection scheme consistent with (i) a grid-scale microphysics scheme and (ii) a sub-grid scale cloud scheme. In most NWP and climate models, convective and grid-scale microphysical processes, e.g. generation of precipitation, are described differently. A grid-scale scheme usually incorporates more of the essential physics. A more consistent treatment is required. As to parameterisation of the sub-grid scale cloudiness, there is consensus of opinion that a statistical sub-grid scale cloud scheme is the most promising alternative. The statistical cloud scheme has the great potential but is sensitive to the input. The key quantities are the sub-grid scalar variances (variance of temperature and of humidity with respect to their grid-box means) that enter the formulations of the cloud fraction and of the cloud water content within a grid box. As both “convection” and “turbulence” contribute to the sub-grid scalar variances, a coherent convection-turbulence formulation is required.

Three avenues of inquiry (development strategies) have been outlined that are loosely referred to as short term, medium term, and long term strategies.

(1) Short term.

Traditional mass-flux convection schemes are kept.

Doing it this way, one should put up with numerous shortcomings of the current mass-flux convection schemes. Although the overall performance of the current schemes within NWP and climate models with comparatively low resolution is not entirely unsatisfactory, many assumptions that stand behind them are too restrictive. These are, first of all, the assumptions that (a) convection is quasi-stationary (no time-rate-of-change terms in the mass-flux equations), and that (b) in a triple decomposition of a quantity in question (vertical velocity, temperature, humidity) into the contributions from updraughts, from downdraughts, and from the so-called environment, a mean over the environment is equal to a mean over the entire grid box. The former assumption deprives a convection scheme of memory. As a result, a scheme responds to external forcing practically instantaneously, leading to a premature initiation of convection and an erroneous diurnal cycle. It is common knowledge that none of the existing convection schemes is able to realistically reproduce diurnal cycle of precipitation. The latter assumption actually means that the area covered by convective updraughts and downdraughts is small as compared to the size of grid-box. This assumption is valid, to a good approximation, for the horizontal grid-size of order 200-300 km. It can probably be tolerated if the grid size is of order 50 km. It is no longer acceptable for the grid size of order 10 km or less, where it leads to a far too active convection, the result of double counting of a considerable range of energy-containing scales of motion.

A way towards improvement of the model performance in the framework of the short term strategy basically lies with tuning/revising some formulations in the existing mass-flux schemes. It should be realised, however, that considerable progress along this line is not very likely. Some improvement can be achieved through tuning/revising (i) convective trigger function, (ii) formulation of entrainment and detrainment, and (iii) the way convective precipitation is generated and evaporated. An attempt should be made to suppress generation of convective precipitation in favour of grid-scale precipitation, e.g. by making the cloud condensate produced by a convection scheme available to a grid-scale microphysics scheme for potential precipitation.

It is recommended to keep away from the “grey zone”. That is, the existing convection schemes should be applied in the numerical models whose grid size is greater than about 10 km. With a smaller grid size, a parameterisation rule should be introduced to slow down deep convection. That parameterisation rule can use a number of criteria to recognise deep convection, such as (i) CAPE, (ii) the mass flux intensity as computed by the convection scheme, and (iii) condensate production and precipitation generation in the convection scheme.

(2) Medium term.

Convection schemes based on the mass-flux approach are kept but should be further developed to eliminate their most notable drawbacks.

Doing it this way, one should introduce memory to the mass-flux equation and relax (or get rid of) the assumption that the mean over the environment is equal to the grid-box mean. One way of doing it is to introduce an equation for the fractional area of convective updraughts and an equation for the vertical velocity in the updraught. Both equations should include the time-rate-of-change term. We recall that the current mass-flux convection schemes carry a steady-state equation for the updraught mass flux, which is, by definition, the product of the mean density, the area fraction covered by convective updraughts, and the difference between the updraught vertical velocity and the grid-box mean vertical velocity (a similar equation is carried for the downdraught mass flux). The scheme solves for the mass flux as function of height. However, by virtue of the above assumption (b), there is no way to separately determine the updraught area fraction and the updraught vertical velocity.

The above two additional evolution equations require boundary conditions at the cloud base. One way to specify the updraught fractional area and the updraught vertical velocity at the cloud base is to relate them to the properties of the boundary-layer turbulence through the Deardorff-type convective scaling. Account must be taken of the skewed nature of convective turbulence. An extended mass-flux scheme will require an advanced formulation for the rate of turbulent entrainment and detrainment. Recall that in the current mass-flux scheme the rate of turbulent entrainment and detrainment is either set to a constant value independent of height or is determined through a buoyancy sorting procedure. An advanced formulation should account, in a physically plausible way, for the dependence of entrainment/detrainment rate on height and on the buoyancy difference between the updraught and the environment. Other formulations (parameterisation rules) that will require modification in the advanced mass flux-scheme include formulations of convective precipitation and of convective downdrafts. Suppressing convective precipitation in favour of grid-scale precipitation, e.g. by making the cloud condensate produced by a convection scheme available to a grid-scale microphysics scheme for potential precipitation, should be tried out. A better parameterisation of convective downdrafts is an unresolved problem that calls for further research. An improved representation of microphysics and precipitation generation in convection schemes may require an iterative procedure to compute the updraught buoyancy and the microphysical quantities.

An extended mass-flux scheme is expected to offer a reasonably accurate solution for the “grey zone”, but this remains to be seen. The work towards an extended mass-flux scheme has been initiated (see the presentation by Luc Gerard).

### (3) Long term.

A separate convection scheme is no longer used. A unified convection-turbulence scheme based on the second-order closure ideas is developed. The scheme accounts for non-local features of convective mixing and treats all sub-grid scale mixing processes in a unified framework.

Doing it this way, part of the work performed presently by the convection scheme is delegated to the turbulence scheme. This requires developing a turbulence scheme that includes extended formulations for the third-order moments largely responsible for non-local transport properties of convective motions. Furthermore, the incorporation of transport equations for variances of scalar quantities, such as temperature and specific humidity, is essential if not indispensable. The mass-flux approach is used as a guidance to develop advanced non-local formulations for the quantities in question, however a unified scheme is formulated in terms of statistical moments of turbulence. This approach has a number of advantages.

First, a unified scheme is more transparent and more controllable. It does not require splitting of sub-grid motions into a quasi-organised part (convection) and a random, quasi-homogeneous, quasi-isotropic part (turbulence). It therefore avoids a number of conceptual difficulties inherent in the mass-flux approach. Next, a unified scheme is “rescalable”, that is, an increased resolution can be accounted for in a physically plausible way through formulations of dissipation and return-to-isotropy length (time) scales. In mass-flux convection schemes, this dependence is hidden in various closure formulations, first of all, in the formulations of entrainment and detrainment. Those closure formulations are difficult to reformulate/adjust as the resolution is increased. Then, communication between a unified scheme and a sub-grid scale cloud scheme is facilitated. The quality of the input information for statistical sub-grid cloud scheme is to be improved. At present, neither the convection scheme nor the turbulence scheme provides necessary input information for the sub-grid cloud scheme. A description of scalar variances is far less satisfactory than is required. It is going to be considerably improved through the use of transport equations for the sub-grid scalar variances. Finally, in view of ever increasing computer power and an increasing horizontal resolution of NWP and climate modelling systems, an extended turbulence scheme has a higher life expectancy than a convection scheme and is, therefore, more worth an effort.

Gryanik and Hartmann (2002) have developed a closure model that satisfies most of the above requirements. Its salient feature is a skewness-dependent formulation for the third-order and fourth-order moments that are largely responsible for non-local mixing (see e.g. Abdella and McFarlane 1997, Zilitinkevich et al. 1999, Mironov et al 1999, Abdella and McFarlane 1999, and Abdella and Petersen 2000). The closure model is developed for the dry convective boundary layer. Its further development to incorporate moisture and, possibly, other hydrometeors, and its testing to see if convection over a wide range of scales (from a few tens of metres to about 50 km) can be described realistically is not trivial. This seems to be manageable, however.

A unified second-order closure scheme is no doubt the most promising alternative to treat shallow convection. It is likely to be a better alternative for deep convection too. Treatment of precipitation processes within the second-order modelling framework seems to be more difficult than within the mass-flux framework. This is not an issue for high-resolution models where only shallow convection should be parameterised. It is, however, an issue for coarse-resolution models where a parameterisation for deep precipitating convection is required.

## References:

- Abdella, K., and N. McFarlane, 1997: A new second-order turbulence closure scheme for the planetary boundary layer. *J. Atmos. Sci.*, 54, 1850-1867.
- Abdella, K., and N. McFarlane, 1999: Reply. *J. Atmos. Sci.*, 56, 3482-3483.
- Abdella, K., and A. C. Petersen, 2000: Third-order moment closure through the mass-flux approach. *Boundary Layer Meteorol.*, 95, 303-318.
- Gryanik, V. M., and J. Hartmann, 2002: A turbulence closure for the convective boundary layer based on a two-scale mass-flux approach. *J. Atmos. Sci.*, 59, 2729-2744.
- Mironov, D. V., V. M. Gryanik, V. N. Lykossov, and S. S. Zilitinkevich, 1999: Comments on "A New Second-Order Turbulence Closure Scheme for the Planetary Boundary Layer" by K. Abdella and N. McFarlane. *J. Atmos. Sci.*, 56, 3478-3481.
- Zilitinkevich, S. S., V. M. Gryanik, V. N. Lykossov, and D. V. Mironov, 1999: Third-order transport and non-local turbulence closures for convective boundary layers. *J. Atmos. Sci.*, 56, 3463-3477.

## **Report of the Working Group Discussion on "Development of Microphysics for the fine scale"**

Jean Quiby

The classical species in a complete scheme of micro-physics and precipitations are: Water vapour, cloud ice crystals, cloud droplets, rain, snow, graupel and hail. A long discussion took place about the degree of sophistication that a micro-physical scheme should have for high resolution NWP models. The discussion concentrates primarily on hail and graupel.

As hail can only form in cumulo-nimbus, the working group considered that it does not belong to the classical micro-physics as it is used today, that is for the grid-scale (or stratiform) precipitations only. This simple fact already shows how more meaningful it would be to have an integrated precipitation scheme combining stratiform and convective precipitations, along the line presented by Luc Gérard during the Workshop.

Concerning the graupel, the discussion revealed two aspects: on one side it has been claimed that graupel is much more abundant in clouds than non-specialists generally believe. Consequently, it should be explicitly represented. On the other side, graupel is connected to snow as it is produced by accretion (the freezing of super-cooled water droplets on ice crystals). The discussion led nevertheless to the conclusion that, because of the steadily increasing complexity of our models (we want to mirror the atmosphere as precisely as we can), graupel should today be part of a micro-physical scheme of a very high resolution NWP model.

An important point was the discussion on super-cooled cloud droplets because these latter not only play a very important role in cloud micro-physics, but also because of their importance in aviation: they are the cause of air-plane icing. It has been confirmed by Paul Schultz that - after definition of thresholds - forecast maps showing the amount of cloud water where the temperature is below zero degree can be of great importance for the aviation. It is by temperatures of -2/-3 degrees that icing is the most dangerous, when glazed, transparent ice forms. At -6/-7 degrees, rimed, opaque ice forms, which is less dangerous as it remains on the edges of the wings and does not spread on the wings as the glazed ice.

Considering that many coefficients used today in the micro-physical schemes are very empirical, the question of whether our cloud physics is realistic has been asked. Paul Schultz and Jean-Pierre Pinty answered that large improvements coming on one side from the measurements made by research airplanes and on the other side from laboratory experiments with cloud chambers - they are still in use! - have been made during the last 15 years.

### Micro-physics versus Dynamics

- It has been accepted that the micro-physics (without sedimentation) of our models can accept large time-steps, time-steps of several minutes without damage. But we have to be careful that mixing-rates do not become negative (particularly true for Eulerian schemes).

- Micro-physics and Semi-lagrangian advection: The answer to that question is that - as long as sedimentation is not considered - there is no specific problem with the semi-lagrangian advection: the micro-physics can be treated at the arrival points as in an Eulerian scheme.

### Advectioned precipitations

- The experience made by COSMO - where precipitations are advectioned operationally - is that it is computationally expensive, at least in an Eulerian frame (see below). Paul Schultz has communicated the fall speeds that we should use: for drizzle: 3-4 m/s; for rain: 5-6 m/s. These values have been measured by wind profilers in the United States.

### Advectioned precipitations and Semi-lagrangian advection

Little has been done in this field until today. There anyway exists a radical solution: the precipitations can be advectioned in the vertical (the fall of the precipitations) in an Eulerian way, with an implicit scheme in order to keep reasonable time steps in view of the thinness of the model layers in the boundary layer). But, as it has rightly been remarked, this solution would very expensive.

### Fractional cloudiness

Due to lack of time, only one point has been discussed:

Do very high resolution models still need a parameterization of the fractional cloudiness?

The answer of the working group is a clear yes. Even with a grid point distance of one km, we need a parameterization of the partial cloudiness. Example: the small cumuli capping the boundary layer in summer by fair weather. But the parameterization can no longer be only a function of height and relative humidity as it is often the case in today's operational models: moist eddy diffusivity has also to be considered, maybe integrated in a shallow convection scheme.

## Notes from the working session on analysis, diagnostics and validation

Carl Fortelius

The working session started with three keynote presentations by:

Paul Schultz on the Local Analysis and Prediction System (LAPS)

(<http://laps.fsl.noaa.gov/>)

Laura Rontu on the Helsinki Testbed project

([http://www.fmi.fi/research\\_meteorology/meteorology\\_30.html](http://www.fmi.fi/research_meteorology/meteorology_30.html))

Javier Calvo on the single column Hirlam

The following points were noted during the discussions:

### Analysis

A LAPS-type analysis system is able to add value to conventional data assimilation in the context of very short range forecasting at highresolution. Well demonstrated for intense convective systems, but remains to be demonstrated in other contexts.

### Validation

A single column version of HIRLAM is maintained in step with the reference system and provides an environment for testing of parameterization schemes with a high degree of control over external conditions.

Intercomparisons of SCM and LES-simulations subject to identical external forcing are recommended.

2-d modelling as e.g. within the COSMO-consortium is likewise recommended.

For process validation in a full 3-d environment, it can be recommended to examine the relationship between those factors that are supposed to control a given process and the behaviour of the process itself. E.g. the relationship between cloud cover and surface radiation.

Especially at high resolution, verification methods that are insensitive to phase errors are needed. Such methods include comparing statistical properties of observed and modelled parameters.

Another avenue is to apply methods of fuzzy logic, that do not overly penalize small phase errors.

# Report of the Working Group Discussion on “Physics-Dynamics Interfacing”

Jean-Francois Geleyn

The basis for these discussions was a document prepared by J.-F. Geleyn, B. Catry, B. Hansen-Sass, P. Termonia and M. Tudor after the Workshop on the same topic held in Prague, November 22<sup>nd</sup> to 26<sup>th</sup> 2004. This document synthesises all its proposals within five rules, named from A to E, mainly targeted for the HIRLAM-AROME-ALADIN collaboration. The basic aim of each rule will be recalled thereafter before the account of the discussion concerning it.

Bart Catry made two presentations at the Workshop. The full presentation recalled the spirit and meaning of each of the five rules (in some sense the following thus contains a short abstract of it). The mini-presentation that introduced the WG discussions emphasized the importance of having a clear vertical discretisation strategy cleanly adapted to the models choices (type of coordinate, explicit or implicit physical time-stepping, etc.). Errors of the order of 10% or less on the budget-terms arising when neglecting this constraint were shown to sometimes have a strong impact on individual cases' results (for instance in terms of precipitation maps).

## *Rule A*

Summary: This rule introduces a distinction between (a) options of a general nature that are automatically part of some critical-path interfacing computations and (b) more 'local' options that can in principle be handled independently at the level of some parameterisation computations. The idea is that the latter computations should all have the same positioning with respect to the options of category '(a)' and ideally be written with algorithms that make them completely transparent to the related choices.

### Discussion:

- When following the HIRLAM line of thoughts it was sometimes difficult to separate Rule A from Rule E below. This was sort of a surprise for people used to the IFS/ARPEGE/ALADIN world and this difference of approach is probably linked to a different 'culture' in the use of switches to activate code options.
- The idea to make even the high-level choices routine-dependent was addressed, but rejected because probably leading to an exaggerated complexity.
- Some doubts were raised about the wisdom of using a parallel strategy for calling parameterisation routines concerned with different processes at high resolution, but this remained at the edge of the discussed topic.
- HIRLAM was requested to analyse its current situation and to also set its 'minimum requirements' with respect to the following flexibility issues:
  - physics before of after dynamics;
  - physics and dynamics parallel or sequential;
  - positioning of the physics forcing along the time-space semi-Lagrangian trajectory;
  - which 'physical' information to pass from one time step to the next;
  - the 'spectral model constraints' (e.g. no physics calls after the Helmholtz solver).
- There is a need to know where the combination of the AROME prototype and of the conservation rules will lead in term of practical interfacing constraints. HIRLAM should receive one example as soon as possible. This should not prevent the above-mentioned analysis to start in-between, on the contrary (a first early feed back might indeed help to better target the example).

- HIRLAM will face the problem that its parallelisation structure influences the data-flow of the physics interfacing in the HIRLAM model. Hence there will be a choice between grouping as much as possible the calls from the ALADIN dynamics (which practically amounts to follow for the time being the whole AROME time sequence) or developing a way to use symmetrically the GFL/GMV structure of IFS and the HIRLAM equivalent but without touching too much the low-level physics code (*Remark N°1: this point is transversal to all rules; it is mentioned here because of the chronology of the discussion as it happened in Tartu. Remark N°2: subsequent discussions showed that the 'code-related' starting point of the discussion on this item was erroneous; nevertheless the dilemma between sticking to the AROME time-space arrangement or maintaining HIRLAM's own specificities in this domain remains a true one*).

### **Rule B**

Summary: The link between individual tendencies computed by parameterisation routines and the projection of the total forcing on the evolution of the model's prognostic variables should obey a single set of governing diabatic equations. These equations are derived from first principles (under an agreed set of basic hypotheses) independently of the choice of the dynamical core they are applied to when discretisation takes place. Only at time of this discretisation should the general switches mentioned in Rule A matter.

#### Discussion:

- HIRLAM wishes to see and study all definitive papers about equations, but in principle, like already said in Prague, it is ready to adapt to the proposed choices.

### **Rule C**

Summary: The basis for articulating the "tendencies  $\leftrightarrow$  fluxes" conversions necessary for a smooth application of Rule B will be the DDH-type diagnostics of IFS/ARPEGE/ALADIN with a mandatory minimum of flux-type information to initialise. When this framework will be (temporarily) at odds with some of the choices made in the basic parameterisation routines (which should evolve to match the said conversion rules), the output of those will be re-tailored to deliver a 'dummy output production' technically compatible with this rule 'C' and scientifically close to the previous solution.

#### Discussion:

- Contrary to what will likely happen for the Meso-NH routines in AROME, HIRLAM shall most likely place its 'dummy output production' (for a full thermodynamic interfacing) inside its own codes.
- A first interfacing verification exercise should be based on both 1D models, before going to 3D applications.

### **Rule D**

Summary: In order to simplify the application of the preceding rules (especially for the distinction between 'parallel' and 'sequential' computations of the physical evolutions) parameterisation routines should communicate on the basis of three different statuses (reference, initial and final) rather than on the basis of only the last two ones like generally done. The use of the 'reference' additional input information to the parameterisation routines should allow keeping correct thermodynamic budget calculations within any sequence of evolutions for non-linear conservative quantities like enthalpy.

#### Discussion:

- NB: *this rule should be reassessed following the introduction of the 'dummy output production' proposal that partly overlaps with its own targets.*

- On a matter of principle, HIRLAM is much in favour of the spirit of this rule and asks that its reassessment should be done as soon as possible, in order to avoid a double effort in recoding the interfaces of the HIRLAM physics routines. The ALADIN-2 team will see how and when to satisfy this request in order that HIRLAM can consider Rules A, B and D nearly as a whole when starting its recoding actions.

### **Rule E**

Summary: The application of the above proposed architecture of 'rules' ultimately assumes that some high-level control procedure knows about the type of 'mandatory' budget terms that should be produced given the high-level 'a'-type choices. It should also know about which routines are used and which ones contribute to which 'mandatory' terms. Furthermore some 'cross-checking' could take place to ensure that neither double-accountings nor misses happen inadvertently. This introduces a welcome distinction between 'processes' and 'schemes', but will need time to be fully implemented.

Discussion:

- Symmetrically it was partly mixed with rule A and the idea of the a-priori control was challenged by the possibility of having a running-time control of which routines to call for which 'physical' purpose. Like for a more versatile version of rule A (cf. supra), this was judged too ambitious and it was concluded that one shall stick to high level choices setting of options rather than situation dependent switching between process (which is indeed a modelling rather than interfacing issue).
- HIRLAM supports very much the idea of relying on a distinction between 'processes' and 'schemes' to perform this a-priori control, even if this is not the most immediate priority of the interfacing design and upgrading. It shall find adequate manpower resources to promote this issue (*Remark N°3: preliminary contacts on this issue started shortly after the Tartu meeting*).

Use of reflectivity to validate Hirlam - Irene Sanz and José Antonio García-Moya .....	76
Satellite Data in the Verification of Model Cloud Forecasts: a convective case in summer 2003 seen from NOAA satellites - Christoph Zingerle .....	82
Precipitation and temperature forecasts in two HIRLAM versions - Kalle Eerola .....	86
What can a LAM-NWP system tell us about the atmospheric water cycle - Carl Fortelius	90
Convective indexes calculated from HIRLAM output - Anna Kanukhina .....	95
The flood case 27–29 July 2004 - Sami Niemelä .....	100
Case study based on one dimensional model with Kain-Fritsch convection parameterization scheme - Paulius Jalinskas .....	107
Summary of the working group discussion on the representation of convection in high resolution numerical models - Dmitrii Mironov and Colin Jones .....	113
Report of the working group discussion on "Development of microphysics for the fine scale" - Jean Quiby .....	117
Notes from the working session discussion on analysis, diagnostics and validation - Carl Fortelius .....	119
Report of the working group discussion on "Physics-dynamics-interfacing" - Jean-Francois Geleyn .....	120

---

#### Nordic Network on Fine-scale Atmospheric Modelling (NetFAM)

NetFAM unites eighteen Nordic, Baltic and French meteorological institutes into a research and training network funded by Nordic Research Board (NordForsk).

"Nordic Network on Fine-scale Atmospheric Modelling (NetFAM) aims at complex and comprehensive promotion of fine-scale atmospheric modeling of Nordic-Baltic regional weather and climate processes and man–environment interactions, with strong emphasis on specific qualities of Nordic natural environment and the Baltic Sea influence. To achieve these objectives, the network is designed to cover the whole chain from basic research and researcher training towards the application of the models. The network shares modelling tools, observational and physiographic data, computing and educational resources, in order to strengthen the expertise in the area of fine-scale atmospheric modelling in the Nordic countries and adjacent areas around the Baltic Sea. " (From the network plan, 2004.)

More information: <http://netfam.fmi.fi> .

Proceedings of HIRLAM/NetFAM Workshop on Convection and Clouds.  
Tartu, Estonia, 24-26.1.2005

---

CONTENTS

Introduction .....	1
Programme of the workshop .....	2
List of participants .....	6
The HIRLAM physics towards meso-scale - Per Undén .....	7
Non-hydrostatic semi-implicit semi-lagrangian dynamics (NH SISL) for HIRLAM - Rein Rõõm and Aarne Männik .....	10
A brief review of some key issues related to modelling of cloud and precipitation - Bent Hansen Sass .....	17
Explicit microphysics and diabatic initialization - Paul Schultz .....	20
Experiments with the MesoNH-AROME microphysical scheme and evaluation by remote sensing tools - Jean-Pierre Pinty, Jean-Pierre Chaboureau, Evelyne Richard, Frank Lascaux and Yann Seity .....	23
Performance of Kain-Fritsch/Rasch-Kristjansson in HIRLAM. A review - Javier Calvo ....	28
Combining a statistical cloud parameterisation and moist conservative turbulence scheme in the HIRLAM model - Colin Jones .....	34
Experiences with a statistical cloud scheme in combination with Kain-Fritsch convection in HIRLAM - Wim de Rooy .....	43
Why do moisture convergence deep convection schemes work for more scales than those which they were in principle designed for? - Jean-Francois Geleyn and Jean-Marcel Piriou ..	47
An integrated prognostic approach for clouds, precipitation and convection - Luc Gerard ..	53
Towards an operational implementation of Lopez's prognostic large scale cloud and precipitation scheme in ARPEGE/ALADIN NWP models - Francois Bouyssel, Yves Bouteloup and Pascal Marquet .....	56
Preliminary tests with the use of separate prognostic treatment of cloud water and ice in HIRLAM - Karl-Ivar Ivarsson .....	61
Parameterization of Convection in the Global NWP System GME of the German Weather Service - Dmitrii Mironov and Bodo Ritter .....	68
Testing of bulk parameterisation of microphysics in ALARO 10 - Tomislav Kovacic .....	73

**LIST CONTINUES on the back side ...**